The relationship between time series models for water table depth and physical information

M. Knotters
M.F.P. Bierkens

Report 167
DLO Winand Staring Centre, Wageningen (The Netherlands), 1998

ABSTRACT

M. Knotters, M.F.P. Bierkens, 1998. *The relationship between time series models for water table depth and physical information;* Wageningen (The Netherlands), DLO Winand Staring Centre, Report 167 112 pp.; 7 Figs; 23 Tables; 4 Annexes; 26 Refs.

The relationship between parameters of autoregressive moving average exogenous variable (ARMAX) models and physical information that can be derived from databases such as digital topographical maps, digital elevation maps and soil profile descriptions was investigated at 51 locations with open sandy soils in the Pleistocene part of the Netherlands. The ARMAX parameters appeared to be weakly related with physical information. Water table depths predicted with ARMAX models which were guessed using physical information have large systematic errors but relatively small random errors. It is concluded that the relationships between time series model parameters and physical information can be improved with respect to the modelling as well as the quality of the data used. Furthermore it is recommended to estimate the spatial distribution of time series model parameters is inversely using additional observations on water table depth.

Keywords: ARMAX model, Kalman filter, unsaturated zone, water balance

ISSN 0927-4499

P.O. Box 125, NL-6700 AC Wageningen (The Netherlands)
Phone: 31 (317) 474200; fax: 31 (317) 424812; e-mail: postkamer@sc.dlo.nl

Project 671

Contents

Preface

The study reported here forms part of DWK Research Program 328 of the Netherlandish Ministry of Agriculture, Nature and Fisheries (LNV). A large number of groundwater observation wells was visited in the field. The authors are grateful to all the individual land owners and nature conservation authorities who gave their permission as well as their support to the fieldwork. In particular we wish to thank those functionaries of the State Forest Service (SBB), the Nature Conservation Society (Natuurmonumenten) and the Provincial Landscape Foundations, who guided us towards often hidden but always picturesque well sites. We thank Ir. K. van der Meulen (SBB) and W. Niemeyer (Natuurmonumenten) for their help in the selection of groundwater data. Our colleague W.J.M. te Riele is gratefully acknowledged for his help during the fieldwork and for his advises at all stages of the project. We are greatly indebted to Dr. J.J. de Gruijter (SC-DLO) for his useful advises on statistics, to G. Thijssen for his help on the soil profile descriptions and to Drs.ing. J.W.J. van der Gaast (SC-DLO), Ir. H.Th.L. Massop (SC-DLO) and Ir. J.G. Wesseling (SC-DLO) for the fruitful discussions and valuable support on the use of physical information.

Summary

The dynamic behaviour of the water table depth can be explained from precipitation excess with empirical time series models such as transfer function-noise models (TFN, Knotters and Van Walsum, 1997), dynamic regression models (DR, Knotters and De Gooijer, 1999) or ARMAX models (Bierkens *et al.*, submitted) and threshold autoregressive self-exciting open-loop models (TARSO, Knotters and De Gooijer, 1999). Comparative studies by Knotters and Van Walsum (1997), Knotters and De Gooijer (1999) and Bierkens and Walvoort (1998) concluded that empirical time series models are able to simulate water table depths as well as more physically based models. The models can be fitted on observed series of water table depths of restricted length, say two to ten years. Since data on precipitation excess are generally available over long time, the models can be used to simulate extensive time series of water table depths with a length of, say, 30 years. Hence all desirable characteristics such as Mean Highest and Mean Lowest Watertable (Knotters and Van Walsum, 1997) and durations (Knotters and De Gooijer, 1999) can be calculated.

The aim of this study is to analyze how the parameters in the empirical time series models mentioned above are related to physical quantities that can be derived from databases such as digital topographical maps, digital elevation maps and soil profile descriptions. For this purpose 51 time series of water table depths which represent a wide range of hydrological situations in the Pleistocene part of the Netherlands are analyzed. This analysis will give insight into the usefulness of databases on soil, topography, and elevation in predicting time series of water table depths. Regression models are given which describe the relationship between physical information and parameters of time series models.

The linear TFN model for the relationship between precipitation excess and water table depth is given by

$$\begin{aligned} H_t^* &= \textstyle\sum_{i=1}^{r} \delta_i H_{t-i}^* + \sum_{j=0}^{s} \omega_j P_{t-j-b}, \\ (N_t^* - \mu) &= \textstyle\sum_{i=1}^{p} \phi_i (N_{t-i}^* - \mu) + \epsilon_t + \sum_{j=1}^{q} \theta_j \epsilon_{t-j}, \\ H_t &= H_t^* + N_t^*, \end{aligned}$$

where H_t^* denotes that part of the water table depth H_t which is explained by the precipitation excess P_t, b is a delay factor, which is an integer greater or equal to zero, $\{\epsilon_t\}$ is a white noise process with zero mean and finite variance, and where μ is the mean of the noise process $\{N_t^*\}$.

It can be shown that if $\delta_i, i = 1, \ldots, r$ equals $\phi_i, i = 1, \ldots, p$ the TFN model can be written as an ARMAX model (Hipel and McLeod, 1994):

$$(H_t - \mu) = \sum_{i=1}^{m} a_i (H_{t-i} - \mu) + \sum_{i=0}^{m'} b_i P_{t-i} + \epsilon_t$$

The ARMAX model with $m = 1$ and $m' = 0$ can be written in water balance terms in the following way:

$$\begin{aligned} h(t) &= \left\{e^{-\Delta t/\varphi\gamma}\right\} h(t-\Delta t) \\ &\quad +\gamma\left\{1-e^{-\Delta t/\varphi\gamma}\right\} P(t) \\ &\quad +\left\{\gamma q_b + H_s\right\}\left\{1-e^{-\Delta t/\varphi\gamma}\right\} \\ &\quad +\gamma\left\{\left[E_p(t)-E_a(t)\right]-\frac{\Delta V}{\Delta t}\right\}\left\{1-e^{-\Delta t/\varphi\gamma}\right\}, \end{aligned}$$

where $h(t)$ is the water table depth [L] at time t, φ is the effective porosity [-], γ is the drainage resistance [T], q_b is the regional groundwater flux [LT^{-1}], H_s is the drainage level [L], E_p is the potential evapotranspiration [LT^{-1}], E_a is the actual evapotranspiration [LT^{-1}], and ΔV is the change of the moisture content in the unsaturated zone [L]. Now the ARMAX model parameters can be expressed in physical terms:

$$\begin{aligned} a_1 &= e^{-\Delta t/\varphi\gamma} \\ b_0 &= \gamma\left\{1-e^{-\Delta t/\varphi\gamma}\right\} \\ &= \gamma\left\{1-a_1\right\} \\ \mu &= \gamma q_b + H_s. \end{aligned}$$

In the presence of two drainage levels these relationships can be written as follows:

$$\begin{aligned} a_1 &= \beta, \\ b_0 &= \frac{1-\beta}{\alpha}, \\ \mu &= \frac{\left\{q_b+\frac{H_1}{\gamma_1}+\frac{H_2}{\gamma_2}\right\}}{\alpha}, \end{aligned}$$

with

$$\alpha = \frac{1}{\gamma_1}+\frac{1}{\gamma_2},$$

and

$$\beta = e^{-\frac{\Delta t}{\varphi}\alpha}.$$

Time series of water table depths which represent a wide range of hydrological situations in the Pleistocene part of the Netherlands were selected from the Groundwater Archive (Van Bracht, 1989). A total number of 51 wells were selected after inspection in the field. Drainage levels and bottom depths of drainage devices in the neighbourhood of the wells were collected. The soil profiles were described at least up to the permanently reduced zone, and texture and organic matter content were estimated.

Values of q_b were "guessed" from digital groundsurface elevation data and information on the hydraulic conductivity of the subsoil. Values of γ were guessed using the drainage formula of Ernst (1956). Inputs on the distance between drainage devices, on bottom depths and on wetted perimeters were guessed from digital topographic maps, field observations and research by Van

der Gaast and Van Bakel (1997). Inputs on hydraulic conductivities were guessed from the soil profile descriptions and a table published by Bierkens (1994). The drainage resistance was guessed for a neighbourhood circle with a radius of 400 m and 600 m. The effective porosity φ was guessed from the soil profile descriptions and soil physical standard curves (Wösten et al., 1987). Hence values of the ARMAX parameters a_1, b_0, μ and σ_ϵ were guessed.

The regional groundwater flux estimated from calibrating ARMAX models appeared to be unrelated with the regional groundwater flux that was guessed from auxiliary information on groundsurface elevation and hydraulic conductivity of the subsoil. The effective porosity estimated from ARMAX models is only weakly related to the effective porosity guessed from auxiliary information on soil physical properties ($R^2_{\text{adj.}} = 21.7\%$). The drainage resistance estimated from time series is moderately related to the drainage resistance guessed from auxiliary information on drainage devices and hydraulic conductivities; $R^2_{\text{adj.}} = 74.5\%$ for guessed values based on a neighbourhood circle with a radius of 600 m, and $R^2_{\text{adj.}} = 54.2\%$ for guessed values based on neighbourhood circles with a radius of 400 m and 600 m. Regression analysis indicated only weak relationships between guessed ARMAX parameters and ARMAX parameters estimated from time series. The percentages of variance accounted for are roughly in between 4% and 35%.

Reasons for the weak relationships between ARMAX parameters and physical information can be divided into three categories:

1. Assumptions in the time series model. The ARMAX model assumes a linear relationship between precipitation excess and water table depth. However, nonlinearities may exist for instance because of the presence of thresholds such as distinct soil physical boundaries and drainage levels. Ignoring the nonlinear behaviour may weaken the relationship between the time series model parameters and the physical information;

2. Assumptions in the models that describe the relationship between time series model parameters and physical information. In the calculation of the regional groundwater flux it is assumed that the gradients of the water table can be approximated by the gradients in the groundsurface. However, the water table is smoother than the groundsurface. The effect of storage in puddles and bypass flow through preferential flowpaths, macropores and soil cracks is ignored in the calculation of the effective porosity. The drainage resistance is guessed on the basis of neighbourhood circles with a fixed radius of 600 m or iteratively from neighbourhood circles with a radius of 400 m and 600 m. It would be more realistic, however, to calculate the drainage resistance iteratively for a wide range of radius values;

3. The quality of the data used. Uncertainty exists about the hydraulic conductivities of the subsoil, the soil physical properties, entrance resistances, drainage levels, and wetted perimeters and bottom depths of drainage devices such as trenches, ditches and channels.

The relationships between ARMAX parameters and auxiliary information on elevation, topography and soil physical properties can be improved in several ways. A first improvement can be obtained if the relationship between precipitation excess and water table depth is described by a nonlinear model, for instance a TARSO model (Knotters and De Gooijer, 1999), in particular if distinct threshold nonlinearities in the relationship between precipitation excess and water table depth are present.

The guessed values of the regional groundwater flux can be improved if the gradients of the water table are derived from the results of for instance a stationary model for regional groundwater flow and from contour line maps of the phreatic groundwater surface obtained with such a model. The guessed values of effective porosity can be improved by including the storage in puddles and the effect of bypass flow through macropores, soil cracks and preferential flow paths. Therefore, more information on these processes need to be collected. The guessed values of the drainage resistance can be improved if they are calculated from a wide range of values for the radius of the neighbourhood.

An important improvement in the quality of the elevation data can be expected in near future, if accurate elevation data collected by laser scanning are digitally available in a 5×5 m grid. This may improve the guessed regional groundwater fluxes. Accurate information on the hydraulic conductivity of the subsoil, say in between 1 m and 10 m depth, is extremely important in the calculation drainage resistances and regional groundwater fluxes. However, this information is not widely available yet. Further improvements in the calculation of drainage resistance can be expected if more information on entrance resistances of drainage devices were available. This study also indicated a need for more accurate and more detailed information on the presence and dimensions of drainage devices. Improvements can be made in the calculation of effective porosities if more soil physical standard curves for distinct geologic regions and geologic deposits were available.

Water table depths that are predicted using guessed ARMAX models contain large systematic errors, but the standard deviations of the prediction errors are relatively small. It is expected that the predictions of an ARMAX model that has been guessed from physical information can be improved using more accurate guesses of the regional groundwater flux and the drainage resistances, and more accurate information on the drainage levels. Another possibility is to guess the ARMAX-parameter μ from water table depths that are observed

at a large number of sites at a time that the water table is about its mean level, or to estimate the spatial distribution of μ inversely using observed water table depths.

This study makes clear that parameters of time series models can not be predicted accurately in space on the basis of physical relationships yet. Although some improvements in the modelling are suggested, these will not take away the uncertainties about the data. In particular the quality of data on the hydraulic conductivity of the subsoil, entrance resistances, dimensions of drainage devices, and soil physical properties is extremely important in guessing ARMAX model parameters. Furthermore, a good approximation of the gradients in the phreatic surface is necessary. For economic reasons it is expected that the quality of physical information can only be improved to some extent. Hence it can be concluded that besides physical auxiliary information, observations on the water table depth itself are necessary in the spatial prediction of time series of water table depths. A possible method is to estimate the spatial distribution of time series parameters inversely from additional observations on the water table depth (i.e. calibration). Therefore, research is needed on optimal sampling strategies for the water table depth in both space and time, within the practical and economic limits of a regional survey.

Water table depths predicted by ARMAX models that are guessed from physical information show large systematic errors but relatively small random errors. These predictions can be improved if the ARMAX-parameter μ that reflects the mean water table depth is guessed more accurately. Again, additional observations on the water table depth and inverse estimation of the spatial distribution of the ARMAX-parameters can be useful to reduce the prediction errors, besides more accurate physical information.

1 Introduction

The dynamic behaviour of the water table depth can be explained from precipitation excess using empirical time series models such as transfer function-noise models (TFN) (Gehrels *et al.*, 1994; Knotters and Van Walsum, 1997; Van Geer and Zuur, 1997), transfer function models as described by Tankersley *et al.* (1993) and Tankersley and Graham (1994), dynamic regression models (DR, Knotters and De Gooijer, 1999) or ARMAX models (Bierkens *et al.*, submitted) and threshold autoregressive self-exciting open-loop models (TARSO, Knotters and De Gooijer, 1999). Both TFN and DR models describe linear relationships between input and output. The TARSO model accounts for threshold nonlinearities in the relationship between precipitation excess and water table depth. Knotters and Van Walsum (1997), Knotters and De Gooijer (1999) and Bierkens and Walvoort (1998) evaluated the simulation performance of empirical time series models and physically based models such as the physical descriptive model SWATRE (Belmans et al., 1987), a simple analytical model (Bierkens and Walvoort, 1998) and a stochastic differential equation (Bierkens, 1998). These comparative studies concluded that empirical time series models are able to simulate water table depths as well as more physically based models. An advantage of empirical time series models is that only data on the input and output variable are requested, whereas physically based models need additional information such as drainage levels and soil physical properties.

The models can be fitted on observed series of water table depths of restricted length, say two to ten years. Since data on precipitation excess are generally available over a longer time, the models can be used to simulate extensive time series of water table depths with a length of, say, 30 years. Hence all desirable characteristics such as Mean Highest and Mean Lowest Watertable (Knotters and Van Walsum, 1997) and durations (Knotters and De Gooijer, 1999) can be calculated. It may be desirable, however, not only to be informed about the dynamic behaviour of water table depth at the location of observation wells but also at other locations. In regional surveys generally only few time series of water table depths are available, and the opportunities for collecting additional groundwater data in space and time are limited in most cases. Therefore, there is a need for relationships between widely available physical information and parameters of time series models. Through using these relationships in combination with time series models it may be possible to predict time series models spatially. Hence, input series on precipitation excess can be transformed into output series on water table depth at all points in space. From these spatially predicted or simulated series all desirable characteristics can be calculated.

The aim of this study is to analyze how the parameters in the empirical time series models mentioned above are related to physical quantities that can be

guessed from databases such as digital topographical maps, digital elevation maps and soil profile descriptions. For this purpose 51 time series of water table depths which represent a wide range of hydrological situations in the Pleistocene part of the Netherlands are analyzed. It will be demonstrated that physical quantities such as the regional groundwater flux, the effective porosity of the soil and the drainage resistance are related to time series model parameters. These physical quantities will be "guessed" from databases on soil, topography and ground surface elevation that are available at a national scale. The term "guessed" is used to distinguish from parameters which are "estimated" from time series. This analysis will give insight into the usefulness of databases on soil, topography, and ground surface elevation in predicting time series of water table depths. Regression models are given which describe the relationship between physical information and parameters of time series models.

This report is composed as follows. In Chapter 2 the time series models that describe the relationship between the potential precipitation excess and the water table depth are defined. In Chapter 3 a water balance for the phreatic groundwater zone that can be expressed in terms of linear time series models such as TFN, DR and ARMAX, is derived. In Chapter 4 the selection procedure is given that resulted in a set of 51 observation wells which represent a wide range of hydrological situations in the Pleistocene part of the Netherlands. Chapter 5 describes how physical quantities like the regional groundwater flux, the drainage resistance, and the effective porosity can be guessed from auxiliary information on soil, topography, and elevation. In Chapter 6 the results of the analyses are given. The results of time series modelling are given, guessed values of physical quantities are listed, and regression models that describe the relationship between estimated parameters of time series models and guessed values of physical quantities are presented. The report ends with a discussion on the usefulness of auxiliary information on soil, topography and groundsurface elevation, and some concluding remarks.

2 Time series models

Let H_t be the water table depth at discrete time t. Furthermore, let P_t be defined as the average daily potential precipitation excess between $t-1$ and t, which is calculated from difference between daily precipitation en daily Makkink reference-crop evapotranspiration (De Bruin, 1987). Now the TFN model that describes the relationship between H_t and P_t is given by the linear difference equation

$$H_t^* = \sum_{i=1}^{r} \delta_i H_{t-i}^* + \sum_{j=0}^{s} \omega_j P_{t-j-b} \tag{1}$$

where H_t^* denotes that part of H_t that is explained by P_t. Here b is a delay factor, which is an integer greater or equal to zero.

In practice one could not expect that H_t can be "fully" explained by variations in P_t. There will always be outside disturbances. If it is assumed that the disturbance, or noise N_t, is independent of the level of P_t and is additive with respect to the influence of P_t, then (1) can be written as

$$H_t = H_t^* + N_t^*. \tag{2}$$

Now N_t^* may be related to its own past N_{t-1}^*, N_{t-2}^*, and so on. This behaviour can be described by an AR(I)MA process. Assuming that N_t^* is stationary, this process can be written as

$$(N_t^* - \mu) = \sum_{i=1}^{p} \phi_i (N_{t-i}^* - \mu) + \epsilon_t + \sum_{j=1}^{q} \theta_j \epsilon_{t-j}$$

where $\{\epsilon_t\}$ is a white noise process with zero mean and finite variance, and where μ is the mean of the process $\{N_t^*\}$.

It can be shown that if $\delta_i, i = 1, \ldots, r$ equals $\phi_i, i = 1, \ldots, p$ the TFN model can be written as an autoregressive moving average exogenous variable (ARMAX) model (Hipel and McLeod, 1994):

$$(H_t - \mu) = \sum_{i=1}^{m} a_i (H_{t-i} - \mu) + \sum_{i=0}^{m'} b_i P_{t-i} + \epsilon_t. \tag{3}$$

The dynamic regression (DR) model (Knotters and De Gooijer, 1999) is an alternative notation of the DR model with respect to the constant term:

$$H_t = a_0 + \sum_{i=1}^{m} a_i H_{t-i} + \sum_{i=0}^{m'} b_i P_{t-i} + \epsilon_t. \tag{4}$$

The ARMAX model with $m = 1$ and $m' = 0$ was calibrated on time series of P and H using the Kalman filter approach described by Bierkens *et al.*

(submitted). For this purpose a Fortran program called "KALMAX" has been written.

3 A water balance for the phreatic groundwater zone

Figure 2 shows a schematic soil profile with a water table and ingoing and outgoing fluxes. At the top of the soil column two ingoing fluxes are assumed: $P_t[\mathrm{LT}^{-1}]$ and $\{E_{\mathrm{p},t} - E_{\mathrm{a},t}\}[\mathrm{LT}^{-1}]$. The term P_t reflects the potential precipitation excess, which is defined by

$$P_t = P_t^* - E_{\mathrm{p},t},$$

where $P_t^*[\mathrm{LT}^{-1}]$ is the precipitation in between $t-1$ and t, and $E_{\mathrm{p},t}[\mathrm{LT}^{-1}]$ is the potential evapotranspiration in between $t-1$ and t. The generally unknown difference between potential and actual evapotranspiration ($E_{\mathrm{a},t}[\mathrm{LT}^{-1}]$) is expressed by the term $\{E_{\mathrm{p},t} - E_{\mathrm{a},t}\}[\mathrm{LT}^{-1}]$. At the bottom of the soil column the ingoing flux $q_{\mathrm{b},t}[\mathrm{L\ T}^{-1}]$ expresses the regional component of groundwater flow, i.e. upward and downward seepage. The outgoing flux $q_{\mathrm{d},t}[\mathrm{L\ T}^{-1}]$ indicates the drainage to devices such as trenches and ditches, with drainage level $H_{\mathrm{s}}[\mathrm{L}]$. The term $V_t[\mathrm{L}]$ expresses the moisture content in the unsaturated zone, which shows a generally unknown variation in time.

Until now a discrete time scale was used, i.e. equidistant time steps indicated by subscripts t. In the following a water balance will be constructed in terms of a linear time series model. For this purpose the continuous time scale will be used, indicated by (t). In first instance several terms are assumed to be constant, so that a water balance with a linear structure can easily be constructed. Firstly, the drainage level H_{s} is assumed to be constant, so that the drainage flux $q_{\mathrm{d}}(t)$ can be defined by

$$q_{\mathrm{d}}(t) = \frac{H_{\mathrm{s}} - h(t)}{\gamma},$$

where γ is the drainage resistance which is also assumed to be constant. Furthermore, the porosity $\varphi[-]$ of the porous medium in which the water table depth $h(t)$ fluctuates is assumed to be constant. Finally, the regional component of groundwater flow (q_{b}) is assumed to be constant in time. A water balance for the phreatic groundwater zone can now be given by

$$\varphi\frac{\mathrm{d}h}{\mathrm{d}t} = \frac{H_{\mathrm{s}} - h(t)}{\gamma} + P(t) + q_{\mathrm{b}} + \{E_{\mathrm{p}}(t) - E_{\mathrm{a}}(t)\} + \frac{\mathrm{d}V}{\mathrm{d}t}. \tag{5}$$

The change in time of the water table depth can be written as

$$\frac{\mathrm{d}h}{\mathrm{d}t} = \frac{-h(t)}{\varphi\gamma} + \frac{1}{\varphi}\left\{P(t) + q_{\mathrm{b}} + \frac{H_{\mathrm{s}}}{\gamma} + E_{\mathrm{p}}(t) - E_{\mathrm{a}}(t) + \frac{\mathrm{d}V}{\mathrm{d}t}\right\}. \tag{6}$$

The second term at the right hand side of Eq. (6) is called $U(t)$ in the following. Now the impulse-response function can be derived as follows:

$$\begin{aligned} \frac{\mathrm{d}h}{h} &= -\frac{1}{\varphi\gamma}\mathrm{d}t \\ \ln h &= -\frac{t}{\varphi\gamma} + c \end{aligned}$$

$$h(t) = h(0)\mathrm{e}^{-t/\varphi\gamma}. \tag{7}$$

Eq. (7) is the tail recession of h. Now assume that at time $t - \Delta t$ the water table depth is equal to $h(t - \Delta t)$. Then at time t remains

$$h'(t) = h(t - \Delta t)\mathrm{e}^{-\Delta t/\varphi\gamma}.$$

The influence of the input, which is assumed to be constant in between $t - \Delta t$ and t, on h follows from the convolution integral:

$$h''(t) = \int_{t-\Delta t}^{t} \mathrm{e}^{-(t-\tau)/\varphi\gamma} U(\tau)\mathrm{d}\tau.$$

Now because $U(t)$ is constant in between $t - \Delta t$ and t we obtain

$$\begin{aligned} h''(t) &= U(t)\mathrm{e}^{-t/\varphi\gamma} \textstyle\int_{t-\Delta t}^{t} \mathrm{e}^{\tau/\varphi\gamma}\mathrm{d}\tau \\ &= U(t)\mathrm{e}^{-t/\varphi\gamma} \left\{\varphi\gamma\mathrm{e}^{t/\varphi\gamma} - \varphi\gamma\mathrm{e}^{t/\varphi\gamma}\mathrm{e}^{-\Delta t/\varphi\gamma}\right\} \\ &= U(t)\varphi\gamma\left\{1 - \mathrm{e}^{-\Delta t/\varphi\gamma}\right\}. \end{aligned}$$

This results in

$$\begin{aligned} h(t) = h'(t) + h''(t) &= \left\{\mathrm{e}^{-\Delta t/\varphi\gamma}\right\} h(t - \Delta t) \\ &\quad +\gamma\left\{1 - \mathrm{e}^{-\Delta t/\varphi\gamma}\right\} P(t) \\ &\quad +\left\{\gamma q_{\mathrm{b}} + H_{\mathrm{s}}\right\}\left\{1 - \mathrm{e}^{-\Delta t/\varphi\gamma}\right\} \\ &\quad +\gamma\left\{\left[E_{\mathrm{p}}(t) - E_{\mathrm{a}}(t)\right] - \frac{\Delta V}{\Delta t}\right\}\left\{1 - \mathrm{e}^{-\Delta t/\varphi\gamma}\right\}. \end{aligned} \tag{8}$$

The first two terms at the right hand side of Eq. (8) describe the dynamic relationship between the input $P(t)$ and the output $h(t)$. The third term at the right hand side contains only terms that are assumed to be constant in time. The last term at the right hand side of Eq. (8) is the residual term $\epsilon(t)$. In its structure Eq. (8) equals the DR model and the ARMAX model which are given in Eqs. (4) and (3), respectively. Eq. (8) can now be written as

$$h(t) - \mu = a_1\left\{h(t - \Delta t) - \mu\right\} + b_0 P(t) + \epsilon(t), \tag{9}$$

with

$$\begin{aligned} a_1 &= \mathrm{e}^{-\Delta t/\varphi\gamma} \\ b_0 &= \gamma\left\{1 - \mathrm{e}^{-\Delta t/\varphi\gamma}\right\} \\ &= \gamma\left\{1 - a_1\right\} \\ \mu &= \gamma q_{\mathrm{b}} + H_{\mathrm{s}}. \end{aligned} \tag{10}$$

From Eq. (9) follows that $0 \leq a_1 < 1$ and $0 \leq b_1 < \infty$, as they should. The physical quantities γ, φ, and q_b can now be calculated from time series parameters in the following way:

$$\begin{aligned} \gamma &= \frac{b_1}{1-a_1} \\ \varphi &= \frac{-\Delta t}{\gamma \ln(a_1)} \\ q_b &= \frac{\mu - H_s}{\gamma} \end{aligned} \tag{11}$$

Until now we assumed the presence of one drainage level. It may be desirable, however, to distinguish more drainage levels. Assuming two drainage levels a water balance can be written as

$$\varphi \frac{\mathrm{d}h}{\mathrm{d}t} = \frac{H_1 - h(t)}{\gamma_1} + \frac{H_2 - h(t)}{\gamma_2} + P(t) + q_b + \{E_p(t) - E_a(t)\} + \frac{\mathrm{d}V}{\mathrm{d}t} \tag{12}$$

After some derivations we obtain

$$\begin{aligned} h(t) &= \beta h(t - \Delta t) + \tfrac{1-\beta}{\alpha} P(t) \\ &\quad + \tfrac{1-\beta}{\alpha} \left\{ q_b + \tfrac{H_1}{\gamma_1} + \tfrac{H_2}{\gamma_2} \right\} + \tfrac{1-\beta}{\alpha} \left\{ E_p(t) - E_a(t) + \tfrac{\mathrm{d}V}{\mathrm{d}t} \right\}, \end{aligned} \tag{13}$$

with

$$\alpha = \frac{1}{\gamma_1} + \frac{1}{\gamma_2},$$

and

$$\beta = \mathrm{e}^{-\frac{\Delta t}{\varphi}\alpha}.$$

Eq. (13) is analogous to the following ARMAX model:

$$h(t) - \mu = a_1 \{h(t-1) - \mu\} + b_0 P(t) + \epsilon(t),$$

with

$$\begin{aligned} a_1 &= \beta, \\ b_0 &= \tfrac{1-\beta}{\alpha}, \\ \mu &= \frac{\left\{ q_b + \frac{H_1}{\gamma_1} + \frac{H_2}{\gamma_2} \right\}}{\alpha}. \end{aligned} \tag{14}$$

The parameters γ, φ, q_b and σ_ϵ are calibrated on time series on P and H using the Kalman filter algorithm described by Bierkens *et al.* (submitted) with the Fortran program "KALWAT".

4 Selection of time series

Time series of water table depths which represent a wide range of hydrological situations in the Pleistocene part of the Netherlands were selected from the Groundwater Archive (OLGA) of the TNO Institute of Applied Geoscience (Van Bracht, 1989). Both the database for the agricultural areas (OLGA) and the nature areas (OLGA-SUN) were used. The selected time series obey the following conditions:

1. Length of at least three years;
2. Water table depths are observed semi-monthly;
3. The wells are situated in the Pleistocene part of the Netherlands with open sandy profiles, i.e. no stagnation of soil water;
4. The filter depth is within 6 m below the groundsurface.

This selection resulted in a set of 1700 observation wells. From this set a balanced sample was taken of 51 well locations with respect to

1. Region: north, middle and south;
2. land use: agriculture or nature;
3. soil type;
4. water table class.

Preliminary information on soil type and water table class was derived from the digital soil map of the Netherlands (Finke *et al.*, 1998). The following soil classes are represented on the basis of the material in the first 1.20 m:

1. "loamy sands": soils with horizons containing less than 15% organic matter, and with a mineral fraction containing 8% clay (mineral material with particle-size $< 2\mu$m), 17.5% to 50% loam (mineral material with particle-size $< 50\mu$m, a median of the sand fraction (M50, mineral material with particle-size $> 50\mu$m) which is smaller than 210μm, and with an anthropogenic top layer not thicker than 0.5 m;
2. "fine sands": soils with horizons containing less than 15% organic matter, and with a mineral fraction containing less than 5% clay (mineral material with particle-size $< 2\mu$m), less than 17.5% loam, an M50 smaller than 210μm, and with an anthropogenic top layer not thicker than 0.5 m;

3. "coarse sands": soils with horizons containing less than 15% organic matter, and with a mineral fraction containing less than 8% clay, less than 17.5% loam, an M50 larger than 210μm, and with an anthropogenic top layer not thicker than 0.5 m;

4. "anthropogenic sandy soils": soils with an anthropogenic top layer that is thicker than 0.5 m, containing fine sandy material (M50 $<$ 210μm) with an organic matter content in between 2.5% and 15%, less than 8% clay and less than 50% loam;

5. "peaty sandy soils": sandy soils with at most 0.4 m peaty material ($>$ 15% organic matter) in the upper 0.8 m of the soil profile.

Five different fluctuation classes of the water table are represented:

1. a wet class with only few drainage devices: the Mean Highest Watertable (MHW, Van Heesen, 1970) is not deeper than 0.25 m below the groundsurface, and the Mean Lowest Watertable (MLW) is not deeper than 1.20 m below the groundsurface;

2. a wet class with drainage devices: the MHW is in between 0.25 m and 0.40 m, and the MLW is not deeper than 1.20 m;

3. a class with large fluctuations up to shallow depths: the MHW is not deeper than 0.40 m, and the MLW is deeper than 1.20 m;

4. a dry class: the MHW is in between 0.40 m and 0.80 m, and the MLW is deeper than 1.20 m;

5. a very dry class: the MHW is deeper than 0.80 m, and the MLW is deeper than 1.20 m.

Preliminary information on land use was derived from the National Land use Map of the Netherlands. For each pixel of 25 by 25 m the land use is known. Two groups of land use were distinguished: 1) agriculture and 2) nature, including forest.

Tables 1 and 2 show the distribution of the 1700 candidate wells over the strata. The 51 bold face numbers in Tables 1 and 2 indicate the strata in which the 51 observation wells were searched.

All 51 observation wells were selected after inspection in the field. Drainage levels and bottom depths of drainage devices in the neighbourhood of the wells were collected. The soil profiles were described at least up to the permanently reduced zone. Texture and organic matter content were estimated, and the

colour of the horizons was measured using Munsell's soil colour charts. The soil profile descriptions are given in Annex 4. An explanation of these soil profile descriptions is given by Ten Cate *et al.* (1995).

Time series on daily precipitation and Makkink reference crop evapotranspiration were selected from the reports of the Royal Dutch Meteorological Institute (KNMI). Tables 3 and 4 list the coordinates of the observation wells and the meteorological stations. Figure 1 shows the locations of the observation wells and the meteorological stations. The beginning and ending dates of the series used in the model calibration are listed in Tables 5 and 6.

5 Physical information

5.1 Regional groundwater flux

From Eq. (10) it is clear that the ARMAX-parameter μ depends on the regional groundwater flux q_b. The driving force of regional groundwater flow is gravity: the groundwater flows from relatively high areas such as ridges of coarse sands and ice-pushed ridges to relatively low areas such as brook valleys. Therefore, a relation between q_b and elevation may be expected. The relation with elevation is described by Darcy's law for groundwater flow between from point A to point B:

$$q_b = -k_{sat}\frac{h'_A - h'_B}{s} \tag{15}$$

where k_{sat} is the saturated hydraulic conductivity, h'_A and h'_B is the phreatic groundwater level relative to NAP at points A and B, respectively, and s is the distance between A and B. In this study the difference $h'_A - h'_B$ is approximated by the difference between the groundsurface elevation of points A and B. It should be noted, however, that this approximation overestimates the gradient of the water table, because the water table is smoother than the groundsurface: high groundsurface elevations generally go with deep water tables, whereas low groundsurface elevations generally go with shallow water tables. Elevation data for the groundsurface are available from digital maps with on average one datum per hectare. In near future precise elevation data are digitally available in a 5×5 m as well as a 25×25 m grid.

An auxiliary variable that can be derived from digital elevation data is the relative groundsurface elevation, which can be defined as the elevation relative to the mean elevation in a surrounding area with a given radius. Te Riele and Brus (1992), Stolp *et al.* (1994), and Te Riele et al. (1995) used relative groundsurface elevation as an auxiliary variable in the spatial prediction of water table depths and characteristics such as the Mean Highest and Mean Lowest water table (MHW and MLW, respectively). In these three studies linear relationships were found between relative groundsurface elevation and water table depth or characteristics like MHW. Besides the relative groundsurface elevation, the groundsurface relative to NAP (Dutch ordnance datum) was included into the regression models in all three studies.

For each of the 51 locations the relative groundsurface elevation was calculated for ten circles with a radius ranging from 300 to 3000 m. For this purpose the elevation data from the digital elevation map were declustered by means of nearest neighbour interpolation to a 25×25 m grid. The relative groundsurface

elevation of a well location is subsequently calculated as follows:

$$\tilde{z}_r = \frac{1}{n_r} \sum_{i=1}^{n_r} (z - \tilde{z}_i) \tag{16}$$

where n_r is the number of declustered elevation data $\tilde{z}_i$ in a circle with radius $r, r = 300, 600, \ldots, 3000$ m.

A drawback of relative groundsurface elevation as a predictor of regional groundwater flux may be that the gradient and the saturated conductivity of the subsoil are not included. Therefore we calculated a "guess" of q_b in the following way:

$$\tilde{q}_b = \max_r \left| -\tilde{k}_{sat} \text{median}_i \left\{ \frac{(z - \tilde{z}_{i,r})}{s_{i,r}} \right\} \right| \tag{17}$$

where $s_{i,r}$ is the distance from the observation well to the ith declustered point with elevation $\tilde{z}_{i,r}$ in the circle with radius $r, r = 300, 600, \ldots, 3000$ m. The maximum operator is included in Eq. (17) in order to find the scale at which the regional flow dominates. Values for $\tilde{k}_{sat}$ were derived from the soil profile descriptions and a table with horizontal hydraulic conductivities published by Bierkens (1994).

5.2 Drainage

As Eq. (10) indicates, all three ARMAX parameters depend on the drainage resistance γ. Furthermore, the parameter μ also depends on the drainage level H_s. Drainage levels are known from the local water management authorities, or otherwise they can be observed in the field. The drainage resistance can not be observed directly in the field, but can be calculated from the distance between drainage devices, the depth of drainage devices, the horizontal, vertical, and radial saturated conductivities of the subsoil, and the entrance resistance of drainage devices. In this study the formula of Ernst (1956) is used in calculating drainage resistances, which is given by

$$\tilde{\gamma} = \frac{D_v}{k_v} + \frac{L^2}{8 \sum k_h D_h} + \frac{L}{\pi k_r} \ln \frac{\alpha D_r}{u} + \frac{L c_e}{u} \tag{18}$$

where the first term at the right hand side is the vertical component, the second term is the horizontal component, the third term is the radial component, and the fourth term is the entrance component. D_v, D_h, and D_r are the thicknesses of the layers with vertical, horizontal, and radial flow, respectively (m). k_v, k_h, and k_r are the vertical, horizontal, and radial hydraulic conductivity in the layers with vertical, horizontal, and radial flow, respectively (m d^{-1}), with $k_v = \sqrt{k_h k_v}$. L is the distance between the drainage devices (m), u is the wetted perimeter (m), α is a factor accounting for the geometry of radial

flow (-), and c_e is the entrance resistance (d). Three profile types can be distinguished: i) homogeneous profiles; ii) profiles with a boundary between two layers above the bottom of the drainage devices, and iii) profiles with a boundary between two layers below the bottom of the drainage devices, see Werkgroep Herziening Cultuurtechnisch Vademecum (1988, pp. 518-522) for a detailed description of the calculation method and a diagram for the determination of α.

The distance between drainage devices can be derived from digital topographic maps (1:10,000) for areas with a specified radius. In this study we applied a radius of 400 m and 600 m. Mean distances between drainage devices were calculated using the GIS-package ARCVIEW (ESRI, 1996). Bottom depths and wetted perimeters were observed in the field or derived from Van der Gaast and Van Bakel (1997). Hydraulic conductivities were derived from the soil profile descriptions and a table given by Bierkens (1994). Tables 7 and 8 list the hydraulic conductivities that are applied in the calculation of the drainage resistances. The broken numbers in these Tables 7 and 8 are effective horizontal and vertical conductivities for multilayered profile types. These effective conductivities are calculated in the following way:

$$k_{\mathrm{h,eff.}} = \frac{1}{n}\sum_{i=1}^{n} k_{\mathrm{h},i},$$

$$k_{\mathrm{v,eff.}} = \frac{1}{\sum_{i=1}^{n}\frac{1}{k_{\mathrm{v},i}}}.$$

The entrance resistance c_e was assumed to be 1 day. Four types of drainage device were distinguished:

1. trenches and periodically dry ditches;
2. ditches with a width up to 3 m;
3. ditches with a width in between 3 m and 6 m;
4. channels, brooks and rivers wider than 6 m;

In the presence of n drainage types the total drainage resistance can be calculated as follows:

$$\tilde{\gamma} = \frac{1}{\sum_{i=1}^{n}\frac{1}{\min_R(\gamma_{i,R})}} \tag{19}$$

with $R = 400, 600$m being the radius of the area for which the drainage resistance is calculated. In this way the smallest drainage resistance is calculated iteratively from drainage resistances for several drainage types in two neighbourhoods of different size.

5.3 Effective porosity

The parameters a_1 and b_0 of the ARMAX model, Eq. (10), depend on the effective porosity φ. The effective porosity is the ratio between a change in the water balance during Δt and the resulting change in water table depth, see Eq. (5). The effective porosity depends not only on the porosity of the medium in which the water table fluctuates, but also on the storage of water in puddles and preferential flow or "bypass flow". Only on porosity prior information is available from the soil profile descriptions and the soil physical standard curves for the main soil horizons in the Netherlands (Wösten *et al.*, 1987). From this information various quantities which may be related to the effective porosity can be calculated, for instance:

1. the moisture content of a soil profile at saturation;

2. the moisture content if the pressure head profile is in equilibrium;

3. the porosity of a soil profile;

4. the storage coefficient if the pressure head profile is in equilibrium.

These quantities were calculated for the soil profiles up to the permanently reduced zone using the program CAPSEV (Wesseling, 1991). The storage coefficient μ_s was calculated in the following way:

$$\mu_s = \frac{\sum_{i=1}^{n} \{\theta_{\text{sat},i} - \theta(h_p(z_i)) + \theta_{\text{residual},i}\}}{z_g} \tag{20}$$

where n is the number of discretisation intervals (0.01 m) between the ground-surface and the permanently reduced zone, z_g is the water table depth (m) which is set equal to the depth of the permanently reduced zone here, z_i is the depth of the ith discretisation interval of 0.01 m, $\theta_{\text{sat},i}$ is the saturated moisture content in the ith discretisation interval (m^3m^{-3}), $\theta(h_p(z_i))$ is the moisture content corresponding to the pressure head h_p at depth z_i (m^3m^{-3}), and $\theta_{\text{residual},i}$ is the residual moisture content in the ith discretisation interval (m^3m^{-3}). The effective porosity can be guessed for instance by μ_s or by the fraction of pores in the soil profile up to the permanently reduced zone, that is $\theta_{\text{sat.},i} z_g^{-1}$.

5.4 Guessing ARMAX parameters from physical information

The ARMAX parameter a_1 (Eq. (3)) is guessed from physical information in the following way:

$$\tilde{a}_1 = \mathrm{e}^{-\frac{1}{\tilde{\varphi}}\left\{\frac{1}{\tilde{\gamma}_{\mathrm{tot}}}\right\}}, \tag{21}$$

where the total drainage resistance γ_{tot} is calculated from physical information using Eqs. (18) and (19).

The ARMAX parameter b_0 (Eq. (3)) is guessed from physical information by

$$\tilde{b}_0 = \frac{1-\tilde{a}_1}{\frac{1}{\tilde{\gamma}_{\mathrm{tot.}}}}. \tag{22}$$

The ARMAX parameter μ (Eq. (3)) is guessed from physical information as follows:

$$\tilde{\mu} = \frac{\left\{\tilde{q}_{\mathrm{b}} + \frac{H_1}{\tilde{\gamma}_1} + \frac{H_2}{\tilde{\gamma}_2} + \frac{H_3}{\tilde{\gamma}_3} + \frac{H_4}{\tilde{\gamma}_4}\right\}}{\frac{1}{\tilde{\gamma}_{\mathrm{tot.}}}} \tag{23}$$

6 Results

6.1 Parameter values guessed from physical information

6.1.1 Regional groundwater flux

Table 13 lists the guessed values of q_b based on Eq. (17) as well as the radius for which the maximum absolute value of regional groundwater flow is found. The values of $\tilde{q}_b$ are rather large, say -38 mm day^{-1} to 130 mm day^{-1}. In general the regional groundwater flux is assumed to range from -2 mm day^{-1} to 2 mm day^{-1}. The first possible reason for the relatively large guessed values is that the saturated hydraulic conductivity of the subsoil is overestimated by the horizontal hydraulic conductivities which were derived from Bierkens (1994). Another possible reason is that the gradients of the water table are overestimated by the gradients of the groundsurface. In order to obtain more realistic values for the regional groundwater flux the guessed values are scaled in a way that the maximum infiltration flux is equal to 200 mm year^{-1}.

6.1.2 Drainage resistance

Tables 14 to 17 list the guessed values of γ for four drainage systems separately as well as for the total drainage resistance. The values in Tables 14 and 15 are based on a radius of 600 m. The guessed the drainage resistances have relatively large values: the guessed total drainage resistance ranges from 92 days to 17288 days. Some large values are due to an overestimated distance between drainage devices, because of omissions in the digital topographical maps used. Furthermore, drain pipes were assumed to be absent. Another reason for the large guessed drainage resistances may be that a circle with 600 m radius does not represent the scale at which the drainage fluxes influence the water table. This scale depends on the drainage resistance itself and therefore the drainage resistance should be calculated iteratively for a large number of circles with varying radius. The values in Tables 16 and 17 are based on a radius of 400 m. In general these values are smaller than those based on a radius of 600 m only.

6.1.3 Effective porosity

The effective porosity is guessed using the following quantities derived from soil profile descriptions and soil physical standard curves for the main soil horizons in the Netherlands (Wösten *et al.*, 1987):

1. the moisture content of a soil profile at saturation, $\theta_{\text{sat.}}$;

2. the moisture content if the pressure head profile is in equilibrium, θ_{v};

3. the porosity of a soil profile, $\theta_{\text{sat.}} d_{\text{r}}^{-1}$;

4. the storage coefficient if the pressure head profile is in equilibrium.

All these quantities are calculated for the soil profile up to the depth of the permanently reduced zone, d_{r}. Tables 18 and 19 list the results of the calculations by the program CAPSEV (Wesseling, 1991).

6.2 KALWAT and KALMAX

Tables 9 and 10 list the parameter estimates obtained by the program KALWAT. The estimated effective porosity $\hat{\varphi}$ is generally about 0.1 to 0.2. However, for some observation wells large values are found. For wells 27DP7603 and 50AP7608 the values of $\hat{\varphi}$ are 0.789 and 0.495, respectively. A possible explanation is that both observation wells are situated in peaty soils. For wells 27DL0031 and 33BL0003 the effective porosity is estimated at 0.821 and 0.433, respectively. Here peaty layers are absent in the soil profile. Both observation wells are situated close to the ice-pushed hills of the Veluwe region. In these two cases the relatively large values of $\hat{\varphi}$ may be explained from a strong time-varying regional groundwater flux which damps the fluctuation of the water table depth, and for which the model does not account for. The effect of the regional hydrology may be compensated by large estimates of the effective porosity.

The ARMAX parameter estimates by the program KALMAX are given in Tables 11 and 12. Figures 3 to 6 show that the estimates of a_1, b_0, μ and σ_ϵ obtained by KALMAX are close to those obtained by KALWAT.

6.3 Regression analysis: physical parameters

In this Section the relationships between the parameters $\hat{q}_{\text{b}}$, $\hat{\gamma}$, $\hat{\varphi}$, which were estimated by KALWAT, and physical information will be reported. The results for wells 21FL0016, 34BL0012, and 50AP7608 were excluded from the analysis because for these wells extremely high drainage resistances were calculated from the auxiliary information, possibly due to errors in the data.

The estimated regional flux $\hat{q}_b$ appeared to be unrelated to the guessed regional flux $\tilde{q}_b$:

$$\begin{array}{rcccccl} \hat{q}_b & = & 0.116 & + & 4.67\tilde{q}_b & + & \varepsilon, \quad \hat{\sigma}_\varepsilon = 1.950 \\ & & (0.282) & & (5.90) & & \end{array}$$

(standard errors in brackets), where the residual variance exceeds the variance of $\hat{q}_b$. A possible reason for the absence of a relationship may be that the gradients in the water table are not satisfactory approximated by the gradients in the groundsurface (Eq. 17). Another reason may be that the hydraulic conductivity of the subsoil is not satisfactory described by the values given in Table 13. It is interesting to analyze whether $\hat{q}_b$ or $\tilde{q}_b$ is more representative for the geohydrologic situation at the well location. For this purpose $\hat{q}_b$ and $\tilde{q}_b$ are compared with the soil profile descriptions in Annex 4. The presence of an E-horizon and a B-horizon as a result of podzolization indicates a downward (negative) flux, whereas the presence of a gley horizon indicates an upward (positive) flux. $\hat{q}_b$ and $\tilde{q}_b$ resemble with the soil profile characteristics at 63% and 59% of the well locations, respectively. In some cases, however, it may be expected that gley horizons are "fossil", i.e. they do not represent the actual hydrological situation. Then a gley horizon goes with a negative regional groundwater flux. If these situations are excluded from the analysis, then $\hat{q}_b$ and $\tilde{q}_b$ resemble with the soil profile characteristics both at 73% of the well locations, In summary, $\hat{q}_b$ indicates the direction of the regional groundwater flux slightly better than $\tilde{q}_b$.

The estimated effective porosity $\hat{\varphi}$ is only weakly related to the guessed effective porosity $\tilde{\varphi}$:

$$\begin{array}{rcccccl} \hat{\varphi}' & = & -0.930 & + & 1.203\tilde{\varphi}' & + & \varepsilon, \quad \hat{\sigma}_\varepsilon = 0.6544 \\ & & (0.152) & & (0.321) & & \end{array}$$

with $R^2_{\text{adj.}} = 21.7\%$, and with $\hat{\varphi}'$ and $\tilde{\varphi}'$ being the logistically transformed $\hat{\varphi}$ and $\tilde{\varphi}$, respectively, in order to obtain response between 0 and 1 and a linear relationship. The guessed effective porosity $\tilde{\varphi}$ is based on the fraction of pores which is given in Tables 18 and 19 by $\theta_{\text{sat.}} d_r^{-1}$, because this guess showed the best relationship in terms of $R^2_{\text{adj.}}$ with the estimated effective porosity $\hat{\varphi}$.

A reason for the weak relationship between $\hat{\varphi}'$ and $\tilde{\varphi}'$ may be that $\tilde{\varphi}'$ does not account for storage in puddles and bypass flow. Furthermore, the soil physical standard curves that are used in the calculation of $\tilde{\varphi}'$ may not represent the soil physical conditions at the well site.

The estimated drainage resistance $\hat{\gamma}$ is linearly related to the guessed drainage resistance $\tilde{\gamma}$ on the basis of a 600 m radius in the following way:

$$\begin{array}{rcccccl} \hat{\gamma} & = & 85.7 & + & 0.6447\tilde{\gamma} & + & \varepsilon, \quad \hat{\sigma}_\varepsilon = 162.57 \\ & & (30.9) & & (0.0548) & & \end{array}$$

with $R^2_{\text{adj.}} = 74.5\%$. Note that the data of four wells with extremely high guessed drainage resistances were discarded before the above model was fitted. The above relationship indicates that the guessed drainage resistances are relatively high as compared with the estimated drainage resistances.

As Eq. (10) indicates, the ARMAX parameters a_1 and b_0 depend on the multiplication $\varphi\gamma$. The estimated term $\hat{\varphi}\hat{\gamma}$ is related to the guessed term $\tilde{\varphi}\tilde{\gamma}$ on the basis of a 600 m radius in the following way:

$$\begin{array}{rcccc} \hat{\varphi}\hat{\gamma} & = & 5.85 & + & 0.4484\tilde{\varphi}\tilde{\gamma} \\ & & (9.13) & & (0.0429) \end{array} + \varepsilon, \quad \hat{\sigma}_\varepsilon = 46.71$$

with $R^2_{\text{adj.}} = 69.7\%$.

If the drainage resistance $\tilde{\gamma}$ is guessed on the basis of a radius of both 600 m and 400 m (Eq. (19)) the relationship with $\hat{\gamma}$ becomes

$$\begin{array}{rcccc} \hat{\gamma} & = & 119.1 & + & 0.926\tilde{\gamma} \\ & & (41.4) & & (0.123) \end{array} + \varepsilon, \quad \hat{\sigma}_\varepsilon = 217.80$$

with $R^2_{\text{adj.}} = 54.2\%$. Now the relationship between $\hat{\varphi}\hat{\gamma}$ and $\tilde{\varphi}\tilde{\gamma}$ is

$$\begin{array}{rcccc} \hat{\varphi}\hat{\gamma} & = & 6.64 & + & 0.7376\tilde{\varphi}\tilde{\gamma} \\ & & (9.92) & & (0.0785) \end{array} + \varepsilon, \quad \hat{\sigma}_\varepsilon = 50.25$$

with $R^2_{\text{adj.}} = 65.0\%$.

6.4 Regression analysis: ARMAX parameters

In this section the relationships between the estimated ARMAX parameters $\hat{a}_1$, $\hat{b}_0$, and $\hat{\mu}$ and their values as guessed from physical information are given. Again, the results for wells 21FL0016, 34BL0012, and 50AP7608 were excluded from the analysis because for these wells extremely high drainage resistances were calculated from the auxiliary information.

For the parameter a_1 the following relation is found if the drainage resistance is guessed on the basis of a radius of 600 m:

$$\begin{array}{rcccc} \hat{a}'_1 & = & 1.072 & + & 0.593\tilde{a}'_1 \\ & & (0.534) & & (0.117) \end{array} + \varepsilon, \quad \hat{\sigma}_\varepsilon = 0.817$$

with $R^2_{\text{adj.}} = 34.6\%$, and $\hat{a}'_1$ and $\tilde{a}'_1$ being the logistically transformed $\hat{a}_1$ and $\tilde{a}_1$, in order to obtain a response in between 0 and 1 and a linear relationship. If the drainage resistance is guessed on the basis of a radius of both 600 m and 400 m this relation becomes

$$\begin{array}{rcccc} \hat{a}'_1 & = & 1.322 & + & 0.600\tilde{a}'_1 \\ & & (0.507) & & (0.123) \end{array} + \varepsilon, \quad \hat{\sigma}_\varepsilon = 0.8295$$

with $R^2_{\text{adj.}} = 32.6\%$.

The parameter estimates for b_0 appear to be unrelated with guessed values if the drainage resistance is guessed on the basis of a radius of 600 m:

$$\begin{array}{rcccccl} \hat{b}'_0 & = & 0.418 & + & 1.348\tilde{b}'_0 & + & \varepsilon, \quad \hat{\sigma}_\varepsilon = 0.4433 \\ & & (0.440) & & (0.485) & & \end{array}$$

with $R^2_{\text{adj.}} = 12.5\%$, and with $\hat{b}'_0$ and $\tilde{b}'_0$ being the logarithmically transformed $\hat{b}_0$ and $\tilde{b}_0$, respectively, in order to obtain a positive response and a linear relationship. If the drainage resistance is guessed on the basis of a radius of both 600 m and 400 m this relation becomes

$$\begin{array}{rcccccl} \hat{b}'_0 & = & 0.494 & + & 1.267\tilde{b}'_0 & + & \varepsilon, \quad \hat{\sigma}_\varepsilon = 0.4472 \\ & & (0.439) & & (0.486) & & \end{array}$$

with $R^2_{\text{adj.}} = 11.0\%$.

For the parameter μ the following relation is found if the drainage resistance is guessed on the basis of a radius of 600 m:

$$\begin{array}{rcccccl} \hat{\mu} & = & -107.2 & + & 0.263\tilde{\mu} & + & \varepsilon, \quad \hat{\sigma}_\varepsilon = 62.27 \\ & & (18.8) & & (0.150) & & \end{array}$$

with $R^2_{\text{adj.}} = 4.2\%$. If the drainage resistance is guessed on the basis of a radius of both 600 m and 400 m this relation becomes

$$\begin{array}{rcccccl} \hat{\mu} & = & -103.0 & + & 0.301\tilde{\mu} & + & \varepsilon, \quad \hat{\sigma}_\varepsilon = 61.92 \\ & & (19.5) & & (0.158) & & \end{array}$$

with $R^2_{\text{adj.}} = 5.3\%$.

The guessed parameter $\tilde{b}_0$ can be assumed to be a guess for σ_ϵ, see Eq. (13). If the drainage resistance is guessed on the basis of a radius of 600 m the following relationship is found:

$$\begin{array}{rcccccl} \hat{\sigma}'_\epsilon & = & 1.414 & + & 1.237\tilde{b}'_0 & + & \varepsilon, \quad \hat{\sigma}_\varepsilon = 0.5358 \\ & & (0.532) & & (0.586) & & \end{array}$$

with $R^2_{\text{adj.}} = 6.8\%$, and $\hat{\sigma}'_\epsilon$ and $\tilde{b}'_0$ are the logarithmically transformed $\hat{\sigma}_\epsilon$ and $\tilde{b}_0$, in order to obtain a positive response and a linear relationship. If the drainage resistance is guessed on the basis of both a radius of 400 m and 600 m the relationship is

$$\begin{array}{rcccccl} \hat{\sigma}'_\epsilon & = & 1.477 & + & 1.174\tilde{b}'_0 & + & \varepsilon, \quad \hat{\sigma}_\varepsilon = 0.5381 \\ & & (0.528) & & (0.585) & & \end{array}$$

with $R^2_{\text{adj.}} = 6.0\%$.

6.5 Prediction of water table depths using guessed ARMAX parameters

In this section the prediction performance of ARMAX models with parameters that are guessed from physical information will be evaluated. For this purpose we used daily precipitation excess series and time series of water table depths, collected at the locations and during the periods listed in Tables 3 to 6. Note that these data are not used in guessing the ARMAX parameters. The ARMAX parameters are guessed from physical information by Eqs. (21) to (23), with drainage resistances based on a neighbourhood radius of 600 m. The prediction performance is evaluated by the following criteria:

- the mean prediction error as a measure of systematic error:

$$ME = \frac{1}{n}\sum_{i=1}^{n} e_i$$

  where n is the number of observations and $e_i = h_i - \tilde{h}_i$. This criterion indicates systematic prediction errors.

- the standard deviation of the prediction errors as a measure of precision:

$$SDE = \sqrt{\frac{1}{n}\sum_{i=1}^{n}(e_i - \bar{e})^2}$$

- the root mean squared error as a measure of accuracy:

$$RMSE = \sqrt{\frac{1}{n}\sum_{i=1}^{n} e_i^2}$$

Tables 22 and 23 list the prediction results. The ME values indicate that large systematic errors occur. The SDE values are relatively small as compared with the ME values. It is interesting to compare the SDE values in Tables 22 and 23 with the standard deviations estimated for the innovations of the calibrated models ($\hat{\sigma}_\varepsilon$) in Tables 11 and 12. Interestingly, for nine observation wells the SDE values are smaller than the values of $\hat{\sigma}_\varepsilon$, as for 21 observation wells relatively small SDE values (smaller than 20 cm) are found. The accuracy of the predictions, expressed by the RMSE, can be improved mainly by reducing the systematic error, that is, by improving the guess of the parameter μ in Eq. (9). From Eq. (14) it can be seen that the parameter μ which reflects the average water table depth depends on the regional groundwater flux q_b, the drainage levels $H_1, H_2, \ldots$ and the drainage resistances $\gamma_1, \gamma_2, \ldots$. Thus, it is expected that the predictions of an ARMAX model that has been guessed from physical

information can be improved using by more accurate guesses of the regional groundwater flux and the drainage resistances, and more accurate information on the drainage levels. Another possibility is to guess the ARMAX-parameter μ directly from water table depths that are observed at a large number of sites at a time that the water table is about its mean level, or to estimate the spatial distribution of μ inversely using observed water table depths.

7 Discussion and conclusions

7.1 Introduction

The intended result of this study was a set of regression models that describe the relationship between parameters of time series models and physical interpretation from databases such as the digital soil map, the digital topographical map and digital elevation values. These regression models could be used to predict time series model parameters in space. In the previous chapter it was seen that relationships between ARMAX parameters and auxiliary information are generally absent or only weakly present. Several reasons for these weak relationships were mentioned. It was also shown in the previous chapter that the predictions with guessed ARMAX models contain large systematic errors, but that they are relatively precise, i.e., the standard deviations of the prediction errors are relatively small.

In the present chapter the possible reasons for the weak relationships between estimated and guessed parameters will be summarized and discussed. Possible improvements are suggested. Finally conclusions will be drawn on the usefulness of auxiliary physical information in the interpolation of time series models.

7.2 Discussion of results

Reasons for the weak relationships between ARMAX parameters and physical information can be divided into three categories:

1. Assumptions underlying the time series model;
2. Assumptions underlying the models that describe the relationship between ARMAX parameters and physical information, and
3. The quality of the data used.

Ad 1. The ARMAX model assumes a linear relationship between precipitation excess and water table depth. However, Knotters and Van Walsum (1997) and Knotters and De Gooijer (1999) demonstrated that several forms of nonlinearity can exist. Ignoring the nonlinear behaviour may weaken the relationship between the time series model parameters and the physical information. For instance threshold nonlinearities can exist because of the presence of soil layers with clearly distinctive soil physical properties. Then the effective porosity as

well as the change of the moisture volume in the unsaturated zone depend on the water table depth and therefore vary with time. In the presence of more than one drainage device both the drainage resistance and regional groundwater flux may also depend on the water table depth.

Ad 2. Below the most important assumptions in the relations between ARMAX parameters and physical auxiliary information will be addressed:

- An important assumption in the model that describes the relationship between the regional groundwater flux and groundsurface elevation is that the gradient of the water table can be approximated by the gradient of the soil surface. However, that the water table is usually smoother than the groundsurface. Therefore, it may be expected that Eq. (17) result in absolute guessed values that are too large;
- The effective porosity is guessed only from soil profile descriptions and soil physical standard curves. The effect of bypass flow through macropores, cracks or preferential flow paths is ignored which will result in guessed values that are too large. Besides this, storage in puddles is ignored which will result in guessed values that are to small;
- The drainage resistance is calculated for a neighbourhood circle with a fixed radius of 600 m or iteratively for neighbourhood circles with a radius of 400 m and 600 m. Therefore, it is implicitly assumed that areas with a radius of 400 m or 600 m represent the scale of drainage flow for all 51 observation wells. It would be better, however, to calculate the drainage resistance for a wide range of values for the radius using Eq. (19).

Ad 3. The auxiliary physical information may contain errors, may be incomplete or may not represent the physical conditions at the well site otherwise. Weak representativeness of the physical information will result in weak relationships between physical information and time series model parameters. The representativeness of the following physical information is uncertain:

- The elevation data are not up to date, because they were collected roughly in between 1950 and 1970. Moreover, they were collected in an unequally spaced pattern and therefore they need to be declustered before calculating areal means, see Section 5.1;
- The hydraulic conductivity of the subsoil. The hydraulic conductivity was guessed from the soil profile descriptions, generally up to a depth of 2 m, and a table given by Bierkens (1994). The hydraulic conductivity guessed in this way was used in guessing the regional groundwater flux and the drainage resistance;

- The soil physical standard curves (Wösten *et al.*, 1987) may not represent the conditions at the well sites. This will influence the guessed effective porosity;
- Information on entrance resistances is not available. This influences the guessed drainage resistances;
- Information on the wetted perimeters of the drainage devices as well as the drainage levels and bottom depths is generally contaminated with measurement errors. This will influence the guessed drainage resistances;
- Information on the presence of drain pipes is not available at digital topographical maps. Ignoring the presence of drain pipes will result in guessed drainage resistances that are too large.

7.3 Possible improvements

From the above section it is clear that the relationships between ARMAX parameters and auxiliary information on elevation, topography and soil physical properties can be improved in several ways. A first improvement may be to describe the relationship between precipitation excess and water table depth by a nonlinear model, for instance a TARSO model (Knotters and De Gooijer, 1999). It may be expected that the parameters of the TARSO model are more closely related to physical information than parameters of a linear time series model, especially if distinct threshold nonlinearities in the relationship between precipitation excess and water table depth are present. These may be the result of for instance soil physical boundaries and clearly distinctive drainage levels. In a TARSO model the relationship between precipitation excess and water table depth is divided into several regimes be so called thresholds. These regimes are conditional on the water table depth at a previous time step. The thresholds can for instance be the result of soil physical boundaries or drainage levels. An extension of the water balance to the TARSO model is given in Annex 3.

The guessed values of the regional groundwater flux indicate the direction of the flow reasonably well, as was pointed out in Section 6.3. There is no relationship with the values estimated from the ARMAX model, however. As was pointed out in Section 6.5, the predictions with guessed ARMAX models contain large systematic errors, which means that the guesses of the parameter μ (Eq. (23)) need to be improved. This implies that the regional groundwater flow needs to be guessed more accurately. The guessed values of the regional groundwater flux can be improved with respect to the approximation of the gradients in the water table. In this study the gradients in the water table were approximated by the gradients in the groundsurface. It may be expected,

however, that more realistic approximations can be obtained from the results of a stationary model for regional groundwater flow and from contour line maps of the phreatic groundwater surface obtained with such a model. Besides better approximation of the gradients, more accurate data on the saturated hydraulic conductivity of the subsoil are needed. Furthermore, it may be necessary to divide the regional groundwater flux into several regimes depending on the water table depth. In such situations it may be expected that the guessed values of the regional groundwater flux are better related to the parameters of a TARSO model than to the parameters of a linear model such as the ARMAX model.

The guessed values of the effective porosity can be improved by including the storage in puddles and the effect of bypass flow through macropores, soil cracks and preferential flow paths into the calculations. Therefore, more information on these processes need to be collected. Besides this, the effective porosity may be divided into several regimes as a result of the presence of distinct soil physical boundaries. In such cases it may be expected that the guessed values for separate regimes correspond better with the parameters of a TARSO model than with the parameters of a linear time series model.

The guessed values of the drainage resistance can be improved if they are calculated from a wide range of values for the radius of the neighbourhood (Eq. (19)). Furthermore, more accurate data on the saturated conductivities in the subsoil as well as more accurate observations of bottom depths are needed. Finally, better relationships between physical information and time series model parameters can be obtained if the drainage resistance is calculated for separate regimes depending on the water table depth. Next these values can be used to guess the parameters of a TARSO model with corresponding regimes.

An important improvement in the quality of the elevation data can be expected in near future, if accurate elevation data collected by laser scanning are digitally available in a 5×5 m grid. This may improve the guessed regional groundwater fluxes. Accurate information on the hydraulic conductivity of the subsoil, say in between 1 m and 10 m depth, is extremely important in the calculation drainage resistances and regional groundwater fluxes. However, this information is not widely available yet. Further improvements in the calculation of drainage resistance can be made if more information on entrance resistances were available. This study also indicated a need for more accurate and more detailed information on the presence and dimensions of drainage devices. Improvements can be made in the calculation of effective porosities if more soil physical standard curves for distinct geologic regions and geologic deposits were available.

The results of the predictions with guessed ARMAX models (Section 6.5)

indicated that the accuracy of the predictions can be increased drastically if the parameter μ (Eqs. (9) and (23)) can be guessed more accurately. An improved guess of μ can be obtained from observed water table depths which are measured at a large number of sites at one strategic moment at which the water table is about its mean level. This moment can be chosen on the basis of time series on water table depth that are collected in the study area. In the soil mapping in the Netherlands it is practice to measure the water table depth at a large number of locations at the moment that the water table reaches the Mean Highest Watertable (MHW) and the Mean Lowest Watertable (MLW). The average of these two levels may also be a useful guess of μ. Besides this, it is common practice in soil mapping to collect time series of one season length at a relatively large number of locations. These time series can be used to estimate the random errors and systematic errors of predictions with guessed ARMAX parameters. Next the random errors that occurred at the moments that the water table depth was measured at a large number of locations can be interpolated spatially to these locations, in order to improve the guesses of μ. Finally, the so obtained guesses of μ can be interpolated spatially to unvisited locations.

The above procedure is direct, and is based on what is common practice in soil mapping. Further study is needed on inverse estimation of the spatial structure of time series model parameters within a Kalman-filter approach, using observations on water table depth.

7.4 Conclusions

This study shows that at present the parameters of linear time series models can not be predicted accurately in space on the basis of physical relationships. Some improvements in the relationship between time series model parameters and physical information may be possible with regard to the time series modelling as well as to the models that describe the relationship between time series model parameters and physical information. These improvements in the modelling will not take away the uncertainties about the data, however. In particular the quality of data on the hydraulic conductivity of the subsoil, entrance resistances, dimensions of drainage devices, and soil physical properties is extremely important in guessing ARMAX model parameters. Furthermore, a good approximation of the gradients in the phreatic surface is necessary. This study showed that an approximation on the basis of groundsurface elevation data is inappropriate.

For economic reasons it is expected that the quality of physical information can only be improved to some extent. Hence it can be concluded that besides physical auxiliary information, observations on the water table depth itself are

necessary in the spatial prediction of time series of water table depths. A possible method is to estimate the spatial distribution of time series parameters inversely from additional observations on the water table depth (i.e. calibration). Therefore, research is needed on optimal sampling strategies for the water table depth in both space and time, within the practical and economic limits of a regional survey.

Water table depths predicted by ARMAX models that are guessed from physical information show large systematic errors but relatively small random errors. Therefore, the predictions can be improved significantly if the ARMAX-parameter μ that reflects the mean water table depth is guessed more accurately. Again, additional observations on the water table depth and inverse estimation of the spatial distribution of the ARMAX-parameters can be useful to reduce the prediction errors, besides more accurate physical information.

References

Bierkens, M.F.P., 1994. *Complex confining layers: a stochastic analysis of hydraulic properties at various scales*, Utrecht, thesis, 1994.

Bierkens, M.F.P., 1998. modelling water table fluctuations by means of a stochastic differential equation. *Water Resources Research* **34**: 2485-2499.

Bierkens, M.F.P., M. Knotters and F.C. Van Geer, submitted to Water Resources Research. Calibration of transfer function-noise models to sparsely or irregularly observed time series.

Bierkens, M.F.P. and D.J.J. Walvoort, 1998. Simple stochastic models for fluctuations of the water table depth. Part 2: A combined soil-groundwater model with stochastic input (in Dutch). *Stromingen* **4**: 5-20.

Box, G.E.P. and G.M. Jenkins, 1976. Time series analysis, forecasting and control. Revised Edition. Holden-Day, San Francisco.

De Bruin, H.A.R., 1987. From Penman to Makkink. In: J.C. Hooghart (editor), *Evaporation and Weather.* CHO-TNO Mededeling 39, Den Haag.

Ernst, L.F., 1956. Calculation of the steady flow of groundwater in vertical cross-sections. *Netherlands Journal of Agricultural Science* **4**: 126-131.

ESRI, 1996. *ArcView GIS. The Geographic Information System for Everyone.* Environmental Systems Research Institute, Redlands.

Finke, P.A., W.J.M. de Groot, M.J.D. Hack-ten Broeke, Y. van Randen, J.H. Oude Voshaar and F. de Vries, 1998. Linking digital soil maps and databases to simulation models: functional soil map generalization in The Netherlands. In: Heineke *et al.* (eds.) Land-Information systems. Developments for planning the sustainable use of land resources. European Soil Bureau Research Report 4, EUR 17729 EN, (1998), 546 pp. Office for Official Publications of the European Communities, Luxembourg.

Gehrels, J.C., F.C. van Geer and J.J. de Vries, 1994. Decomposition of groundwater level fluctuations using transfer modelling in an area with shallow to deep unsaturated zones. *Journal of Hydrology* **157**: 105-138.

Hipel, K.W. and A.I. McLeod, 1994. *Time series modelling of water resources and environmental systems.* Elsevier, Amsterdam.

Knotters, M. and J.G. De Gooijer, 1999. TARSO modeling of water table depths, Water Resources Research (in press).

Knotters, M. and P.E.V. Van Walsum, 1997. Estimating fluctuation quanti-

ties from time series of water-table depths using models with a stochastic component, *Journal of Hydrology* **197**: 25-46.

Stolp, J., M. Knotters and G. Pleijter, 1994. *Geostatistical interpolation of the mean lowest water table using elevation data in a part of the rural development area Aardenburg* (in Dutch). Wageningen, DLO Winand Staring Centre. Rapport 344.

Tankersley, C.D., W.D. Graham and K. Hatfield, 1993. Comparison of univariate and transfer function models of groundwater fluctuations. *Water Resources Research* **29**: 3517-3533.

Tankersley, C.D. and W.D. Graham, 1994. Development of an optimal control system for maintaining minimum groundwater levels. *Water Resources Research* **30**: 3171-3181.

Ten Cate, J.A.M., A.F. van Holst, H. Kleijer and J. Stolp, 1995. *Manual Soil Survey. Guidelines and Instructions. Part A: Soil* (in Dutch). Wageningen, DLO Winand Staring Centre. Technical Document 19A.

Te Riele, W.J.M. and D.J. Brus, 1992. *The use of physical-geographical preliminary information in the spatial prediction of water table depths and fluctuation characteristics (MHW and MLW)* (in Dutch). Wageningen, DLO Winand Staring Centre. Rapport 209.

Te Riele, W.J.M., E.P. Querner, M. Knotters and A.B. Pomper, 1995. *Geostatistical interpolation of water table depths using physical-geographical information and the results of a model for regional groundwater flow* (in Dutch). Wageningen, DLO Winand Staring Centre. Rapport 414.

Van Bracht, M.J., 1989. OLGA (On Line Groundwater Archive). An information system for groundwater data in the Netherlands. TNO Institute of Applied Geoscience, Report PN 89-14-A, TNO-GG, Delft, 10 pp.

Van der Gaast, J.W.J. and P.J.T. Van Bakel, 1997. *Differentiating drainage devices for pesticide policy in the Netherlands* (in Dutch). Wageningen, DLO Winand Staring Centre. Rapport 526.

Van Geer, F.C. and A.F. Zuur, 1997. An extension of Box-Jenkins transfer/noise models for spatial interpolation of groundwater head series. *Journal of Hydrology* **192**: 65-80.

Van Heesen, H.C., 1970. Presentation of the seasonal fluctuation of the water-table on soil maps. Geoderma **4**: 257-278.

Werkgroep Herziening Cultuurtechnisch Vademecum, 1988. *Cultuurtechnisch*

vademecum (in Dutch). Utrecht, Cultuurtechnische Vereniging.

Wesseling, J.G., 1991. *CAPSEV: Steady state moisture flow theory. Program description. User manual.* Wageningen, DLO Winand Staring Centre. Report 37.

Wösten, J.H.M., M.H. Bannink and J. Beuving, 1987. *Water retention and hydraulic conductivity characteristics of topsoils and subsoils in the Netherlands: the Staring series* (in Dutch). Wageningen, Institute for Land and Water Management Research (ICW). Rapport 18.

Annex 1 Tables

Table 1: Selection scheme of observation wells. Bold face: groups from which an observation well has been selected.

			Region		
Soil type	Fluctuation class	Landuse	North	Middle	South
1	1	1	7	**42**	6
		2	3	**26**	6
	2	1	8	**39**	3
		2	0	1	1
	3	1	**13**	**17**	**10**
		2	4	4	1
	4	1	**21**	**46**	**18**
		2	5	**12**	1
	5	1	3	6	2
		2	0	3	2
2	1	1	2	**21**	8
		2	0	**14**	**15**
	2	1	**14**	**22**	1
		2	0	0	0
	3	1	**28**	**37**	**18**
		2	1	**20**	**21**
	4	1	**82**	**111**	**27**
		2	**24**	**35**	**21**
	5	1	**27**	**47**	**13**
		2	**43**	**41**	**62**
3	1	1	0	**15**	7
		2	0	7	9
	2	1	**8**	**5**	1
		2	0	1	1
	3	1	0	3	**9**
		2	0	1	6
	4	1	4	9	5
		2	0	2	6
	5	1	1	6	5
		2	0	8	**19**

Table 2: Selection scheme of observation wells (continued).

Soil type	Fluctuation class	Landuse	Region		
			North	Middle	South
4	1	1	0	0	0
		2	0	0	0
	2	1	0	0	3
		2	0	0	0
	3	1	0	1	**11**
		2	0	0	0
	4	1	4	**12**	**14**
		2	0	4	2
	5	1	**7**	**48**	**13**
		2	2	**10**	1
5	1	1	**39**	**21**	**11**
		2	**7**	9	**17**
	2	1	**27**	**21**	0
		2	1	0	0
	3	1	**27**	0	0
		2	**9**	4	0
	4	1	8	**11**	0
		2	2	0	0

Table 3: Locations of observation wells and meteorological stations.

Observation well	Municipality	Province	X-coor.	Y-coor.	Precipitation station	X-coor.	Y-coor.	Evapo-transpiration station	X-coor.	Y-coor.
12EL0026	Anloo	Drenthe	246985	564849	Eelde	235030	571460	Eelde	235030	571460
12FL0033	Veendam	Groningen	255640	565330	Vlagtwedde	271000	561000	Eelde	235030	571460
16EL0035	Weststellingwerf	Friesland	204860	544540	Appelscha	219300	552860	Eelde	235030	571460
16FP7053	Havelte	Drenthe	212205	542620	Appelscha	219300	552860	Eelde	235030	571460
16GL0007	Havelte	Drenthe	209640	531240	Appelscha	219300	552860	Eelde	235030	571460
21FL0016	Staphorst	Overijssel	215440	515050	Dedemsvaart	226400	512040	Eelde	235030	571460
21FL0033	Staphorst	Overijssel	213410	519940	Dedemsvaart	226400	512040	Eelde	235030	571460
21HL0018	Nieuwleusen	Overijssel	213960	511260	Dedemsvaart	226400	512040	Eelde	235030	571460
21HL0019	Nieuwleusen	Overijssel	211200	510520	Dedemsvaart	226400	512040	Eelde	235030	571460
22CL0044	Ommen	Overijssel	221100	513480	Vilsteren	219460	504180	Twente VB	257980	477070
27DL0031	Epe	Gelderland	199970	483000	Apeldoorn	194800	470875	De Bilt	141000	456750
27DP7603	Epe	Gelderland	192100	483560	Apeldoorn	194800	470875	De Bilt	141000	456750
27HP0064	Diepenveen	Overijssel	211560	479000	Lettele	216060	475330	Twente VB	257980	477070
28BL0051	Hellendoorn	Overijssel	236620	496140	Almelo	242470	485430	Twente VB	257980	477070
28BL0052	Hellendoorn	Overijssel	238150	495470	Almelo	242470	485430	Twente VB	257980	477070
28DL0026	Markelo	Overijssel	234480	476120	Almelo	242470	485430	Twente VB	257980	477070
28DL0044	Wierden	Overijssel	237250	482440	Almelo	242470	485430	Twente VB	257980	477070
28DP7037	Markelo	Overijssel	234610	477230	Almelo	242470	485430	Twente VB	257980	477070
28FL0125	Denekamp	Overijssel	259530	491660	Almelo	242470	485430	Twente VB	257980	477070
28FP7015	Denekamp	Overijssel	259390	488910	Almelo	242470	485430	Twente VB	257980	477070
28FP7017	Denekamp	Overijssel	258780	488660	Almelo	242470	485430	Twente VB	257980	477070
28GL0008	Borne	Overijssel	247000	481700	Almelo	242470	485430	Twente VB	257980	477070
28GL0075	Borne	Overijssel	249450	481200	Almelo	242470	485430	Twente VB	257980	477070
28HL0079	Weerselo	Overijssel	251670	485210	Almelo	242470	485430	Twente VB	257980	477070
29CL0021	Losser	Overijssel	267000	486720	Almelo	242470	485430	Twente VB	257980	477070

Table 4: Locations of observation wells and meteorological stations (continued).

Observation well	Municipality	Province	X-coor.	Y-coor.	Precipitation station	X-coor.	Y-coor.	Evapo-transpiration station	X-coor.	Y-coor.
32GL0021	Ede	Gelderland	169720	450080	Lunteren	172375	454500	De Bilt	141000	456750
32HL0105	Ede	Gelderland	171240	451900	Lunteren	172375	454500	De Bilt	141000	456750
33BL0003	Apeldoorn	Gelderland	195579	464336	Beekbergen	193000	463700	De Bilt	141000	456750
33FL0049	Gorssel	Gelderland	212095	469420	Deventer	208400	475120	Twente VB	257980	477070
34BL0013	Markelo	Overijssel	235200	472910	Almelo	242470	485430	Twente VB	257980	477070
34BP0192	Borculo	Gelderland	232030	464295	Almelo	242470	485430	Twente VB	257980	477070
34CP7003	Lochem	Gelderland	229610	459270	Borculo	231700	456600	Twente VB	257980	477070
34CP7016	Lochem	Gelderland	229645	458560	Borculo	231700	456600	Twente VB	257980	477070
34DP0155	Neede	Gelderland	235620	461420	Borculo	231700	456600	Twente VB	257980	477070
34GL0007	Eibergen	Gelderland	245570	458910	Rekken	246630	456950	Twente VB	257980	477070
34GL0012	Eibergen	Gelderland	245032	454985	Rekken	246630	456950	Twente VB	257980	477070
41AL0059	Doetinchem	Gelderland	220830	439920	Doetinchem	216570	443100	Twente VB	257980	477070
41BP7014	Aalten	Gelderland	234990	441410	Winterswijk	245200	442500	Twente VB	257980	477070
41BP7018	Aalten	Gelderland	233610	441890	Winterswijk	245200	442500	Twente VB	257980	477070
44HP7804	Loon op Zand	Noord Brabant	131175	403045	Boxtel	151300	400300	Eindhoven VB	156700	384000
45CL0024	Udenhout	Noord Brabant	145540	401300	Boxtel	151300	400300	Eindhoven VB	156700	384000
50AP7608	Rucphen	Noord Brabant	102698	391811	Oudenbosch	95300	398800	Eindhoven VB	156700	384000
50AP7615	Rijsbergen	Noord Brabant	102890	391260	Oudenbosch	95300	398800	Eindhoven VB	156700	384000
50AP7618	Rucphen	Noord Brabant	102233	392175	Oudenbosch	95300	398800	Eindhoven VB	156700	384000
51AL0003	Boxtel	Noord Brabant	148850	399040	Boxtel	151300	400300	Eindhoven VB	156700	384000
51FL0004	Beek en Donk	Noord Brabant	175500	398385	Venray	196550	388250	Eindhoven VB	156700	384000
51GP0087	Waalre	Noord Brabant	162830	377370	Someren	176750	377710	Eindhoven VB	156700	384000
52CL0044	Deurne	Noord Brabant	181475	383543	Venray	196550	388250	Eindhoven VB	156700	384000
52DL0010	Horst	Limburg	198410	384110	Venray	196550	388250	Eindhoven VB	156700	384000
57AP7802	Hoogeloon	Noord Brabant	146396	372129	Someren	176750	377710	Eindhoven VB	156700	384000
57EL0006	Leende	Noord Brabant	164880	371480	Someren	176750	377710	Eindhoven VB	156700	384000

Table 5: Starting and ending of the calibration periods (day-month-year); numbers of observed water table depths (n).

Observation well	n	starting date	ending date
12EL0026	184	28- 7-1988	28- 3-1996
12FL0033	138	14- 1-1985	28-12-1990
16EL0035	223	14-10-1986	28- 3-1996
16FP7053	74	15- 7-1991	29- 8-1994
16GL0007	108	14- 1-1985	14-12-1989
21FL0016	264	14- 1-1985	28- 3-1996
21FL0033	256	14- 1-1985	28- 3-1996
21HL0018	223	15-12-1986	28- 3-1996
21HL0019	266	14- 1-1985	28- 3-1996
22CL0044	124	28- 6-1989	28- 3-1995
27DL0031	189	15- 1-1988	14-11-1996
27DP7603	157	28- 6-1989	14-11-1996
27HP0064	173	28- 8-1987	28- 3-1994
28BL0051	185	18- 6-1987	14- 3-1995
28BL0052	184	13- 7-1987	14- 3-1995
28DL0026	134	28-12-1987	15- 7-1993
28DL0044	228	15- 1-1985	17- 3-1995
28DP7037	48	15- 4-1993	30- 3-1995
28FL0125	244	14- 1-1985	28- 3-1995
28FP7015	126	16-10-1986	17- 2-1992
28FP7017	126	16-10-1986	17- 2-1992
28GL0008	188	11- 3-1987	14- 3-1995
28GL0075	200	15- 4-1985	30-11-1993
28HL0079	230	28- 3-1985	28- 3-1995
29CL0021	236	29- 4-1985	28- 3-1995

Table 6: Starting and ending of the calibration periods (day-month-year); numbers of observed water table depths (n).

Observation well	n	starting date	ending date
32GL0021	253	14- 1-1985	28- 3-1996
32HL0105	264	28- 1-1985	28- 5-1996
33BL0003	163	14- 9-1988	28- 6-1995
33FL0049	243	14- 1-1985	28- 3-1995
34BL0013	201	13- 6-1986	28- 3-1995
34BP0192	244	14- 1-1985	28- 3-1995
34CP7003	201	29- 1-1985	27- 3-1997
34CP7016	93	1- 3-1993	27- 3-1997
34DP0155	287	14- 1-1985	26- 3-1997
34GL0007	220	14- 1-1988	26- 3-1997
34GL0012	156	29- 8-1988	28- 3-1995
41AL0059	291	14- 1-1985	26- 3-1997
41BP7014	64	14- 8-1985	30- 5-1988
41BP7018	55	14-11-1994	27- 3-1997
44HP7804	114	14- 8-1985	28-11-1990
45CL0024	216	14- 3-1985	28- 1-1994
50AP7608	81	28- 4-1991	28-10-1994
50AP7615	88	28- 4-1991	16- 1-1995
50AP7618	89	28- 4-1991	16- 1-1995
51AL0003	246	14- 1-1985	28- 3-1995
51FL0004	125	1- 3-1990	27- 4-1995
51GP0087	55	14- 1-1988	13- 4-1990
52CL0044	144	14- 3-1989	28- 2-1995
52DL0010	245	14- 1-1985	28- 4-1995
57AP7802	174	14- 4-1987	28- 4-1995
57EL0006	241	14- 1-1985	28- 3-1995

Table 7: Hydraulic conductivities used in the calculation of drainage resistances.

Observation well	number of layers	d_1	$k_{\text{hor.},1}$	$k_{\text{vert.},1}$	d_2	$k_{\text{hor.},2}$	$k_{\text{vert.},2}$	d_3	$k_{\text{hor.},3}$	$k_{\text{vert.},3}$
12EL0026	2	105	13.28571	5	55	15	15			
12FL0033	1	140	15	15						
16EL0035	1	190	15	15						
16FP7053	2	115	1.61739	0.43396	35	15	15			
16GL0007	2	140	13.625	4.94118	20	15	15			
21FL0016	2	150	15	15	30	3	1			
21FL0033	1	180	15	15						
21HL0018	1	120	15	15						
21HL0019	1	100	15	15						
22CL0044	1	160	15	15						
27DL0031	2	95	3	1	55	15	15			
27DP7603	2	60	0.3	0.25	60	50	50			
27HP0064	2	110	3	1	50	15	15			
28BL0051	2	110	1.40909	0.61111	70	3	1			
28BL0052	2	140	3	1	30	15	15			
28DL0026	1	200	15	15						
28DL0044	1	250	15	15						
28DP7037	2	25	1.5	0.625	115	15	15			
28FL0125	1	200	15	15						
28FP7015	1	180	15	15						
28FP7017	1	150	15	15						
28GL0008	2	40	3	1	140	15	15			
28GL0075	3	95	3	1	25	0.05	0.05	80	15	15
28HL0079	2	75	3	1	125	15	15			
29CL0021	1	160	15	15						

Note: d_i = thickness of ith layer (cm); $k_{\text{hor.},i}$ = horizontal hydraulic conductivity of ith layer (m d^{-1}); $k_{\text{vert.},i}$ = vertical hydraulic conductivity of ith layer (m d^{-1}).

Table 8: Hydraulic conductivities used in the calculation of drainage resistances (continued).

Observation well	number of layers	d_1	$k_{\text{hor.},1}$	$k_{\text{vert.},1}$	d_2	$k_{\text{hor.},2}$	$k_{\text{vert.},2}$	d_3	$k_{\text{hor.},3}$	$k_{\text{vert.},3}$
32GL0021	1	180	15	15						
32HL0105	2	80	3	1	60	15	15			
33BL0003	1	180	15	15						
33FL0049	3	140	15	15	20	3	1	140	15	15
34BL0013	1	260	15	15						
34BP0192	2	40	3	1	130	15	15			
34CP7003	2	120	15	15	20	3	1			
34CP7016	1	180	15	15						
34DP0155	3	65	3	1	25	0.05	0.05	90	15	15
34GL0007	1	150	15	15						
34GL0012	1	150	15	15						
41AL0059	2	180	2.01667	0.13636	40	15	15			
41BP7014	1	150	15	15						
41BP7018	1	100	15	15						
44HP7804	2	135	15	15	55	3	1			
45CL0024	2	80	3	1	60	15	15			
50AP7608	2	45	1.88889	0.69231	35	15	15			
50AP7615	2	40	12	3.33333	40	3	1			
50AP7618	2	110	5.18182	1.20438	20	15	15			
51AL0003	1	200	15	15						
51FL0004	1	170	15	15						
51GP0087	2	175	15	15	5	3	1			
52CL0044	2	180	15	15	20	3	1			
52DL0010	2	100	3	1	85	15	15			
57AP7802	2	100	10.675	2.25564	20	50	50			
57EL0006	2	180	8.33333	1.70886	100	3	1			

Note: see Table 7.

Table 9: Results of KALWAT.

Observation well	H_s	$\hat{q}_b$	$\hat{\gamma}$	$\hat{\varphi}$	$\hat{a}_1$	$\hat{b}_0$	$\hat{\mu}$	$\hat{\sigma}_\epsilon$
12EL0026	-100	-0.93590	247.26	0.13484	0.97045	7.3061	-123.14	10.527
12FLfl00	-140	-1.5997	97.892	0.16399	0.93961	5.9120	-155.66	15.244
16EL0035	-220	0.61450	293.71	0.22288	0.98484	4.4527	-201.95	8.4029
16FP7053	-96	0.38275	281.71	0.21848	0.98388	4.5401	-85.218	9.3041
16GL0007	-60	-2.5607	248.25	0.12431	0.96812	7.9152	-123.57	25.396
21FL0016	-216	0.87405	405.30	0.18656	0.98686	5.3250	-180.57	11.086
21FL0033	-301	2.5363	420.03	0.15365	0.98463	6.4580	-194.47	19.060
21HL0018	-100	-0.03162	154.59	0.11272	0.94423	8.6221	-100.49	21.791
21HL0019	-65	3.8922	39.803	0.08719	0.74964	9.9651	-49.508	43.448
22CL0044	-150	0.15385	180.22	0.35426	0.98446	2.8008	-147.23	12.313
27DL0031	-110	0.53247	66.103	0.82059	0.98173	1.2075	-106.48	13.656
27DP7603	-40	4.6439	48.996	0.78885	0.97444	1.2514	-17.261	2.5636
27HP0064	-85	-1.1671	67.916	0.12409	0.88812	7.5987	-92.926	15.040
28BL0051	-150	-2.8826	78.898	0.19222	0.93617	5.0345	-172.73	12.192
28BL0052	-130	-0.11224	85.846	0.21070	0.94622	4.6172	-130.96	10.196
28DL0026	-225	0.65054	330.01	0.21554	0.98604	4.6071	-203.53	6.5383
28DL0044	-166	-2.9909	140.57	0.14682	0.95270	6.6486	-208.04	18.092
28DP7037	-90	6.7748	58.061	0.090611	0.82689	10.051	-50.665	14.695
28FL0125	-200	1.5220	426.18	0.17508	0.98669	5.6737	-135.13	16.713
28FP7015	-50	-1.8122	313.68	0.14613	0.97842	6.7690	-106.85	15.715
28FP7017	-140	-0.37425	297.60	0.17399	0.98087	5.6924	-151.14	13.843
28GL0008	-130	0.65604	237.45	0.17541	0.97628	5.6330	-114.42	17.849
28GL0075	-180	0.97811	303.53	0.22206	0.98527	4.4700	-150.31	15.521
28HL0079	-190	0.61324	477.43	0.21191	0.99016	4.6958	-160.72	12.651
29CL0021	-110	-0.90727	138.72	0.19626	0.96394	5.0028	-122.59	16.529

Note: H_s = drainage level (cm); $\hat{q}_b$ = regional groundwater flux (mm d^{-1}); $\hat{\gamma}$ = drainage resistance (d); $\hat{\varphi}$ = effective porosity (-); $\hat{a}_1$, $\hat{b}_0$ and $\hat{\mu}$ are ARMAX parameters; $\hat{\sigma}_\epsilon$ = standard deviation of innovations (cm).

Table 10: Results of KALWAT (continued).

Observation well	H_s	$\hat{q}_b$	$\hat{\gamma}$	$\hat{\varphi}$	$\hat{a}_1$	$\hat{b}_0$	$\hat{\mu}$	$\hat{\sigma}_\epsilon$
32GL0021	-130	0.51099	179.41	0.11532	0.95282	8.4651	-120.83	21.708
32HL0105	-87	0.66119	234.27	0.14271	0.97053	6.9036	-71.511	18.511
33BL0003	-240	1.9390	340.22	0.43296	0.99323	2.3019	-174.03	3.1279
33FL0049	-210	-0.97537	767.38	0.30299	0.99571	3.2934	-284.85	7.0330
34BL0013	-200	-0.87417	918.44	0.30292	0.99641	3.2953	-280.29	5.5413
34BP0192	-80	-2.2641	197.43	0.21171	0.97636	4.6673	-124.70	16.931
34CP7003	-150	0.76384	243.65	0.16792	0.97585	5.8832	-131.39	20.470
34CP7016	-75	-1.6211	285.60	0.17201	0.97985	5.7550	-121.30	7.9475
34DP0155	-140	3.1333	143.63	0.16671	0.95910	5.8750	-94.998	15.648
34GL0007	-100	-1.3984	200.45	0.13848	0.96462	7.0927	-128.03	15.004
34GL0012	-160	0.42774	372.21	0.16744	0.98408	5.9246	-144.08	13.916
41AL0059	-200	0.43928	222.09	0.34533	0.98705	2.8769	-190.24	6.6769
41BP7014	-50	-2.4660	155.37	0.094052	0.93386	10.277	-88.314	24.649
41BP7018	-80	-0.5999	391.75	0.17026	0.98512	5.8296	-103.50	12.214
44HP7804	-100	-1.2689	1030.1	0.27085	0.99642	3.6854	-230.70	10.972
45CL0024	-230	1.6773	587.63	0.17298	0.99021	5.7527	-131.44	13.488
50AP7608	-50	0.68587	225.53	0.49740	0.99113	2.0015	-34.531	5.7446
50AP7615	-60	2.5290	109.70	0.31267	0.97127	3.1521	-32.256	10.747
50AP7618	-60	-1.1864	218.27	0.13239	0.96599	7.4243	-85.895	15.201
51AL0003	-120	0.79116	297.15	0.16047	0.97925	6.1669	-116.49	10.969
51FL0004	-120	-0.79906	124.71	0.16351	0.95214	5.9683	-129.96	13.277
51GP0087	-140	-0.37920	1124.3	0.18674	0.99525	5.3423	-182.64	10.208
52CL0044	-180	-0.27298	1050.3	0.22381	0.99576	4.4585	-208.67	5.6472
52DL0010	-70	-2.0624	163.16	0.13177	0.95455	7.4152	-103.65	21.726
57AP7802	-130	0.63810	275.30	0.31703	0.98861	3.1363	-112.43	4.2036
57EL0006	-250	-0.39906	1720.6	0.27194	0.99787	3.6733	-318.66	5.0093

Note: see Table 9.

Table 11: Results of KALMAX.

Observation well	$\hat{a}_1$	$\hat{b}_0$	$\hat{\mu}$	$\hat{\sigma}_\epsilon$
12EL0026	0.97054	7.3042	-123.10	10.466
12FL0033	0.94878	5.2405	-155.88	14.794
16EL0035	0.97648	4.1423	-182.90	8.4511
16FP7053	0.96940	5.0404	-69.799	9.7027
16GL0007	0.96862	7.6933	-122.61	24.805
21FL0016	0.98807	5.4153	-186.34	9.1259
21FL0033	0.97044	6.6821	-174.42	16.708
21HL0018	0.94590	8.3307	-100.84	21.582
21HL0019	0.77858	8.8504	-49.617	35.546
22CL0044	0.98698	2.7200	-152.56	12.305
27DL0031	0.98262	1.0397	-105.83	13.266
27DP7603	0.97547	0.96342	-16.642	2.4998
27HP0064	0.89111	7.6256	-93.267	14.704
28BL0051	0.93542	5.2236	-173.03	12.585
28BL0052	0.94541	4.6951	-131.15	10.592
28DL0026	0.98165	4.6398	-195.54	6.385
28DL0044	0.95385	6.5655	-207.35	17.999
28DP7037	0.82377	10.293	-50.609	17.808
28FL0125	0.98365	5.5567	-124.82	17.431
28FP7015	0.98595	6.3743	-121.74	17.103
28FP7017	0.98104	5.6512	-150.67	14.080
28GL0008	0.97920	5.5773	-119.72	17.971
28GL0075	0.99014	4.8925	-171.04	13.869
28HL0079	0.98549	4.7610	-142.69	12.578
29CL0021	0.96468	4.9681	-122.68	16.148

Note: $\hat{\sigma}_\epsilon$ = standard deviation of innovations (cm).

Table 12: Results of KALMAX (continued).

Observation well	$\hat{a}_1$	$\hat{b}_0$	$\hat{\mu}$	$\hat{\sigma}_\epsilon$
32GL0021	0.93835	7.8621	-116.02	39.658
32HL0105	0.96869	6.8462	-68.420	19.014
33BL0003	0.99065	2.3075	-160.59	3.1153
33FL0049	0.99531	3.4648	-287.02	6.9497
34BL0013	0.99645	3.2796	-274.73	5.7035
34BP0192	0.97606	4.6447	-125.06	16.471
34CP7003	0.97206	5.7576	-126.15	21.482
34CP7016	0.97960	5.7795	-120.63	8.3108
34DP0155	0.95734	6.1627	-95.654	15.961
34GL0007	0.96487	7.0756	-128.89	15.082
34GL0012	0.98425	5.8119	-143.65	13.983
41AL0059	0.98784	2.9144	-191.90	6.7897
41BP7014	0.93518	10.023	-88.436	25.771
41BP7018	0.98514	5.8768	-104.23	12.529
44HP7804	0.99586	3.7528	-218.63	11.353
45CL0024	0.98185	6.0802	-114.37	9.1315
50AP7608	0.97790	2.0201	-19.065	6.4523
50AP7615	0.97043	3.2243	-31.467	10.915
50AP7618	0.96649	7.3830	-86.707	15.730
51AL0003	0.98021	6.1188	-117.50	10.989
51FL0004	0.95099	6.0256	-130.62	14.126
51GP0087	0.99259	5.7067	-155.12	11.591
52CL0044	0.99817	4.3326	-270.14	5.6244
52DL0010	0.95457	7.2332	-103.84	22.003
57AP7802	0.98748	3.1330	-109.53	4.3023
57EL0006	0.99863	3.7009	-376.25	5.0055

Note: $\hat{\sigma}_\epsilon$ = standard deviation of innovations (cm).

Table 13: Guessed values of the regional groundwater flux.

Observation well	$k_{sat.}$	$\tilde{q}_b$	$\tilde{q}_{b,\ scaled}$	radius	Observation well	$k_{sat.}$	$\tilde{q}_b$	$\tilde{q}_{b,\ scaled}$	radius
12EL0026	15	-38.432	-0.5479	300	32GL0021	15	-6.0384	-0.0861	600
12FL0033	15	15.770	0.2248	300	32HL0105	15	7.8044	0.1113	300
16EL0035	15	-36.877	-0.5258	300	33BL0003	15	34.161	0.4871	300
16FP7053	15	26.778	0.3818	1200	33FL0049	15	-21.954	-0.313	300
16GL0007	15	42.251	0.6024	900	34BL0013	15	49.912	-0.7116	300
21FL0016	3	1.8273	0.0261	300	34BP0192	15	64.384	0.9180	300
21FL0033	15	-34.717	-0.4950	300	34CP7003	3	-3.6241	-0.0517	300
21HL0018	15	-22.031	-0.3141	300	34CP7016	15	2.7083	0.0386	2700
21HL0019	15	4.3515	0.0620	300	34DP0155	15	-6.7573	-0.0963	300
22CL0044	15	13.007	0.1854	300	34GL0007	15	-13.661	-0.1948	300
27DL0031	15	-11.270	-0.1607	300	34GL0012	15	-21.243	-0.3029	300
27DP7603	50	85.429	1.218	300	41AL0059	15	-15.732	-0.2243	300
27HP0064	15	-36.670	-0.5228	300	41BP7014	15	36.173	0.5157	300
28BL0051	3	-7.1673	-0.1022	300	41BP7018	15	-10.551	-0.1504	300
28BL0052	15	-6.0902	-0.0868	300	44HP7804	3	0.53514	0.0076	3000
28DL0026	15	-30.058	-0.4285	300	45CL0024	15	-14.521	-0.2070	300
28DL0044	15	-33.733	-0.4809	300	50AP7608	15	40.655	0.5796	1200
28DP7037	15	15.653	0.2232	1800	50AP7615	3	15.785	0.2251	300
28FL0125	15	-20.970	-0.2990	600	50AP7618	15	33.405	0.4763	1500
28FP7015	15	9.1960	0.1311	3000	51AL0003	15	-9.4055	-0.1341	300
28FP7017	15	-29.908	-0.4264	300	51FL0004	15	-23.969	-0.3417	300
28GL0008	15	130.21	1.856	300	51GP0087	3	9.2069	0.1313	300
28GL0075	15	-24.474	-0.3489	300	52CL0044	3	20.313	0.2896	300
28HL0079	15	-8.0926	-0.1154	600	52DL0010	15	-5.7732	-0.0823	300
29CL0021	15	-26.673	-0.3803	300	57AP7802	50	68.068	0.9705	1500
					57EL0006	3	6.6034	0.0941	300

Note: $k_{sat.}$ = hydraulic conductivity of the subsoil; radius of the neighbourhood (m).

Table 14: Guessed values of the drainage resistance, radius = 600 m.

Observation well	$H_{s,1}$	$\tilde{\gamma}_1$	$H_{s,2}$	$\tilde{\gamma}_2$	$H_{s,3}$	$\tilde{\gamma}_3$	$H_{s,4}$	$\tilde{\gamma}_4$	$\tilde{\gamma}_{tot.}$
12EL0026	1.22	329.28	1.57	513.54	1.45	6128.2	1.45	61.1743	186.10
12FL0033	0.8	634.39	1.4	3114.7	2	1333.2	2	39.684	143.65
16EL0035	1	371.24	2.2	461.33	0.01	1.00E+07	2.2	1100.1	693.18
16FP7053	0.2	1678.7	1	15559	0.01	6.85E+08	1.16	119.69	443.71
16GL0007	0.6	2009.2	0.7	1039.7	0.01	7.58E+07	0.01	7.58E+07	2740.5
21FL0016	0.46	3209.3	0.01	6.58E+07	0.01	6.58E+07	0.01	6.58E+07	12835
21FL0033	1.11	230.06	1.21	4595.9	0.01	1.00E+07	0.01	1.00E+07	876.35
21HL0018	0.5	277.30	0.8	359.27	0.8	10704	1.3	220.62	363.12
21HL0019	0.5	711.60	0.5	231.02	0.5	294.04	0.01	1.00E+07	437.88
22CL0044	0.4	960.21	2.6	12571	0.01	1.00E+07	1.3	91.6251	332.36
27DL0031	0.8	6048.0	1.1	240.85	0.01	4.51E+08	0.01	4.51E+08	926.49
27DP7603	0.4	562.54	0.4	357.58	0.01	1.06E+07	0.01	1.06E+07	874.43
27HP0064	0.8	1631.3	0.85	24194	2.8	1376.6	2.8	175.52	565.11
28BL0051	1.5	598.20	1.5	423.07	-0.1	959.37	0.01	8120.7	769.10
28BL0052	0.5	3349.5	1.3	213.05	0.01	3.09E+08	0.01	3.09E+08	801.23
28DL0026	0.75	2297.7	1.05	564.28	1.75	435.15	0.01	1.00E+07	887.80
28DL0044	1.26	549.77	2.16	711.30	0.01	1.00E+07	2.16	44.2636	154.94
28DP7037	0.5	720.07	0.8	651.28	0.9	234.04	0.9	27.7073	92.403
28FL0125	0.73	339.41	2.23	478.85	0.01	1.00E+07	0.01	1.00E+07	794.47
28FP7015	0.14	1809.0	1.14	374.66	1.14	506.96	0.01	1.00E+07	770.04
28FP7017	0.9	641.47	1.9	511.81	0.01	1.00E+07	0.01	1.00E+07	1138.6
28GL0008	0.6	473.75	1.3	1200.3	0.01	1.06E+09	0.01	1.06E+09	1358.7
28GL0075	1.2	733.38	2.1	1098.0	2.1	346.40	0.01	4.51E+08	775.02
28HL0079	0.68	2594.8	1.98	1388.4	0.01	5.69E+08	0.01	5.69E+08	3617.8
29CL0021	1.11	659.61	1.31	2066.8	0.01	1.00E+07	1.81	56.9938	204.65

Note: $H_{s,i}$ = drainage level of the ith drainage type; $\tilde{\gamma}_i$ = drainage resistance of the ith drainage type.

Table 15: Guessed values of the drainage resistance, radius = 600 m (continued).

Observation well	$H_{s,1}$	$\tilde{\gamma}_1$	$H_{s,2}$	$\tilde{\gamma}_2$	$H_{s,3}$	$\tilde{\gamma}_3$	$H_{s,4}$	$\tilde{\gamma}_4$	$\tilde{\gamma}_{tot.}$
32GL0021	0.6	480.75	1.3	2201.2	1.3	465.86	0.01	1.00E+07	854.50
32HL0105	0.87	285.05	0.87	1651.4	0.01	5.34E+08	0.01	5.34E+08	972.35
33BL0003	2.13	1175.4	2.43	1055.7	0.01	1.00E+07	0.01	1.00E+07	2224.5
33FL0049	0.8	1.36E+05	1.1	44264	1.1	2946.8	1.1	1587.8	4003.6
34BL0013	1.44	2010.7	0.01	1.00E+07	0.01	1.00E+07	0.01	1.00E+07	8038.0
34BP0192	0.3	2685.5	0.67	785.18	0.01	1.06E+09	0	121.28	404.38
34CP7003	1.11	558.05	1.41	830.99	0.01	7.97E+07	0.01	7.97E+07	1335.4
34CP7016	0.75	297.33	1.43	910.82	0.01	1.00E+07	0.01	1.00E+07	896.59
34DP0155	0	62519	1.4	1866.6	0.01	11728	0.77	88.5312	335.22
34GL0007	0.3	654.59	1	1477.2	0.01	1822.5	1	221.87	550.93
34GL0012	0.9	288.94	1.8	1480.9	0.01	2043.4	0.01	1.00E+07	864.75
41AL0059	1.15	1334.9	1.55	974.44	2	534.41	2	99.416	291.86
41BP7014	0.3	625.49	0.5	760.98	0.01	1.00E+07	0.01	1.00E+07	1373.1
41BP7018	0.3	676.66	0.5	381.58	0.01	1.00E+07	0.01	1.00E+07	975.91
44HP7804	0.58	2078.6	0.98	5993.5	0.01	7.20E+07	0.01	7.20E+07	6173.1
45CL0024	0.58	4185.1	0.78	394.86	0.01	5.34E+08	0.01	5.34E+08	1443.3
50AP7608	0.3	5657.9	0.33	18307	0.01	1.50E+09	0.01	1.50E+09	17288
50AP7615	0.1	1514.1	0.7	823.66	0.01	2.74E+08	0.01	2.74E+08	2133.8
50AP7618	0.6	854.51	0.5	10158	0.01	2.30E+08	0.01	2.30E+08	3152.8
51AL0003	0.5	270.25	1.3	641.04	0.01	1.00E+07	1.51	72.6772	210.31
51FL0004	0.94	271.00	1.24	2796.9	0.01	1.00E+07	1.84	159.35	387.47
51GP0087	0.5	1925.2	0.7	16814	0.01	5.78E+07	0.01	5.78E+07	6909.2
52CL0044	1	3200.4	1.7	1.83E+05	1.8	1205.4	0.01	5.64E+07	3485.7
52DL0010	0.8	2637.6	0.8	12353	1.4	591.70	0.01	4.29E+08	1860.3
57AP7802	1.9	1504.9	1.6	663.46	0.01	1.28E+08	0.01	1.28E+08	1841.8
57EL0006	0.5	1959.0	0.8	5.78E+08	0.01	9.36E+07	0.01	9.36E+07	7835.7

Note: see Table 14.

Table 16: Guessed values of the drainage resistance, radius = 400 m.

Observation well	$H_{s,1}$	$\tilde{\gamma}_1$	$H_{s,2}$	$\tilde{\gamma}_2$	$H_{s,3}$	$\tilde{\gamma}_3$	$H_{s,4}$	$\tilde{\gamma}_4$	$\tilde{\gamma}_{tot.}$
12EL0026	1.22	235.75	1.57	543.59	0.01	1.00E+08	1.45	89.069	231.10
12FL0033	0.8	574.56	1.4	20961	2	670.36	2	30.787	111.85
16EL0035	1	207.22	2.2	465.00	0.01	1.00E+07	0.01	1.00E+07	573.35
16FP7053	0.2	884.00	1	7296.6	0.01	6.85E+08	1.16	80.143	290.99
16GL0007	0.6	1181.4	0.7	9542.7	0.01	7.58E+07	0.01	7.58E+07	4204.8
21FL0016	0.46	5620.9	0.01	6.58E+07	0.01	6.58E+07	0.01	6.58E+07	22478
21FL0033	1.11	153.26	1.21	3736.3	0.01	1.00E+07	0.01	1.00E+07	588.86
21HL0018	0.5	105.51	0.8	227.22	0.01	1.00E+07	1.3	109.49	173.82
21HL0019	0.5	463.95	0.5	111.75	0.5	155.45	0.01	1.00E+07	228.09
22CL0044	0.4	1272.2	2.6	1.68E+05	0.01	1.00E+07	1.3	109.80	404.05
27DL0031	0.8	3000.1	1.1	163.71	0.01	4.51E+08	0.01	4.51E+08	620.94
27DP7603	0.4	529.94	0.4	244.15	0.01	1.06E+07	0.01	1.06E+07	668.56
27HP0064	0.8	741.74	0.85	7265.0	2.8	950.21	2.8	134.86	401.87
28BL0051	1.5	414.68	1.5	414.71	-0.1	1442.8	0.01	8.20E+08	725.17
28BL0052	0.5	3810.1	1.3	159.05	0.01	3.09E+08	0.01	3.09E+08	610.72
28DL0026	0.75	3823.7	1.05	471.03	1.75	282.60	0.01	1.00E+07	675.31
28DL0044	1.26	546.42	2.16	1329.5	0.01	1.00E+07	2.16	29.970	111.27
28DP7037	0.5	1171.3	0.8	540.87	0.9	114.11	0.9	14.496	49.720
28FL0125	0.73	269.30	2.23	512.92	0.01	1.00E+07	0.01	1.00E+07	706.32
28FP7015	0.14	1926.4	1.14	335.01	1.14	306.56	0.01	1.00E+07	591.18
28FP7017	0.9	666.02	1.9	775.14	0.01	1.00E+07	0.01	1.00E+07	1432.8
28GL0008	0.6	575.79	1.3	841.39	0.01	1.06E+09	0.01	1.06E+09	1367.4
28GL0075	1.2	650.48	2.1	671.20	2.1	225.70	0.01	4.51E+08	536.35
28HL0079	0.68	578.73	1.98	3111.3	0.01	5.69E+08	0.01	5.69E+08	1951.8
29CL0021	1.11	400.87	1.31	2135.7	0.01	1.00E+07	0.01	1.00E+07	1350.0

Note: see Table 14.

Table 17: Guessed values of the drainage resistance, radius = 400 m (continued).

Observation well	$H_{s,1}$	$\tilde{\gamma}_1$	$H_{s,2}$	$\tilde{\gamma}_2$	$H_{s,3}$	$\tilde{\gamma}_3$	$H_{s,4}$	$\tilde{\gamma}_4$	$\tilde{\gamma}_{\text{tot.}}$
32GL0021	0.6	358.66	1.3	7456.2	1.3	305.58	0.01	1.00E+07	645.70
32HL0105	0.87	125.15	0.87	1295.4	0.01	5.34E+08	0.01	5.34E+08	456.51
33BL0003	2.13	950.97	2.43	786.01	0.01	1.00E+07	0.01	1.00E+07	1721.2
33FL0049	0.8	2.79E+05	1.1	9361.6	1.1	1553.5	0.01	6.97E+07	5304.2
34BL0013	1.44	2011.5	0.01	1.00E+07	0.01	1.00E+07	0.01	1.00E+07	8041.0
34BP0192	0.3	1393.6	0.67	571.63	0.01	1.06E+09	0	69.938	238.59
34CP7003	1.11	561.04	1.41	426.05	0.01	7.97E+07	0.01	7.97E+07	968.62
34CP7016	0.75	172.38	1.43	1274.1	0.01	1.00E+07	0.01	1.00E+07	607.34
34DP0155	0	2.38E+07	1.4	1388.4	0.01	6.56E+08	0.77	58.816	225.70
34GL0007	0.3	433.86	1	771.70	0.01	1.00E+07	1	129.40	353.09
34GL0012	0.9	178.50	1.8	947.20	0.01	1.00E+07	0.01	1.00E+07	600.76
41AL0059	1.15	898.38	1.55	690.67	2	315.85	2	61.212	181.29
41BP7014	0.3	230.55	0.5	468.49	0.01	1.00E+07	0.01	1.00E+07	618.04
41BP7018	0.3	311.55	0.5	264.68	0.01	1.00E+07	0.01	1.00E+07	572.40
44HP7804	0.58	1041.7	0.98	4326.7	0.01	7.20E+07	0.01	7.20E+07	3358.1
45CL0024	0.58	3730.8	0.78	129.08	0.01	5.34E+08	0.01	5.34E+08	499.05
50AP7608	0.3	2408.0	0.33	11882.2	0.01	1.50E+09	0.01	1.50E+09	8009.0
50AP7615	0.1	505.28	0.7	813.377	0.01	2.74E+08	0.01	2.74E+08	1246.7
50AP7618	0.6	370.95	0.5	2.79E+05	0.01	2.30E+08	0.01	2.30E+08	1481.8
51AL0003	0.5	118.83	1.3	732.67	0.01	1.00E+07	1.51	46.019	126.94
51FL0004	0.94	272.87	1.24	1.68E+05	0.01	1.00E+07	1.84	81.047	249.85
51GP0087	0.5	1261.8	0.7	66.027	0.01	5.78E+07	0.01	5.78E+07	250.98
52CL0044	1	1528.2	1.7	9.27E+07	1.8	683.08	0.01	5.64E+07	1888.3
52DL0010	0.8	802.97	0.8	5791.8	1.4	395.24	0.01	4.29E+08	1013.1
57AP7802	1.9	5092.9	1.6	689.77	0.01	1.28E+08	0.01	1.28E+08	2429.9
57EL0006	0.5	1475.0	0.8	1.07E+08	0.01	9.36E+07	0.01	9.36E+07	5899.7

Note: see Table 14.

Table 18: Results of CAPSEV calculations.

Observation well	θ_v	d_r	$\theta_{sat.}$	μ_s	$\theta_{sat.} d_r^{-1}$
12EL0026	40.67	156	63.33	0.1453	0.4060
12FL0033	45.47	175	70.75	0.1445	0.4043
16EL0035	45.76	207	81.41	0.1722	0.3933
16FP7053	42.86	88	48.62	0.06551	0.5525
16GL0007	35.52	152	58.42	0.1507	0.3843
21FL0016	42.45	208	78.22	0.1720	0.3761
21FL0033	43.15	205	78.95	0.1746	0.3851
21HL0018	33.92	132	50.67	0.1269	0.3839
21HL0019	20.95	66	25.16	0.06386	0.3812
22CL0044	43.14	168	66.78	0.1407	0.3975
27DL0031	45.28	126	54.53	0.07338	0.4328
27DP7603	18.60	24	18.96	0.01496	0.7900
27HP0064	40.47	144	53.62	0.09134	0.3724
28BL0051	81.17	189	106.4	0.1333	0.5628
28BL0052	47.59	148	62.34	0.09969	0.4212
28DL0026	41.43	193	74.59	0.1718	0.3865
28DL0044	46.05	234	90.67	0.1907	0.3875
28DP7037	28.74	70	32.55	0.05440	0.4650
28FL0125	39.05	146	58.23	0.1314	0.3988
28FP7015	32.94	126	48.88	0.1265	0.3879
28FP7017	39.20	176	67.88	0.1630	0.3857
28GL0008	42.06	156	62.08	0.1283	0.3979
28GL0075	60.17	191	79.23	0.09977	0.4148
28HL0079	49.47	167	68.71	0.1152	0.4114
29CL0021	37.53	149	58.37	0.1398	0.3917

Note: θ_v = moisture volume of a soil moisture profile in equilibrium with a water table depth that equals the depth to the permanently reduced zone (d_r (cm)); $\theta_{sat.}$ = saturated moisture volume up to d_r; μ_s = storage capacity of the soil profile in equilibrium, water table depth equals d_r (cm); $\theta_{sat.} d_r^{-1}$ = fraction of pores of the soil profile up to d_r.

Table 19: Results of CAPSEV calculations (continued).

Observation well	θ_v	d_r	$\theta_{sat.}$	s.c.	$\theta_{sat.} d_r^{-1}$
32GL0021	38.29	155	60.65	0.1443	0.3913
32HL0105	37.95	101	43.98	0.05969	0.4354
33BL0003	42.28	160	63.90	0.1351	0.3994
33FL0049	51.61	316	120.3	0.2173	0.3806
34BL0013	47.67	261	100.7	0.2031	0.3857
34BP0192	41.42	151	60.18	0.1242	0.3985
34CP7003	29.40	140	50.35	0.1496	0.3596
34CP7016	34.93	148	56.74	0.1474	0.3834
34DP0155	42.90	120	50.15	0.06042	0.4179
34GL0007	32.87	158	57.93	0.1586	0.3666
34GL0012	33.63	171	62.40	0.1682	0.3649
41AL0059	59.37	207	77.16	0.08595	0.3728
41BP7014	32.79	125	48.50	0.1256	0.3880
41BP7018	34.33	136	52.68	0.1350	0.3874
44HP7804	38.67	208	75.17	0.1755	0.3614
45CL0024	45.05	143	58.89	0.09680	0.4118
50AP7608	19.73	33	20.45	0.02171	0.6197
50AP7615	17.18	49	18.96	0.03638	0.3869
50AP7618	32.55	116	42.98	0.08995	0.3705
51AL0003	41.23	146	59.48	0.1250	0.4074
51FL0004	44.60	155	64.20	0.1265	0.4142
51GP0087	39.36	176	67.63	0.1606	0.3843
52CL0044	42.19	198	76.28	0.1722	0.3853
52DL0010	39.70	136	51.53	0.08701	0.3789
57AP7802	30.62	105	40.15	0.0908	0.3824
57EL0006	50.07	265	93.30	0.1631	0.3521

Note: see Table 18.

Table 20: Relationship between estimated regional groundwater flux and relative groundsurface elevation.

radius	$\hat{\beta}_0$	$\hat{\beta}_1$	$R^2_{\text{adj.}}$
300	0.1274(0.2740)	-0.0010(0.0056)	*
600	0.1150(0.2780)	-0.0015(0.0049)	*
900	0.0560(0.2871)	-0.0031(0.0041)	*
1200	0.0372(0.2919)	-0.0027(0.0033)	*
1500	-0.0654(0.2958)	-0.0043(0.0029)	2.3
1800	-0.1478(0.2996)	-0.0049(0.0026)	4.9
2100	-0.1803(0.3050)	-0.0047(0.0024)	5.3
2400	-0.2509(0.3113)	-0.0049(0.0022)	7.0
2700	-0.2959(0.3181)	-0.0048(0.0021)	7.7
3000	-0.3043(0.3239)	-0.0044(0.0020)	7.3

Note: $\hat{q}_{\text{b}} = \beta_0 + \beta_1 h_{\text{r}} + \varepsilon$, with
$\hat{q}_{\text{b}}$ =regional groundwater flux;
h_{r} =relative groundsurface elevation.

Table 21: Relationship between the constant of the ARMAX model and relative groundsurface elevation.

radius	$\hat{\beta}_0$	$\hat{\beta}_1$	$R^2_{\text{adj.}}$
300	-138.5364(9.6978)	-0.1069(0.1977)	*
600	-141.7653(9.6091)	-0.2802(0.1688)	3.4
900	-145.7535(9.7437)	-0.3146(0.1378)	7.8
1200	-147.0255(9.8915)	-0.2622(0.1116)	8.3
1500	-150.4870(9.9483)	-0.2742(0.0970)	12.3
1800	-152.9338(10.1017)	-0.2661(0.0876)	14.1
2100	-153.9592(10.3280)	-0.2444(0.0815)	13.8
2400	-156.5388(10.5378)	-0.2415(0.0760)	15.4
2700	-158.5090(10.7517)	-0.2342(0.0715)	16.3
3000	-159.2494(10.9415)	-0.2172(0.0670)	16.0

Note: $\hat{\mu} = \beta_0 + \beta_1 h_r + \varepsilon$, with
$\hat{\mu}$ =constant of the ARMAX model;
h_r =relative groundsurface elevation.

Table 22: Results of prediction with guessed ARMAX parameters.

Observation well	ME	SDE	$RMSE$	MAE
12EL0026	36.88484	27.71087	46.13441	38.68887
12FL0033	40.3344	13.52824	42.54265	40.3344
16EL0035	-12.06504	13.55763	18.14868	15.47331
16FP7053	39.51477	15.74568	42.53638	39.51477
16GL0007	-146.5867	23.16572	148.4059	146.5867
21FL0016	-299.6516	75.90086	309.1149	299.6516
21FL0033	-52.00467	19.46751	55.529	52.06157
21HL0018	-1.90463	20.0491	20.13937	16.27576
21HL0019	-5.58342	15.27091	16.25962	13.78393
22CL0044	-19.56704	24.1707	31.0981	26.22205
27DL0031	-13.10310	20.28278	24.14710	18.59498
27DP7603	-21.87072	13.99866	25.96711	22.34582
27HP0064	147.4371	59.06467	158.828	147.4371
28BL0051	-65.89499	14.1547	67.39811	65.89499
28BL0052	-14.21246	12.76365	19.10248	15.82261
28DL0026	-46.80394	13.64881	48.75345	46.87363
28DL0044	12.6237	21.35271	24.80516	18.98816
28DP7037	43.89441	13.50338	45.92451	43.89441
28FL0125	28.0572	28.11289	39.71827	34.27377
28FP7015	5.05963	24.89451	25.40347	22.19455
28FP7017	9.72773	19.99414	22.23498	18.8181
28GL0008	-107.0621	20.76802	109.0578	107.0621
28GL0075	44.12111	31.57634	54.25622	45.8936
28HL0079	-26.91462	24.02401	36.077	29.84546
29CL0021	61.47495	21.06299	64.98322	61.47495

Note: The drainage resistance is guessed on the basis of a neighbourhood with a radius of 600 m. The prediction periods are equal to the calibration periods given in Tables 5 and 6. Values in cm.

Table 23: Results of prediction with guessed ARMAX parameters.

Observation well	ME	SDE	$RMSE$	MAE
32GL0021	-24.04331	19.94566	31.23956	27.00655
32HL0105	12.79732	23.86854	27.08281	22.88904
33BL0003	1.58589	11.11687	11.22942	9.21513
33FL0049	-158.9175	30.64363	161.845	158.9175
34BL0013	-311.0078	73.33863	319.5378	311.0078
34BP0192	-115.8469	20.23414	117.6007	115.8469
34CP7003	-10.46798	18.89086	21.5973	17.95967
34CP7016	-25.92113	20.28433	32.91442	28.05635
34DP0155	-11.19906	17.44146	20.72736	17.22785
34GL0007	-44.10907	18.22693	47.72663	44.35114
34GL0012	-32.65917	25.09083	41.1846	34.26096
41AL0059	14.3913	19.28114	24.05976	20.62195
41BP7014	-85.23621	20.3435	87.6303	85.23621
41BP7018	-47.25457	28.58927	55.22989	47.25457
44HP7804	-183.665	36.67593	187.2911	183.665
45CL0024	-28.67791	25.81346	38.58442	29.93253
50AP7608	-128.0281	64.56054	143.385	128.0281
50AP7615	-24.0902	18.44046	30.3379	25.3896
50AP7618	-95.74882	25.12774	98.99111	95.74882
51AL0003	30.24664	32.11179	44.11379	38.78738
51FL0004	23.987	14.67375	28.1193	24.24862
51GP0087	-123.5875	36.43026	128.845	123.5875
52CL0044	-69.39536	20.92792	72.48237	69.39536
52DL0010	12.33081	19.47475	23.05027	17.2131
57AP7802	4.45955	13.71503	14.42185	10.16468
57EL0006	-265.7693	39.47746	268.6853	265.7693

Note: The drainage resistance is guessed on the basis of a neighbourhood with a radius of 600 m. The prediction periods are equal to the calibration periods given in Tables 5 and 6. Values in cm.

Annex 2 Figures

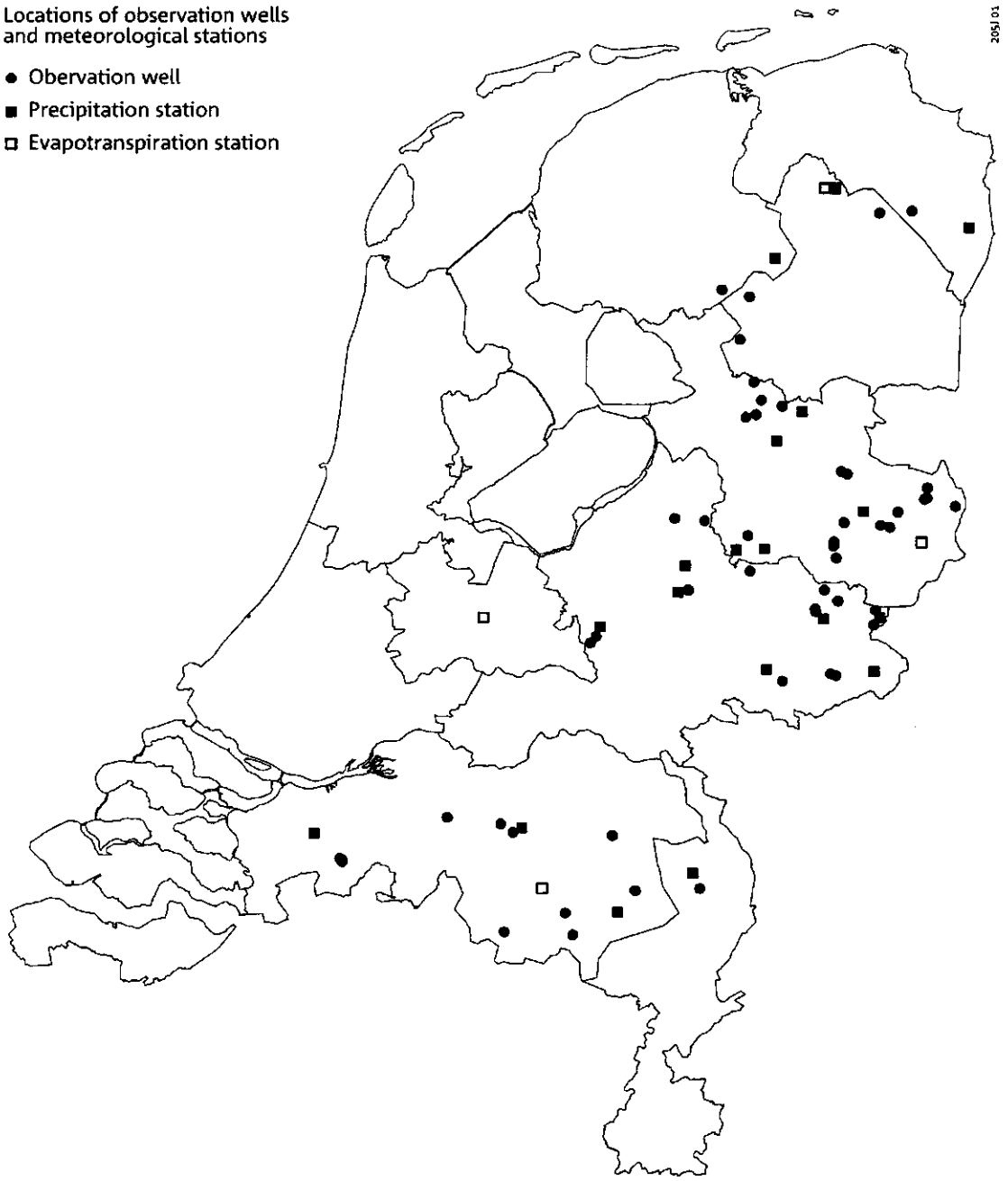

Figure 1: Locations of the observation wells and meteorological stations

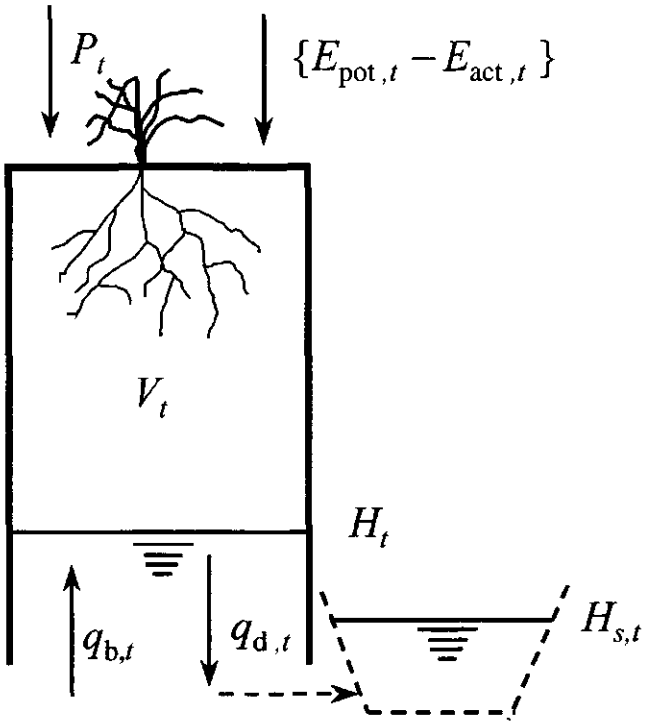

Figure 2: Soil column with water balance terms. P_t = potential precipitation excess, i.e. precipitation – potential evapotranspiration [LT^{-1}]; $E_{\text{pot},t} - E_{\text{act},t}$ = difference between potential and actual evapotranspiration [LT^{-1}]; $q_{\text{b},t}$ = regional groundwater flux [LT^{-1}]; ΔV_t = increase of water content in the unsaturated zone [L]; $q_{\text{d},t}$ = drainage flux [LT^{-1}]; H_t = water table depth [L]; $H_{\text{s},t}$ = drainage level [L].

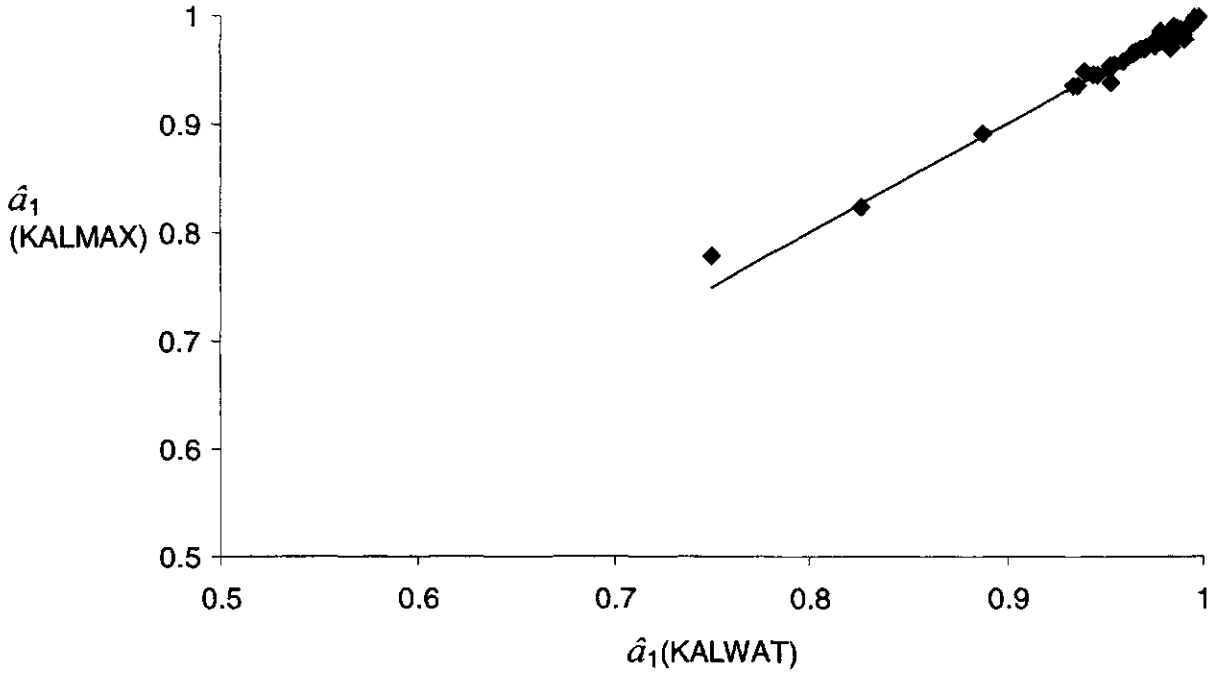

Figure 3: Estimates of the parameter a_1 by the program KALMAX against estimates of the parameter a_1 by the program KALWAT.

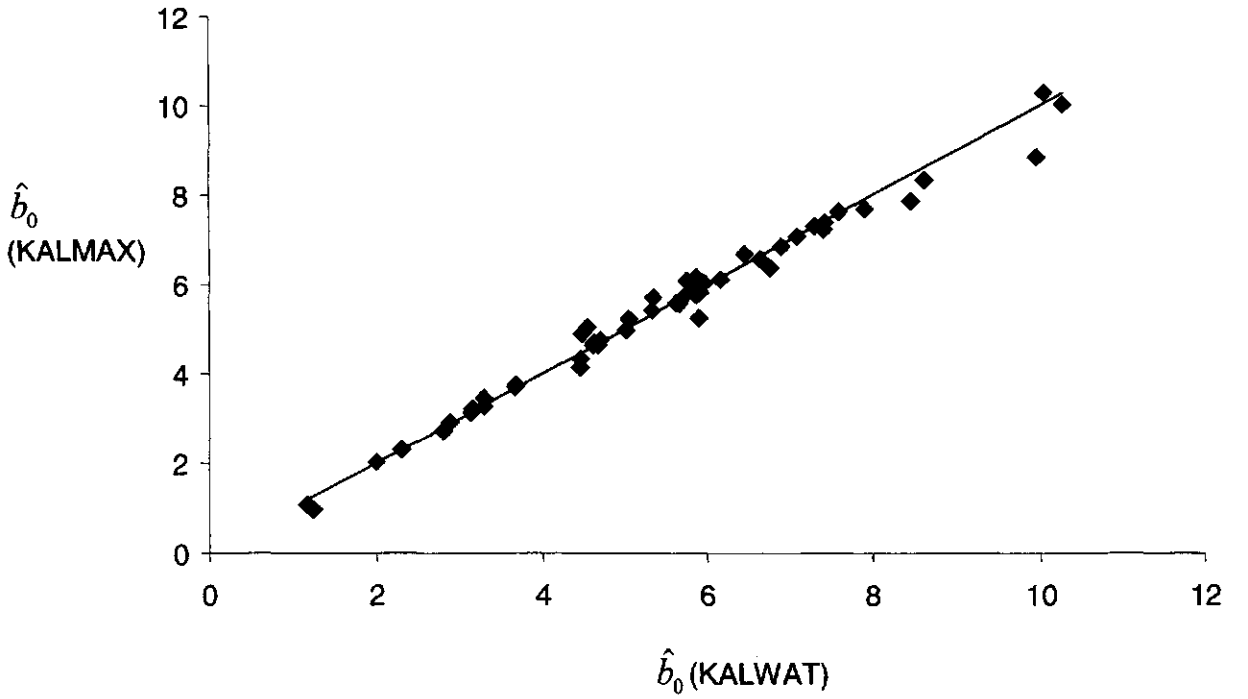

Figure 4: Estimates of the parameter b_1 by the program KALMAX against estimates of the parameter b_1 by the program KALWAT.

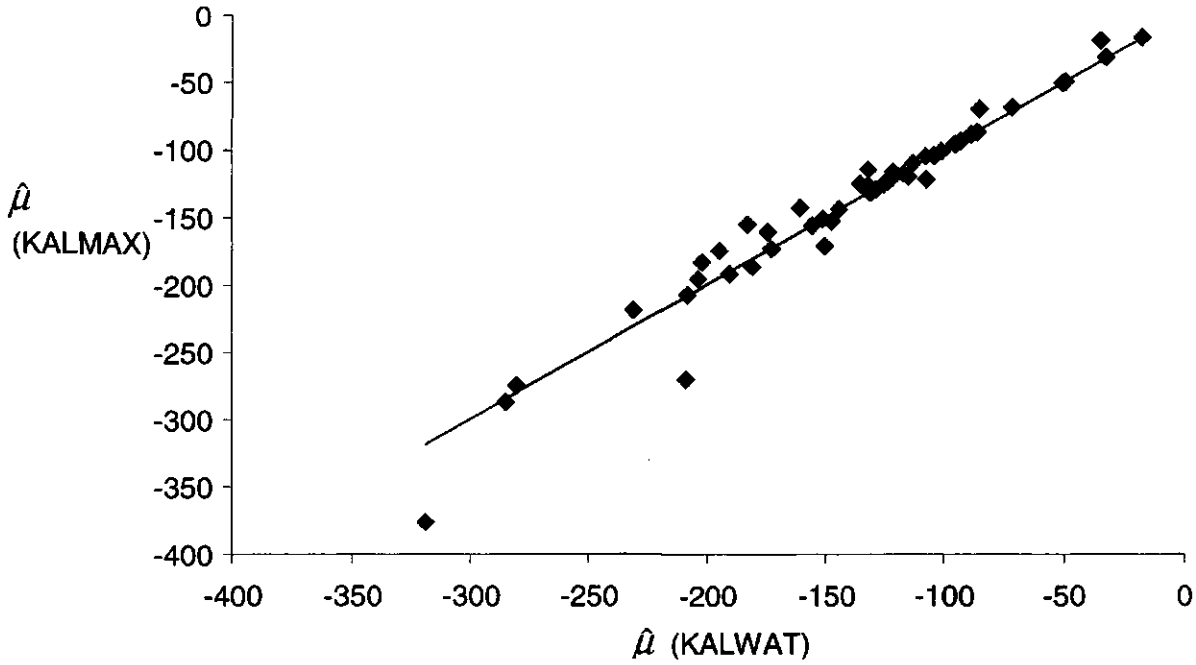

Figure 5: Estimates of the parameter μ by the program KALMAX against estimates of the parameter μ by the program KALWAT.

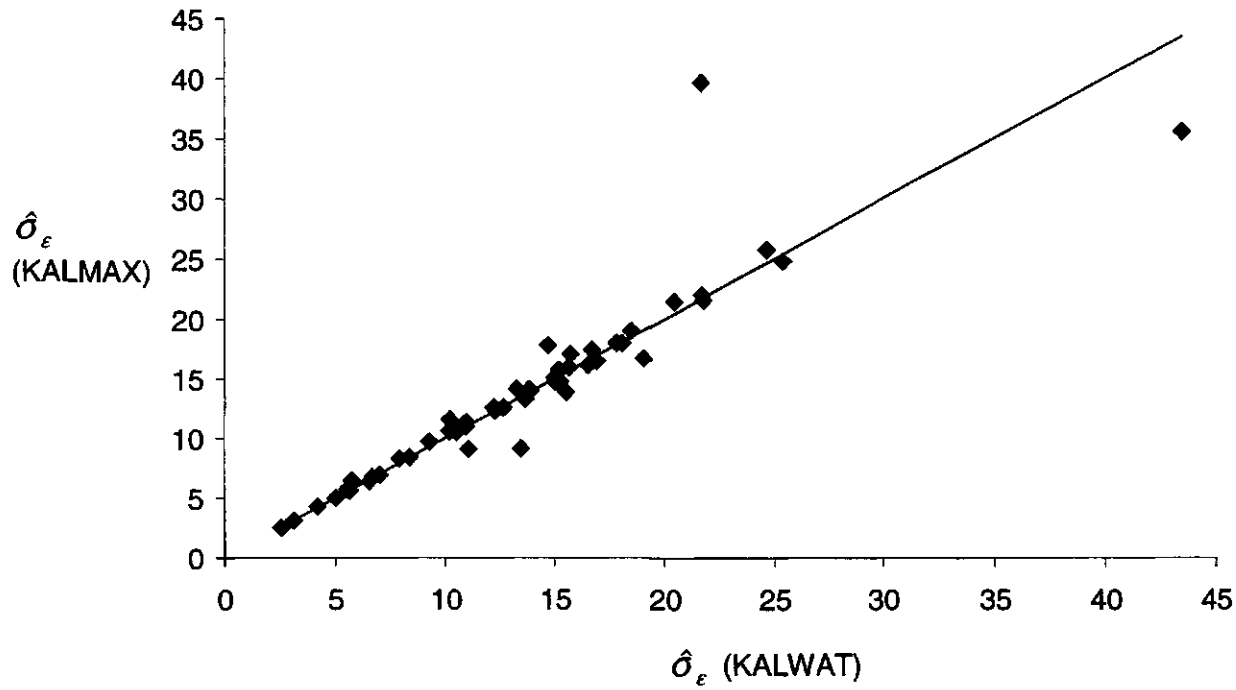

Figure 6: Estimates of the parameter σ_ε by the program KALMAX against estimates of the parameter σ_ε by the program KALWAT.

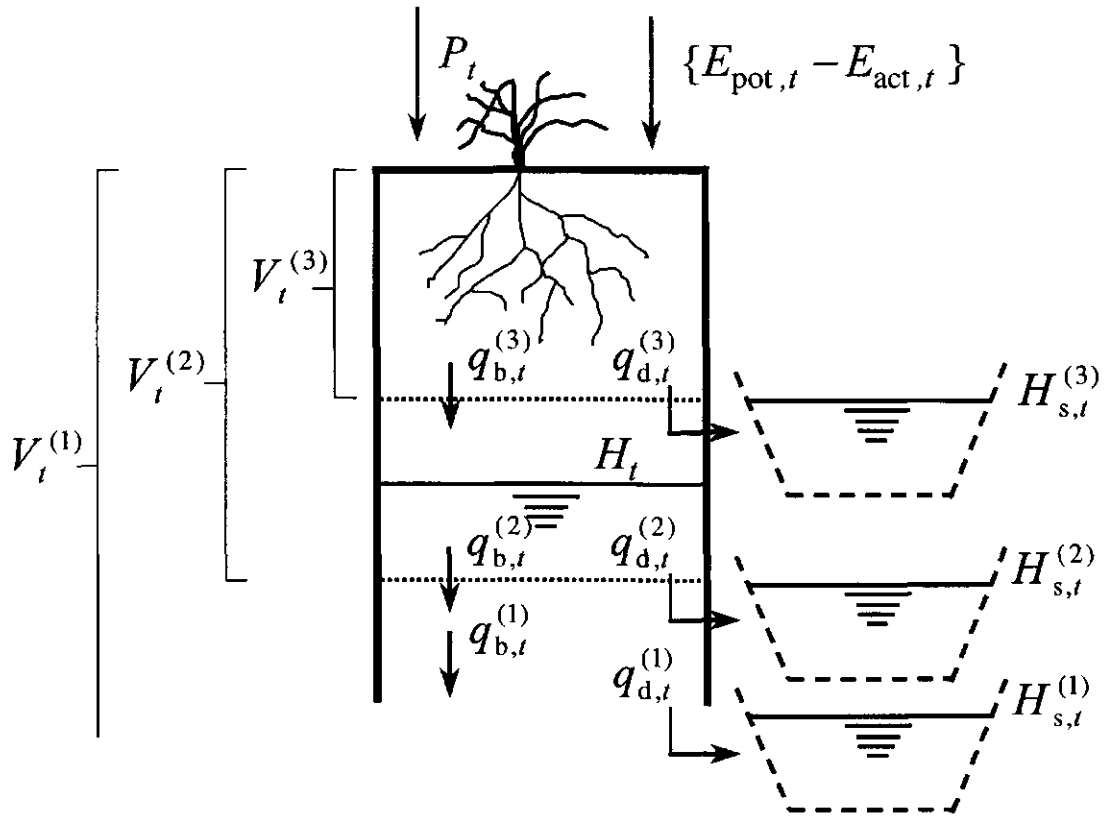

Figure 7: Soil column with water balance terms and three regimes. The superscript $^{(j)}$ indicates the regime in which the water table falls (j = 1,2,3); P_t = potential precipitation excess, i.e. precipitation – potential evapotranspiration [LT^{-1}]; $E_{\mathrm{pot},t} - E_{\mathrm{act},t}$ = difference between potential and actual evapotranspiration [LT^{-1}]; $q_{\mathrm{b}}^{(j)}$ = regional groundwater flux [LT^{-1}]; $\Delta V_t^{(j)}$ = increase of water content in the unsaturated zone [L]; $q_{\mathrm{d}}^{(j)}$ = drainage flux [LT^{-1}]; H_t = water table depth [L]; $H_{\mathrm{s},t}^{(j)}$ = drainage level [L].

Annex 3 TARSO modelling

3.1 The TARSO model

Models such as TFN models and ARMAX models describe linear relationships between input and output. However, the relationship between precipitation excess and water table depth may contain several forms of nonlinearities. One form of nonlinearity is caused by the presence of thresholds which divide the relationship between precipitation excess and water table depth into several regimes. These thresholds are for instance soil physical boundaries or drainage levels. Threshold nonlinearities can be modelled by threshold autoregressive self-exciting open loop models (TARSO, Tong, 1990). Knotters and De Gooijer (1999) apply TARSO models to the relationship between precipitation excess and water table depth. The TARSO model is defined as follows. Let $\{H_t\}$ denote a time series of water table depths (output) and $\{P_t\}$ a time series of precipitation excess (input). Now a discrete self-exciting TARSO process $\{H_t, P_t\}$ with order $(\ell; (m_1, m_1'), \ldots, (m_\ell, m_\ell'))$ and delay parameter d $(d > 0)$ is defined by *Tong* [1990] to be a solution of the equations

$$H_t = a_0^{(j)} + \sum_{i=1}^{m_j} a_i^{(j)} H_{t-i} + \sum_{i=0}^{m_j'} b_i^{(j)} P_{t-i} + \epsilon_t^{(j)}, \qquad \text{if } r_{j-1} \leq H_{t-d} < r_j, \quad (24)$$

where $-\infty = r_0 < r_1 < \ldots < r_\ell = \infty$, $a_i^{(j)}$ and $b_i^{(j)}$ $(j = 1, \ldots, \ell)$ are constants, and $\{\epsilon_t^{(j)}\}$ $(j = 1, \ldots, \ell)$ are heterogeneous white noise sequences with zero mean and finite variances $\sigma_{\epsilon^{(j)}}^2$ and each being independent of $\{P_t\}$. The thresholds are the levels $r_1, \ldots, r_{\ell-1}$. Thus, the real line is partitioned into ℓ intervals, and H_t satisfies one of ℓ dynamic regression models depending on the interval in which H_{t-d} falls.

3.2 The TARSO model in water balance terms

The schematic soil profile in Fig. 2 can easily be extended to a situation with more than one regime, as is shown in Figure 7. Hence, Eq. (5) can be extended to a situation with ℓ regimes:

$$\frac{\mathrm{d}h}{\mathrm{d}t} = \frac{-h(t)}{\varphi^{(j)}\gamma^{(j)}} + \frac{1}{\varphi^{(j)}} \left\{ P(t) + q_{\mathrm{b}}^{(j)} + \frac{H_{\mathrm{s}}^{(j)}}{\gamma^{(j)}} + E_{\mathrm{p}}(t) - E_{\mathrm{a}}(t) + \frac{\mathrm{d}V^{(j)}}{\mathrm{d}t} \right\}. \quad (25)$$

Threshold nonlinearities in the relationship between precipitation excess and water table depth may be caused by soil physical boundaries, which is expressed in Eq. (25) by $\varphi^{(j)}$ and $V^{(j)}$. Another source of threshold nonlinearity may be found in the drainage systems, which are expressed in Eq. (25) by $\gamma^{(j)}$ and $H_{\mathrm{s}}^{(j)}$. Furthermore, the regional flux $q_{\mathrm{b}}^{(j)}$ may vary with regimes which are determined by H_{t-1}, for instance if the regional flux is upward or downward, depending on the water table depth H_t.

After some substitutions Eq. (25) can be written as

$$\begin{aligned} h(t) &= \left\{ e^{-\Delta t/\varphi^{(j)}\gamma^{(j)}} \right\} h(t-\Delta t) \\ &+\gamma^{(j)} \left\{ 1 - e^{-\Delta t/\varphi^{(j)}\gamma^{(j)}} \right\} \\ &+ \left\{ \gamma^{(j)} q_b^{(j)} + H_s^{(j)} \right\} \left\{ 1 - e^{-\Delta t/\varphi^{(j)}\gamma^{(j)}} \right\} \\ &+\gamma^{(j)} \left\{ [E_p(t) - E_a(t)] - \frac{\Delta V^{(j)}}{\Delta t} \right\} \left\{ 1 - e^{-\Delta t/\varphi^{(j)}\gamma^{(j)}} \right\} \end{aligned} \tag{26}$$

The parameters of the TARSO models can be written in terms of physical quantities in the following way:

$$\begin{aligned} a_1^{(j)} &= e^{-\Delta t/\varphi^{(j)}\gamma^{(j)}} \\ b_0^{(j)} &= \gamma^{(j)} \left\{ 1 - a_1^{(j)} \right\} \\ a_0^{(j)} &= \frac{\gamma^{(j)} q_b^{(j)} + H_s^{(j)}}{\left\{ 1 - a_1^{(j)} \right\}} \end{aligned} \tag{27}$$

Annex 4 Soil profile descriptions

Top-krtnr	Veld-krtnr	Bor. nr	Datum	Opst.	X	Y	Vlaknr	Hoogte	Kroonboring		
12E	1	1	10-98	KNO	246985	564849		2.10m+ NAP			

STANDAARDPUNTENCODE tv	subgr	cijf	k	toev.eind	v	Gt	GHG	GLG	Bew. diepte	Bod. gebr	A	B	
	2r	422				IIIb	30	105	35	GR			

BIJZONDERHEDEN: 12EL0026 Anloo, provincie Drenthe

Lg nr	Horizont code	Diepte begin	Diepte eind	M	Org.st. %	Org.st. vs	Textuur <2	Textuur 50	Textuur M50	K	R	Geo frm	K vrz	C	D	Opmerkingen
1	1Ap	0	15		4.0		11	145				411		B2		10YR 3/2
2	2Ah	15	25		15	DV	11	145				110		B15		vz. 10YR 3/1
3	3Bhe	25	35		1.0		11	145				413		O2		10YR 4/3
4	3BCe	35	45		0.5		11	145				413		O2		10YR 4.5/3
5	3Ce	45	85				11	145				413		O2		10YR 6/3
6	3BCer1	85	100		2.0		11	145				413		O2		wh. 10YR 3/2
7	3BCer2	100	105		2.0		30	130				413		O3		wh. 10YR 3/2
8	3Cr	105	160				12	130				413		O2		10YR 6/3

Top-krtnr	Veld-krtnr	Bor. nr	Datum	Opst.	X	Y	Vlaknr	Hoogte	Kroonboring		
12F	1	2	10-98	KNO	255640	565330		3.09m+ NAP			

STANDAARDPUNTENCODE tv	subgr	cijf	k	toev.eind	v	Gt	GHG	GLG	Bew. diepte	Bod. gebr	A	B	
	2r	422			F	IVu	50	100	85	AK			

BIJZONDERHEDEN: 12FL0033 Veendam, provincie Groningen

Lg nr	Horizont code	Diepte begin	Diepte eind	M	Org.st. %	Org.st. vs	Textuur <2	Textuur 50	Textuur M50	K	R	Geo frm	K vrz	C	D	Opmerkingen
1	1A/Bhep	0	30		4.0		11	145				693		B2		10YR 3/1,4/4
2	1A/B/C	30	85		6.0		11	145				693		B2		veenr. 10YR 2/1
3	1Cer	85	100				11	145				411		O2		10YR 6/3
4	1Cr	100	140				11	145				411		O2		10YR 6/3

Top-krtnr	Veld-krtnr	Bor. nr	Datum	Opst.	X	Y	Vlaknr	Hoogte	Kroonboring
16E	1	3	10-98	KNO	204860	544540		2.90m+ NAP	

STANDAARDPUNTENCODE tv	subgr	cijf	k	toev.eind	v	Gt	GHG	GLG	Bew. diepte	Bod. gebr	A	B
	4s	422				VIo	50	170	55	GR		

BIJZONDERHEDEN: 16EL0035 Weststellingwerf, prov. Friesland

Lg nr	Horizont code	Diepte begin	Diepte eind	M	Org.st. %	Org.st. vs	Textuur <2	Textuur 50	Textuur M50	K	R	Geo frm	K vrz	C	D	Opmerkingen
1	1Ap	0	20		6.0		15	140				411		B2		10YR 2/2
2	1Ahb	20	55		8.0		15	140				411		B2		10YR 2/1
3	1Cu	55	145				11	155				411		O2		10YR 5.5/5
4	1Cur	145	170				11	140				411		O2		5Y 6/4
5	1Cr	170	190				11	140				411		O2		5Y 6/2.5

Top-krtnr	Veld-krtnr	Bor. nr	Datum	Opst.	X	Y	Vlaknr	Hoogte	Kroonboring
16F	1	4	10-98	KNO	212205	542620		4.26m+ NAP	

STANDAARDPUNTENCODE tv	subgr	cijf	k	toev.eind	v	Gt	GHG	GLG	Bew. diepte	Bod. gebr	A	B
	v4d	423			v9	IIIa	10	90	20	GR		

BIJZONDERHEDEN: 16FP7053 Havelte, provincie Drenthe

Lg nr	Horizont code	Diepte begin	Diepte eind	M	Org.st. %	Org.st. vs	Textuur <2	Textuur 50	Textuur M50	K	R	Geo frm	K vrz	C	D	Opmerkingen
1	1Ah	0	5		6.0		18	140				411		B3		10YR 2.5/2
2	2Cw	5	35		70	DV						110		O16		10YR 2/1
3	3Cu	35	85				18	140				413		O3		10YR 5/3
4	4Cr	85	115		70	DV						413		O16		10YR 2/1
5	5Cr	115	150				15	140				413		O2		2.5YR 5/2

Top-krtnr	Veld-krtnr	Bor. nr	Datum	Opst.	X	Y	Vlaknr	Hoogte	Kroonboring
16G	1	5	10-98	KNO	209640	531240		1.45m+ NAP	

STANDAARDPUNTENCODE tv	subgr	cijf	k	toev.eind	v	Gt	GHG	GLG	Bew. diepte	Bod. gebr	A	B
	2r	423		g13		Vbo	30	130	30	GR		

BIJZONDERHEDEN: 16GL0007 Havelte, provincie Drenthe

Lg nr	Horizont code	Diepte begin	Diepte eind	M	Org.st. %	Org.st. vs	Textuur <2	Textuur 50	Textuur M50	K	R	Geo frm	K vrz	C	D	Opmerkingen
1	1Ap	0	15		5.0		17	140				411		B2		10YR 3/1
2	2Ahb	15	22		30	DV						110		B16		10YR 2/1
3	3Bhe1	22	35		3.0		17	140				413		O2		7.5YR 3/2
4	3Bhe2	35	55		1.0		8	140				413		O1	g	7.5YR 4/4
5	3BCe	55	65		0.5		8	140				413		O1		10YR 4/4
6	3Ce1	65	100				8	140				413		O1		10YR 5.5/4
7	3Ce2	100	130				6	160				413		O1		10YR 5.5/3
8	3Cr1	130	140				25	130				413		O3	g	2.5YR 5.5/2
9	3Cr2	140	160				6	160				413		O1	g	2.5YR 5/2

Top-krtnr	Veld-krtnr	Bor. nr	Datum	Opst.	X	Y	Vlaknr	Hoogte	Kroonboring
21F	1	6	10-98	KNO	215440	515050		3.36m+ NAP	

STANDAARDPUNTENCODE tv	subgr	cijf	k	toev.eind	v	Gt	GHG	GLG	Bew. diepte	Bod. gebr	A	B
	4i	431			F	VIo	50	150	80	BL		

BIJZONDERHEDEN: 21FL0016 Staphorst, provincie Overijssel

Lg nr	Horizont code	Diepte begin	Diepte eind	M	Org.st. %	Org.st. vs	Textuur <2	Textuur 50	Textuur M50	K	R	Geo frm	K vrz	C	D	Opmerkingen
1	1A/	0	50	1	3.0		8	170	693					B1		10YR 3/1
2	1Bhe/	0	50	1	2.0		8	170	693					B1		7.5YR 4/4
3	1Ce1	50	80				8	170	411					O1		10YR 5/6
4	1Ce2	80	100				8	170	411					O1		2.5Y 6/4
5	1Ce3	100	150				12	140	412					O2		2.5Y 7/4
6	1Cr	150	180				20	130	412					O3		5Y 6/4

Top-krtnr	Veld-krtnr	Bor. nr	Datum	Opst.	X	Y	Vlaknr	Hoogte	Kroonboring
21F	1	7	10-98	KNO	213410	519940		2.31m+ NAP	

STANDAARDPUNTENCODE tv	subgr	cijf	k	toev.eind	v	Gt	GHG	GLG	Bew. diepte	Bod. gebr	A	B
	4s	422				VIo	70	140	55	GR		

BIJZONDERHEDEN: 21FL0033 Staphorst, provincie Overijssel

Lg nr	Horizont code	Diepte begin	Diepte eind	M	Org.st. %	Org.st. vs	Textuur <2	Textuur 50	Textuur M50	K	R	Geo frm	K vrz	C	D	Opmerkingen
1	1Aa	0	55		5.0		12	145	692					B2		10YR 3.5/1
2	1Bheb	55	80		0.5		8	155	411					O1		7.5YR 4/4
3	1BC	80	100		0.5		8	155	411					O1		10YR 5/6
4	1Cu	100	140				8	155	411					O1		10YR 6/5
5	1Cr	140	180				15	135	412					O1		2.5YR 6.5/4

Top-krtnr	Veld-krtnr	Bor. nr	Datum	Opst.	X	Y	Vlaknr	Hoogte	Kroonboring
21H	1	8	10-98	KNO	213960	511260		2.23m+ NAP	

STANDAARDPUNTENCODE tv	subgr	cijf	k	toev.eind	v	Gt	GHG	GLG	Bew. diepte	Bod. gebr	A	B
	2q	432				IIIb	35	110	35	GR		

BIJZONDERHEDEN: 21HL0018 Nieuwleusen, provincie Overijssel

Lg nr	Horizont code	Diepte begin	eind	M	Org.st. %	vs	Textuur <2	50	M50	K	R	Geo frm	K vrz	C	D	Opmerkingen
1	1Aap	0	35		6.0		12	160	692					B2		10YR 2/1
2	1E	35	45				6	160	411					B1		10YR 4/2
3	1Bhe	45	65		3.0		6	160	411					O1		10YR 2/2
4	1BC	65	110		0.5		8	140	411					O1		10YR 4/4
5	1Cr	110	120				8	140	411					O1		10YR 5/4

Top-krtnr	Veld-krtnr	Bor. nr	Datum	Opst.	X	Y	Vlaknr	Hoogte	Kroonboring
21H	1	9	10-98	KNO	211200	510520		0.52m+ NAP	

STANDAARDPUNTENCODE tv	subgr	cijf	k	toev.eind	v	Gt	GHG	GLG	Bew. diepte	Bod. gebr	A	B
	4h	432				IIa	15	70	20	GR		

BIJZONDERHEDEN: 21HL0019 Nieuwleusen, provincie Overijssel

Lg nr	Horizont code	Diepte begin	eind	M	Org.st. %	vs	Textuur <2	50	M50	K	R	Geo frm	K vrz	C	D	Opmerkingen
1	1Apg	0	20		5.0		5	12	190					B2		10YR 2/2
2	2Cg	20	50				6	200	413					O1		10YR 5/5
3	2Cgr	50	70				6	180	413					O1		10YR 5.5/3
4	2Cr	70	100				6	170	413					O1		10YR 6/1.5

Top-krtnr	Veld-krtnr	Bor. nr	Datum	Opst.	X	Y	Vlaknr	Hoogte	Kroonboring		
22C	1	10	10-98	KNO	220400	503060		4.81m+ NAP			

STANDAARDPUNTENCODE tv	subgr	cijf	k	toev.eind	v	Gt	GHG	GLG	Bew. diepte	Bod. gebr	A	B	
4r	422					VIIo	93	152	90	GR			

BIJZONDERHEDEN: 22CL0044 Vilsteren, provincie Overijssel

Lg nr	Horizont code	Diepte begin	Diepte eind	M	Org.st. %	Org.st. vs	Textuur <2	Textuur 50	Textuur M50	K	R	Geo frm	K vrz	C	D	Opmerkingen
1	1Aa	0	15		4.0		11	145	692					B2		bruin, 10YR 3/2
2	1Aag	15	70		4.0		11	155	692					B2		bruin, 10YR 4/3
3	1Ahb	70	90		6.0		13	140	413					B2		10YR 3/1
4	1Cg	90	130				8	160	413					O1		10YR 5/6
5	1Cr	130	160				8	140	413					O1		5Y 5.5/2.5

Top-krtnr	Veld-krtnr	Bor. nr	Datum	Opst.	X	Y	Vlaknr	Hoogte	Kroonboring		
27D	1	11	10-98	KNO	199970	483000		3.16m+ NAP			

STANDAARDPUNTENCODE tv	subgr	cijf	k	toev.eind	v	Gt	GHG	GLG	Bew. diepte	Bod. gebr	A	B	
4r	423					VIo	40	120	70	AK			

BIJZONDERHEDEN: 27DL0031 Epe, provincie Gelderland

Lg nr	Horizont code	Diepte begin	Diepte eind	M	Org.st. %	Org.st. vs	Textuur <2	Textuur 50	Textuur M50	K	R	Geo frm	K vrz	C	D	Opmerkingen
1	1Aap	0	30		6.0		7	25	145			692		B3		10YR 3/2
2	1Aag	30	70		4.0		7	25	145			692		B3		10YR 4/3
3	1ACg	70	95		2.0		4	20	150			321		B3		10YR 4/3
4	2Cg	95	120					14	145			413		O2		10YR 7/2
5	2Cr	120	150					12	145			413		O2		2.5Y 7/2

Top-krtnr	Veld-krtnr	Bor. nr	Datum	Opst.	X	Y	Vlaknr	Hoogte	Kroonboring		
27D	1	12	10-98	KNO	192100	483560		19.35m+ NAP			

STANDAARDPUNTENCODE tv	subgr	cijf	k	toev.eind	v	Gt	GHG	GLG	Bew. diepte	Bod. gebr	A	B	
1v		z6				Ia	10	40	15	WN			

BIJZONDERHEDEN: 27DP7603 Epe, provincie Gelderland

Lg nr	Horizont code	Diepte begin	eind	M	Org.st. %	vs	Textuur <2	50	M50	K	R	Geo frm	K vrz	C	D	Opmerkingen
1	1Ah	0	15		50	DV						110		B16		10YR 3/2
2	1Cu	15	60		70	S						150		B16		10YR 3/2
3	2Cr1	60	75				8	300				631		O5		2.5Y 7/6
4	2Cr2	75	120				8	220				631		O5		2.5Y 7/6

Top-krtnr	Veld-krtnr	Bor. nr	Datum	Opst.	X	Y	Vlaknr	Hoogte	Kroonboring		
27H	1	13	10-98	KNO	211560	479000		5.40m+ NAP			

STANDAARDPUNTENCODE tv	subgr	cijf	k	toev.eind	v	Gt	GHG	GLG	Bew. diepte	Bod. gebr	A	B	
4k	423					IIIb	35	110	30	GR			

BIJZONDERHEDEN: 27HP0064 Diepenveen, provincie Overijssel

Lg nr	Horizont code	Diepte begin	eind	M	Org.st. %	vs	Textuur <2	50	M50	K	R	Geo frm	K vrz	C	D	Opmerkingen
1	1Ap	0	30		4.0		18	145				411		B3		10YR 3/1
2	1Cg1	30	85				22	145				411		O3		10YR 6/4
3	1Cg2	85	110				17	145				411		O3		10YR 7/2
4	1Cr	110	160				12	145				411		O2		10YR 5/1

Top-krtnr	Veld-krtnr	Bor. nr	Datum	Opst.	X	Y	Vlaknr	Hoogte	Kroonboring
28B	1	14	10-98	KNO	236620	496140		9.01m+ NAP	

STANDAARDPUNTENCODE tv	subgr	cijf	k	toev.eind	v	Gt	GHG	GLG	Bew. diepte	Bod. gebr	A	B
	1t	z11		g11		VIo	60	160	110	TU		

BIJZONDERHEDEN: 28BL0051 Hellendoorn, provincie Overijssel

Lg nr	Horizont code	Diepte begin	Diepte eind	M	Org.st. %	Org.st. vs	Textuur <2	Textuur 50	Textuur M50	K	R	Geo frm	K vrz	C	D	Opmerkingen
1	1Aap	0	40		8.0		18	140				692		B3		10YR 3/1
2	2Cw	40	110		50	DV						110		O16		10YR 2/2
3	3Cu	110	160				20	110				413		O3	g	10YR 5.5/4
4	3Cr	160	180				20	110				413		O3		2.5Y 6/3

Top-krtnr	Veld-krtnr	Bor. nr	Datum	Opst.	X	Y	Vlaknr	Hoogte	Kroonboring
28B	1	15	10-98	KNO	238150	495470		9.29m+ NAP	

STANDAARDPUNTENCODE tv	subgr	cijf	k	toev.eind	v	Gt	GHG	GLG	Bew. diepte	Bod. gebr	A	B
	2r	432				VIo	50	140	30	BW		

BIJZONDERHEDEN: 28BL0052 Vriezenveen, provincie Overijssel

Lg nr	Horizont code	Diepte begin	Diepte eind	M	Org.st. %	Org.st. vs	Textuur <2	Textuur 50	Textuur M50	K	R	Geo frm	K vrz	C	D	Opmerkingen
1	1Ap	0	30		12		20	130				413		B15		10YR 2/1 veenr.
2	1Bhe	30	50		4.0		25	110				413		O3		7.5YR 3/2
3	1Ce1	50	70				20	130				413		O3		10YR 6.5/3
4	1Ce2	70	140				11	155				413		O3		10YR 5/4
5	1Cr	140	170				11	155				413		O3		2.5Y 6/3

Top-krtnr	Veld-krtnr	Bor. nr	Datum	Opst.	X	Y	Vlaknr	Hoogte	Kroon boring		
28D	1	16	10-98	KNO	234480	476120		10.74m+ NAP			

STANDAARDPUNTENCODE tv	subgr	cijf	k	toev.eind	v	Gt	GHG	GLG	Bew. diepte	Bod. gebr	A	B	
	2r	422		g13		VIo	70	180	25	GR			

BIJZONDERHEDEN: 28DL0026 Markelo, provincie Overijssel

Lg nr	Horizont code	Diepte begin	Diepte eind	M	Org.st. %	Org.st. vs	Textuur <2	Textuur 50	Textuur M50	K	R	Geo frm	K vrz	C	D	Opmerkingen
1	1Ap	0	25		6.0		14	145				411		B2		10YR 3/2
2	1BC	25	80		0.5		14	145				411		O2		10YR 6/4
3	1Cu1	80	130				14	145				411		O2		10YR 6/2
4	1Cu2	130	180				11	160				413		O2	g	10YR 6/2
5	1Cr	180	200				11	150				413		O2		10YR 6/1.5

Top-krtnr	Veld-krtnr	Bor. nr	Datum	Opst.	X	Y	Vlaknr	Hoogte	Kroon boring		
28D	1	17	10-98	KNO	237250	482440		9.66m+ NAP			

STANDAARDPUNTENCODE tv	subgr	cijf	k	toev.eind	v	Gt	GHG	GLG	Bew. diepte	Bod. gebr	A	B	
	2q	422				VIId	130	210	50	TV			

BIJZONDERHEDEN: 28DL0044 Wierden, provincie Overijssel

Lg nr	Horizont code	Diepte begin	Diepte eind	M	Org.st. %	Org.st. vs	Textuur <2	Textuur 50	Textuur M50	K	R	Geo frm	K vrz	C	D	Opmerkingen
1	1Aap	0	35		5.0		12	145				692		B2		10YR 4/2
2	1Bhe	35	50		1.5		12	145				411		O2		10YR 4/6
3	1Cg	50	150				12	145				411		O2		10YR 8/6

Top-krtnr	Veld-krtnr	Bor. nr	Datum	Opst.	X	Y	Vlaknr	Hoogte	Kroonboring		
28D	1	18	10-98	KNO	234610	477230		9.59m+ NAP			

STANDAARDPUNTENCODE tv	subgr	cijf	k	toev.eind	v	Gt	GHG	GLG	Bew. diepte	Bod. gebr	A	B	
	z4d	422				IIIa	20	110	25	GR			

BIJZONDERHEDEN: 28DP7037 Markelo, provincie Overijsel

Lg nr	Horizont code	Diepte begin	Diepte eind	M	Org.st. %	Org.st. vs	Textuur <2	Textuur 50	Textuur M50	K	R	Geo frm	K vrz	C	D	Opmerkingen
1	1AC	0	10		2.0		20	145				411		B3		10YR 4/2
2	2Ah	10	25		20	DV						110		B16		10YR 2/1
3	3Cu1	25	80				12	150				411		O2		10YR 7/2
4	3Cu2	80	110				14	145				411		O2		2.5Y 7/2
5	3Cr	110	140				12	150				411		O2		2.5Y 6/1

Top-krtnr	Veld-krtnr	Bor. nr	Datum	Opst.	X	Y	Vlaknr	Hoogte	Kroonboring		
28F	1	19	10-98	KNO	259530	491660		21.23m+ NAP			

STANDAARDPUNTENCODE tv	subgr	cijf	k	toev.eind	v	Gt	GHG	GLG	Bew. diepte	Bod. gebr	A	B	
	4s	422				VIo	60	150	65	TV			

BIJZONDERHEDEN: 28FL0125 Denekamp, provincie Overijssel

Lg nr	Horizont code	Diepte begin	Diepte eind	M	Org.st. %	Org.st. vs	Textuur <2	Textuur 50	Textuur M50	K	R	Geo frm	K vrz	C	D	Opmerkingen
1	1Aa	0	55		4.0		15	145				692		B2		10YR 2/1
2	1Bheb	55	65		1.5		12	145				411		O2		10YR 3/2
3	1Cg	65	150				12	145				411		O2		10YR 5/6, 7/2
4	1Cr	150	200				14	140				411		O2		5Y 6/2

Top-krtnr	Veld-krtnr	Bor. nr	Datum	Opst.	X	Y	Vlaknr	Hoogte	Kroonboring
28F	1	20	10-98	KNO	259390	488910		21.04m+ NAP	

STANDAARDPUNTENCODE tv	subgr	cijf	k	toev.eind	v	Gt	GHG	GLG	Bew. diepte	Bod. gebr	A	B
2r	422					Vbo	30	120	70	BL		

BIJZONDERHEDEN: 28FP7015 Denekamp, provincie Overijssel

Lg nr	Horizont code	Diepte begin	Diepte eind	M	Org.st. %	Org.st. vs	Textuur <2	Textuur 50	Textuur M50	K	R	Geo frm	K vrz	C	D	Opmerkingen
1	1Ap	0	20		4.0		14	145				411		B2		10YR 3/1
2	1Bhg	20	70		1.0		14	145				411		O2		5YR 2.5/2, 3/4
3	1Cg	70	120				12	150				411		O2		10YR 7/2, 7/6
4	1Cr	120	180				12	155				411		O2		5Y 7/1, 7/2

Top-krtnr	Veld-krtnr	Bor. nr	Datum	Opst.	X	Y	Vlaknr	Hoogte	Kroonboring
28F	1	21	10-98	KNO	258780	488660		21.51m+ NAP	

STANDAARDPUNTENCODE tv	subgr	cijf	k	toev.eind	v	Gt	GHG	GLG	Bew. diepte	Bod. gebr	A	B
2r	422					VIo	70	140	75	BL		

BIJZONDERHEDEN: P7017 Denekamp, provincie Overijssel

Lg nr	Horizont code	Diepte begin	Diepte eind	M	Org.st. %	Org.st. vs	Textuur <2	Textuur 50	Textuur M50	K	R	Geo frm	K vrz	C	D	Opmerkingen
1	1AEp	0	20		2.0		11	145				411		B2		5YR 3/1
2	1Bhe	20	35		8.0		11	145				411		O2		5YR 2.5/1
3	1BC	35	75		1.5		11	145				411		O2		5YR 3/2
4	1Cu1	75	120				13	145				411		O2		10YR 4/4
5	1Cu2	120	150				11	145				411		O2		10YR 4/6

Top-krtnr	Veld-krtnr	Bor. nr	Datum	Opst.	X	Y	Vlaknr	Hoogte	Kroon boring		
28G	1	22	10-98	KNO	247000	481700		12.88m+ NAP			

STANDAARDPUNTENCODE tv	subgr	cijf	k	toev.eind	v	Gt	GHG	GLG	Bew. diepte	Bod. gebr	A	B	
	c4k	423				VIo	60	140	40	GR			

BIJZONDERHEDEN: 28GL0008 Borne, provincie Overijssel

Lg nr	Horizont code	Diepte begin	Diepte eind	M	Org.st. %	Org.st. vs	Textuur <2	Textuur 50	Textuur M50	K	R	Geo frm	K vrz	C	D	Opmerkingen
1	1Aa	0	40		4.0		22	145	692					B3		10YR 3/1
2	1Cg	40	180				16	140	413					O2		10YR 7/3

Top-krtnr	Veld-krtnr	Bor. nr	Datum	Opst.	X	Y	Vlaknr	Hoogte	Kroon boring		
28G	1	23	10-98	KNO	249450	481200		14.30m+ NAP			

STANDAARDPUNTENCODE tv	subgr	cijf	k	toev.eind	v	Gt	GHG	GLG	Bew. diepte	Bod. gebr	A	B	
	4s	423				VIo	60	150	70	GR			

BIJZONDERHEDEN: 28GL0075 Borne, provincie Overijssel

Lg nr	Horizont code	Diepte begin	Diepte eind	M	Org.st. %	Org.st. vs	Textuur <2	Textuur 50	Textuur M50	K	R	Geo frm	K vrz	C	D	Opmerkingen
1	1Aap	0	30		5.0		22	145	692					B3		10YR 3/1
2	1Aa	30	55		7.0		25	145	692					B3		10YR 3/2
3	1AC	55	70		7.0		25	145	411					B3		10YR 3/2 4/4
4	1Ahb	70	95		20		20	145	411					B3		2.5Y 2/1
5	1Cu1	95	120				55	130	411					O14		10YR 5/2
6	1Cu2	120	150				12	145	411					O2		10YR 5/3
7	1Cr	150	200				12	145	411					O2		10YR 6/2

Top-krtnr	Veld-krtnr	Bor. nr	Datum	Opst.	X	Y	Vlaknr	Hoogte	Kroon boring		
28H	1	24	10-98	KNO	251670	485210		13.68m+ NAP			

STANDAARDPUNTENCODE tv	subgr	cijf	k	toev.eind	v	Gt	GHG	GLG	Bew. diepte	Bod. gebr	A	B	
4s	423					VIo	70	160	75	TV			

BIJZONDERHEDEN: 28HL0079 Weerselo, provincie Overijssel

Lg nr	Horizont code	Diepte begin	Diepte eind	M	Org.st. %	Org.st. vs	Textuur <2	Textuur 50	Textuur M50	K	R	Geo frm	K vrz	C	D	Opmerkingen
1	1Aap	0	40		4.0		23	145	692					B3		10YR 3/2
2	1Aa	40	75		2.0		20	145	692					B3		10YR 4/1, 4/2
3	1Cg	75	160				14	145	411					O2		2.5Y 7/4
4	1Cr	160	200				12	150	411					O2		2.5Y 7/1

Top-krtnr	Veld-krtnr	Bor. nr	Datum	Opst.	X	Y	Vlaknr	Hoogte	Kroon boring		
29C	1	25	10-98	KNO	267000	486720		27.11m+ NAP			

STANDAARDPUNTENCODE tv	subgr	cijf	k	toev.eind	v	Gt	GHG	GLG	Bew. diepte	Bod. gebr	A	B	
2q	432					VIo	60	140	50	TV			

BIJZONDERHEDEN: 29CL0021 Losser, provincie Overijssel

Lg nr	Horizont code	Diepte begin	Diepte eind	M	Org.st. %	Org.st. vs	Textuur <2	Textuur 50	Textuur M50	K	R	Geo frm	K vrz	C	D	Opmerkingen
1	1Aap	0	35		7.0		15	155	692					B2		7.5YR 3/0
2	1Bhep	35	50		1.0		12	160	411					O2		7.5YR 4/4
3	1BC	50	100		0.5		10	170	411					O2		10YR 5/6
4	1Cu	100	160				10	170	411					O2		10YR 5/3

Top-krtnr	Veld-krtnr	Bor. nr	Datum	Opst.	X	Y	Vlaknr	Hoogte	Kroonboring		
32G	1	26	10-98	KNO	169720	450080		8.30m+ NAP			

STANDAARDPUNTENCODE tv	subgr	cijf	k	toev.eind	v	Gt	GHG	GLG	Bew. diepte	Bod. gebr	A	B	
	c4i	422				VIo	50	170	35	TV			

BIJZONDERHEDEN: 32GL0021 Ede, provincie Gelderland

Lg nr	Horizont code	Diepte begin	Diepte eind	M	Org.st. %	Org.st. vs	Textuur <2	Textuur 50	Textuur M50	K	R	Geo frm	K vrz	C	D	Opmerkingen
1	1Aap	0	35		5.0		11	140	692					B2		10YR 2.5/2
2	1Ce1	35	100				11	140	413					O2		10YR 5.5/3.5
3	1Ce2	100	150				11	140	413					O2		10YR 4.5/3
4	1Cu	150	180				11	140	413					O2		10YR 4/3

Top-krtnr	Veld-krtnr	Bor. nr	Datum	Opst.	X	Y	Vlaknr	Hoogte	Kroonboring		
32H	1	27	10-98	KNO	171240	451900		10.57m+ NAP			

STANDAARDPUNTENCODE tv	subgr	cijf	k	toev.eind	v	Gt	GHG	GLG	Bew. diepte	Bod. gebr	A	B	
	4s	423				IIIa	15	110	60	GR			

BIJZONDERHEDEN: 32HL0105 Ede, provincie Gelderland

Lg nr	Horizont code	Diepte begin	Diepte eind	M	Org.st. %	Org.st. vs	Textuur <2	Textuur 50	Textuur M50	K	R	Geo frm	K vrz	C	D	Opmerkingen
1	1Aapg	0	20		4.0		5	20	150	692				B3		10YR 3/2
2	1Aag	20	60		4.0		7	22	145	692				B3		10YR 3/2
3	1Ahb	60	80		7.0		7	22	145	411				B3		10YR 3/1
4	1Cg	80	110					12	145	411				O2		10YR 6/3
5	1Cr	110	140					12	145	411				O2		2.5Y 7/2

Top-krtnr	Veld-krtnr	Bor. nr	Datum	Opst.	X	Y	Vlaknr	Hoogte	Kroonboring	
33B	1	28	10-98	KNO	195579	464336		18.13m+ NAP		

STANDAARDPUNTENCODE tv	subgr	cijf	k	toev.eind	v	Gt	GHG	GLG	Bew. diepte	Bod. gebr	A	B	
	4s	432				VIo	50	150	90	GR			

BIJZONDERHEDEN: 33BL0003 Apeldoorn, provincie Gelderland

Lg nr	Horizont code	Diepte begin	Diepte eind	M	Org.st. %	Org.st. vs	Textuur <2	Textuur 50	Textuur M50	K	R	Geo frm	K vrz	C	D	Opmerkingen
1	1Aa1	0	40		5.0		12	180				692		B2		10YR 3/2
2	1Aa2	40	60		5.0		12	160				692		B2		10YR 4/2
3	1A/C	60	70				8	160				693		B1		10YR 5.5/5
4	1Ahb	70	90				12	180				411		B2		10YR 3/2
5	1Ce	90	150				8	180				411		O1		2.5Y 6/2
6	1Cr	150	180				5	200				411		O1		10YR 5/2

Top-krtnr	Veld-krtnr	Bor. nr	Datum	Opst.	X	Y	Vlaknr	Hoogte	Kroonboring	
33F	1	29	10-98	KNO	212095	469420		8.10m+ NAP		

STANDAARDPUNTENCODE tv	subgr	cijf	k	toev.eind	v	Gt	GHG	GLG	Bew. diepte	Bod. gebr	A	B
2r	422					VIId	140	240	35	BL		

BIJZONDERHEDEN: 33FL0049 Gorssel, provincie Gelderland

Lg nr	Horizont code	Diepte begin	Diepte eind	M	Org.st. %	Org.st. vs	Textuur <2	Textuur 50	Textuur M50	K	R	Geo frm	K vrz	C	D	Opmerkingen
1	1O	-10	0		90	L						170				strooisel-laag
2	2Ah	0	20		3.0		14	145				411		B2		10YR 3/1
3	2Bhe	20	35		1.0		14	145				411		O2		10YR 3/2
4	2Cu	35	60				14	145				411		O2		10YR 7/6
5	2Cg1	60	140				12	150				411		O2		2.5Y 8/4
6	2Cg2	140	160				25	150				412		O3		10YR 7/3
7	2Cg3	160	200				14	150				413		O2		10YR 7/3
8	2Cgr	200	240				12	165				413		O2		10YR 7/3
9	2Cr	240	300				10	165				413		O2		10YR 6/2

Top-krtnr	Veld-krtnr	Bor. nr	Datum	Opst.	X	Y	Vlaknr	Hoogte	Kroonboring	
34B	1	30	10-98	KNO	235200	472910		11.74m+ NAP		

STANDAARDPUNTENCODE tv	subgr	cijf	k	toev.eind	v	Gt	GHG	GLG	Bew. diepte	Bod. gebr	A	B
2r	432					VIId	130	230	50	GR		

BIJZONDERHEDEN: 34BL0013 Markelo, provincie Overijssel

Lg nr	Horizont code	Diepte begin	Diepte eind	M	Org.st. %	Org.st. vs	Textuur <2	Textuur 50	Textuur M50	K	R	Geo frm	K vrz	C	D	Opmerkingen
1	1Ap	0	30		3.0		12	155				411		B2		10YR 3/1
2	1BC	30	50		1.0		16	145				411		O2		7.5YR 4/4
3	1Cu1	50	140				16	145				411		O2		2.5Y 7/4
4	1Cu2	140	230				12	145				411		O2		2.5Y 6/4
5	1Cr	230	260				12	145				411		O2		10YR 5/1

Top-krtnr	Veld-krtnr	Bor. nr	Datum	Opst.	X	Y	Vlaknr	Hoogte	Kroonboring	
34B	1	31	10-98	KNO	232030	464295		12.97m+ NAP		

STANDAARDPUNTENCODE tv	subgr	cijf	k	toev.eind	v	Gt	GHG	GLG	Bew. diepte	Bod. gebr	A	B	
	c4i	423				Vbo	35	140	40	GR			

BIJZONDERHEDEN: 34BP0192 Borculo, provincie Gelderland

Lg nr	Horizont code	Diepte begin	Diepte eind	M	Org.st. %	Org.st. vs	Textuur <2	Textuur 50	Textuur M50	K	R	Geo frm	K vrz	C	D	Opmerkingen
1	1Aa	0	40		5.0		22	145	692					B3		10YR 3/1
2	1Cu	40	140				14	145	411					B3		10YR 6/4
3	1Cr	140	170				12	145	411					B3		2.5Y 6/2

Top-krtnr	Veld-krtnr	Bor. nr	Datum	Opst.	X	Y	Vlaknr	Hoogte	Kroonboring	
34C	1	32	10-98	KNO	229610	459270		14.36m+ NAP		

STANDAARDPUNTENCODE tv	subgr	cijf	k	toev.eind	v	Gt	GHG	GLG	Bew. diepte	Bod. gebr	A	B	
	2r	432				VIo	40	120	15	WD			

BIJZONDERHEDEN: 34CP7003 Lochem, provincie Gelderland

Lg nr	Horizont code	Diepte begin	Diepte eind	M	Org.st. %	Org.st. vs	Textuur <2	Textuur 50	Textuur M50	K	R	Geo frm	K vrz	C	D	Opmerkingen
1	1Ah	0	5		3.0		12	160	411					B2		10YR 2/1
2	1Bhe	5	15		1.0		8	160	411					O1		10YR 4/6 fibers
3	1BC	15	50		0.5		8	160	411					O1		10YR 5.5/6 fib.
4	1Ce	50	120				8	170	411					O1		2.5Y 6.5/4
5	1Cr	120	140		0.5		20	145	412					O3		2.5Y 5/2

Top-krtnr	Veld-krtnr	Bor. nr	Datum	Opst.	X	Y	Vlaknr	Hoogte	Kroonboring
34C	1	33	10-98	KNO	229645	458560		14.63m+ NAP	

STANDAARDPUNTENCODE tv	subgr	cijf	k	toev.eind	v	Gt	GHG	GLG	Bew. diepte	Bod. gebr	A	B
2r	422					VIo	50	120	20	BL		

BIJZONDERHEDEN: 34CP7016 Lochem, provincie Gelderland

Lg nr	Horizont code	Diepte begin	Diepte eind	M	Org.st. %	Org.st. vs	Textuur <2	Textuur 50	Textuur M50	K	R	Geo frm	K vrz	C	D	Opmerkingen
1	1Ap	0	10		2.5		11	145				411		B2		10YR 3/2
2	1Bhe	10	20		0.5		11	145				411		O2		10YR 5/2
3	1Cu1	20	50				11	145				411		O2		10YR 6/4
4	1Cg	50	80				14	155				411		O2		7.5YR 6/8
5	1Cu2	80	120				14	145				411		O2		2.5Y 6/2
6	1Cr	120	180				12	150				411		O2		5Y 6/2

Top-krtnr	Veld-krtnr	Bor. nr	Datum	Opst.	X	Y	Vlaknr	Hoogte	Kroonboring
34D	1	34	10-98	KNO	235620	461420		15.77m+ NAP	

STANDAARDPUNTENCODE tv	subgr	cijf	k	toev.eind	v	Gt	GHG	GLG	Bew. diepte	Bod. gebr	A	B
4r	423					VIo	70	150	65	TV		

BIJZONDERHEDEN: 34DP0155 Neede, provincie Gelderland

Lg nr	Horizont code	Diepte begin	Diepte eind	M	Org.st. %	Org.st. vs	Textuur <2	Textuur 50	Textuur M50	K	R	Geo frm	K vrz	C	D	Opmerkingen
1	1Aa	0	65		3.0		5	24	145			692		B3		10YR 4/2
2	1Cg1	65	90					50	155			411		O14		10YR 5/1
3	1Cg2	90	140					13	140			411		O2		2.5Y 7/2
4	1Cg3	140	180					11	150			411		O2		2.5Y 6/2

Top-krtnr	Veld-krtnr	Bor. nr	Datum	Opst.	X	Y	Vlaknr	Hoogte	Kroonboring
34G	1	35	10-98	KNO	245570	458910		24.72m+ NAP	

STANDAARDPUNTENCODE tv	subgr	cijf	k	toev.eind	v	Gt	GHG	GLG	Bew. diepte	Bod. gebr	A	B
	2r	432				IIIb	35	110	20	GR		

BIJZONDERHEDEN: 34GL0007 Eibergen, provincie Gelderland

Lg nr	Horizont code	Diepte begin	Diepte eind	M	Org.st. %	Org.st. vs	Textuur <2	Textuur 50	Textuur M50	K	R	Geo frm	K vrz	C	D	Opmerkingen
1	1Ap	0	15		5.0		12	160				411		B2		10YR 3/1
2	1Bhe	15	20		1.0		8	160				411		O1		7.5YR 4/4
3	1BC	20	45		0.5		8	160				411		O1		10YR 5/6 fibers
4	1Ce	45	110				8	160				411		O1		10YR 5.5/4
5	1Cr	110	150				8	160				411		O1		2.5Y 6/3

Top-krtnr	Veld-krtnr	Bor. nr	Datum	Opst.	X	Y	Vlaknr	Hoogte	Kroonboring
34G	1	36	10-98	KNO	245032	454985		26.82m+ NAP	

STANDAARDPUNTENCODE tv	subgr	cijf	k	toev.eind	v	Gt	GHG	GLG	Bew. diepte	Bod. gebr	A	B
	2r	422				IIIb	35	110	50	GR		

BIJZONDERHEDEN: 34GL0012 Eibergen, provincie Gelderland

Lg nr	Horizont code	Diepte begin	Diepte eind	M	Org.st. %	Org.st. vs	Textuur <2	Textuur 50	Textuur M50	K	R	Geo frm	K vrz	C	D	Opmerkingen
1	1Ah	0	12		4.0		12	145				411		B2		10YR 3/1
2	1Bhe	12	35		1.0		8	145				411		O1		5YR 3/2
3	1BCe	35	50		0.5		8	145				411		O1		7.5YR 4/4
4	1Ce	50	110				8	160				411		O1		10YR 5.5/4
5	1Cr	110	150				8	160				411		O1		2.5Y 6/3

Top-krtnr	Veld-krtnr	Bor. nr	Datum	Opst.	X	Y	Vlaknr	Hoogte	Kroonboring		
41A	1	37	10-98	KNO	220830	439920		14.55m+ NAP			

STANDAARDPUNTENCODE tv	subgr	cijf	k	toev.eind	v	Gt	GHG	GLG	Bew. diepte	Bod. gebr	A	B	
	4i	423				VIId	90	180	30	GR			

BIJZONDERHEDEN: 41AL0059 Doetinchem, provincie Gelderland

Lg nr	Horizont code	Diepte begin	Diepte eind	M	Org.st. %	Org.st. vs	Textuur <2	Textuur 50	Textuur M50	K	R	Geo frm	K vrz	C	D	Opmerkingen
1	1Ap	0	30		3.0		7	30	150			340		B3		10YR 3/3
2	1Cu	30	50				4	22	150			340		O3		10YR 6/4
3	1Cg	50	90				7	30	150			340		O3		10YR 5/6
4	2Cg1	90	120					65	150			413		O14	bl	7.5YR 5/8
5	2Cg2	120	150		2.0			55	150			413		O14	bl	10YR 5/2
6	2Cg3	150	180					18	155			413		O3		10YR 5/6
7	2Cr	180	220					12	160			413		O2		10YR 5/7

Top-krtnr	Veld-krtnr	Bor. nr	Datum	Opst.	X	Y	Vlaknr	Hoogte	Kroonboring		
41B	1	38	10-98	KNO	234990	441410		19.14m+ NAP			

STANDAARDPUNTENCODE tv	subgr	cijf	k	toev.eind	v	Gt	GHG	GLG	Bew. diepte	Bod. gebr	A	B	
	2r	422				IIIb	35	110	50	GR			

BIJZONDERHEDEN: 41BP7014 Aalten, provincie Gelderland

Lg nr	Horizont code	Diepte begin	Diepte eind	M	Org.st. %	Org.st. vs	Textuur <2	Textuur 50	Textuur M50	K	R	Geo frm	K vrz	C	D	Opmerkingen
1	1Ap	0	20		4.0		13	150				411		B2		10YR 3/1
2	1Bhe	20	50		1.0		13	145				411		O2		7.5YR 5/4
3	1Cu1	50	100				16	155				411		O2		10YR 6/3
4	1Cu2	100	120				12	160				411		O2		10YR 6/3
5	1Cr	120	150				12	150				411		O2		10YR 4/1

Top-krtnr	Veld-krtnr	Bor. nr	Datum	Opst.	X	Y	Vlaknr	Hoogte	Kroonboring		
41B	1	39	10-98	KNO	233610	441890		19.43m+ NAP			

STANDAARDPUNTENCODE tv	subgr	cijf	k	toev.eind	v	Gt	GHG	GLG	Bew. diepte	Bod. gebr	A	B	
2r	432					IIa	10	70	50	GR			

BIJZONDERHEDEN: 41BP7018 Aalten, provincie Gelderland

Lg nr	Horizont code	Diepte begin	Diepte eind	M	Org.st. %	Org.st. vs	Textuur <2	Textuur 50	Textuur M50	K	R	Geo frm	K vrz	C	D	Opmerkingen
1	1Ah	0	15		3.0		11	180				411		B2		7.5YR 3/2
2	1E	15	20				8	180				411		B1		10YR 4/3
3	1Bhe	20	45		1.0		11	180				411		O2		7.5YR 4/3
4	1BC	45	70		0.5		11	180				411		O2		10YR 3/3
5	1Cr	70	100		0.3		11	180				411		O2		10YR 4/3

Top-krtnr	Veld-krtnr	Bor. nr	Datum	Opst.	X	Y	Vlaknr	Hoogte	Kroonboring		
44H	1	40	10-98	KNO	131175	403045		9.08m+ NAP			

STANDAARDPUNTENCODE tv	subgr	cijf	k	toev.eind	v	Gt	GHG	GLG	Bew. diepte	Bod. gebr	A	B	
2r	432					VIo	70	170	75	BL			

BIJZONDERHEDEN: 44HP7804 Loon op zand, provincie N.Brabant

Lg nr	Horizont code	Diepte begin	Diepte eind	M	Org.st. %	Org.st. vs	Textuur <2	Textuur 50	Textuur M50	K	R	Geo frm	K vrz	C	D	Opmerkingen
1	1AO	-3	0		60	L						170				strooisel
2	1AE	0	25		2.0		11	160				411		B2		10YR 3.5/1
3	1Bhe1	25	40		1.0		8	160				411		O1		5YR 3/2
4	1Bhe2	40	75		0.5		8	160				411		O1		7.5YR 4/4
5	1BC1	75	120		0.2		8	160				411		O1		10YR 3/6
6	1BC2	120	135		0.2		8	160				411		O1		10YR 3/4 fibers
7	1BC3	135	145		0.5		30	110				412		O3		10YR 3/3
8	1Ce	145	170				18	145				412		O3		2.5Y 6/3 gel.
9	1Cr	170	190				18	145				412		O3		2.5Y 5.5/2

Top-krtnr	Veld-krtnr	Bor. nr	Datum	Opst.	X	Y	Vlaknr	Hoogte	Kroonboring		
45C	1	41	10-98	KNO	145540	401300		6.98m+ NAP			

STANDAARDPUNTENCODE tv	subgr	cijf	k	toev.eind	v	Gt	GHG	GLG	Bew. diepte	Bod. gebr	A	B	
	c4k	423				IIIb	30	120	70	GR			

BIJZONDERHEDEN: 45CL0024 Udenhout, provincie N.Brabant

Lg nr	Horizont code	Diepte begin	Diepte eind	M	Org.st. %	Org.st. vs	Textuur <2	Textuur 50	Textuur M50	K	R	Geo frm	K vrz	C	D	Opmerkingen
1	1Aag	0	45		5.0		20	145	692					B3		10YR 3/1
2	1ACg	45	80		1.0		35	130	413					B4		10YR 5/4 bont
3	1Cg	80	120				12	160	413					O2		2.5Y 6/4
4	1Cr	120	140				12	160	413					O2		2.5Y 6.5/3

Top-krtnr	Veld-krtnr	Bor. nr	Datum	Opst.	X	Y	Vlaknr	Hoogte	Kroonboring		
50A	1	42	10-98	KNO	102698	391811		6.33m+ NAP			

STANDAARDPUNTENCODE tv	subgr	cijf	k	toev.eind	v	Gt	GHG	GLG	Bew. diepte	Bod. gebr	A	B	
	v4d	423				Ia	0	45	20	WN			

BIJZONDERHEDEN: 50AP7608 Rucphen, provincie N.Brabant

Lg nr	Horizont code	Diepte begin	Diepte eind	M	Org.st. %	Org.st. vs	Textuur <2	Textuur 50	Textuur M50	K	R	Geo frm	K vrz	C	D	Opmerkingen
1	1Cw	0	20		99	S			150					B16		10YR 2/1
2	2Cgr	20	45		5.0		30	130	413					B3		10YR 3/2
3	2Cr	45	80				11	160	413					O2		10YR 5/2

Top-krtnr	Veld-krtnr	Bor. nr	Datum	Opst.	X	Y	Vlaknr	Hoogte	Kroonboring		
50A	1	43	10-98	KNO	102890	391260		7.05m+ NAP			

STANDAARDPUNTENCODE tv	subgr	cijf	k	toev.eind	v	Gt	GHG	GLG	Bew. diepte	Bod. gebr	A	B	
5h	432					Ia	0	50	10	GR			

BIJZONDERHEDEN: 50AP7615 Rijsbergen, provincie N.Brabant

Lg nr	Horizont code	Diepte begin	Diepte eind	M	Org.st. %	Org.st. vs	Textuur <2	Textuur 50	Textuur M50	K	R	Geo frm	K vrz	C	D	Opmerkingen
1	1Ahg	0	10		4.0		25	130	413					B3		10YR 3/2
2	1Cgr1	10	40				15	160	413					O2		10YR 5/2.5
3	1Cgr2	40	50				20	160	413					O3		10YR 4.5/2
4	1Cr	50	80				20	160	413					O3		10YR 4/2 leemb.

Top-krtnr	Veld-krtnr	Bor. nr	Datum	Opst.	X	Y	Vlaknr	Hoogte	Kroonboring		
50A	1	44	10-98	KNO	102233	392175		7.33m+ NAP			

STANDAARDPUNTENCODE tv	subgr	cijf	k	toev.eind	v	Gt	GHG	GLG	Bew. diepte	Bod. gebr	A	B	
2r	423					IIIa	20	110	40	GR			

BIJZONDERHEDEN: 50AP7618 Rucphen, provincie N.Brabant

Lg nr	Horizont code	Diepte begin	Diepte eind	M	Org.st. %	Org.st. vs	Textuur <2	Textuur 50	Textuur M50	K	R	Geo frm	K vrz	C	D	Opmerkingen
1	1Ap	0	20		3.0		18	140	411					B3		10YR 3.5/1.5
2	1BCe1	20	25		0.2		11	160	411					O2		10YR 5/3
3	1BCe2	25	40		0.5		35	110	412					O4		10YR 4/2
4	1Ce	40	55				15	160	413					O2		10YR 5/3
5	1Cg	55	110				20	150	413					O3		10YR 4/2.5 hout
6	1Cr	110	130				11	160	413					O2		10YR 4.5/2

Top-krtnr	Veld-krtnr	Bor. nr	Datum	Opst.	X	Y	Vlaknr	Hoogte	Kroon boring		
51A	1	45	10-98	KNO	148850	399040		7.91m+ NAP			

STANDAARDPUNTENCODE tv	subgr	cijf	k	toev.eind	v	Gt	GHG	GLG	Bew. diepte	Bod. gebr	A	B	
	4s	432				VIo	60	160	100	BL			

BIJZONDERHEDEN: 51AL0003 Boxtel, provincie N.Brabant

Lg nr	Horizont code	Diepte begin	Diepte eind	M	Org.st. %	Org.st. vs	Textuur <2	Textuur 50	Textuur M50	K	R	Geo frm	K vrz	C	D	Opmerkingen
1	1Aa1	0	15		5.0		15	160	692					B2		10YR 3/1
2	1Aa2	15	70		5.0		15	160	692					B2		10YR 3/1
3	1Ahb	70	80		8.0		15	160	411					B2		10YR 2/1
4	1Bhb	80	100		2.0		15	160	411					O2		10YR 3/2
5	1BC	100	110		1.0		15	160	411					O2		10YR 4/2
6	1Ce	110	125				11	160	411					O2		2.5YR 6/2
7	1Cg	125	160				11	160	411					O2		2.5YR 6.5/4
8	1Cr	160	200				11	160	411					O2		2.5YR 6.5/1

Top-krtnr	Veld-krtnr	Bor. nr	Datum	Opst.	X	Y	Vlaknr	Hoogte	Kroon boring		
51F	1	46	10-98	KNO	175500	398385		15.94m+ NAP			

STANDAARDPUNTENCODE tv	subgr	cijf	k	toev.eind	v	Gt	GHG	GLG	Bew. diepte	Bod. gebr	A	B	
	4s	432			F	VIo	40	130	120	GR			

BIJZONDERHEDEN: 51FL0004 Beek en Donk, provincie N.Brabant

Lg nr	Horizont code	Diepte begin	Diepte eind	M	Org.st. %	Org.st. vs	Textuur <2	Textuur 50	Textuur M50	K	R	Geo frm	K vrz	C	D	Opmerkingen
1	1Aa	0	120		5.0		12	160	693					B2		10YR 3/2 hetrog
2	1ACg	120	130		1.0		6	190	411					O1		10YR 5.5/2
3	1ACr	130	170		1.0		6	190	411					O1		10YR 5.5/2

Top-krtnr	Veld-krtnr	Bor. nr	Datum	Opst.	X	Y	Vlaknr	Hoogte	Kroonboring	
51G	1	47	10-98	KNO	162830	377370		21.94m+ NAP		

STANDAARDPUNTENCODE tv	subgr	cijf	k	toev.eind	v	Gt	GHG	GLG	Bew. diepte	Bod. gebr	A	B	
	2r	432				VIo	70	150	35	BL			

BIJZONDERHEDEN: 51GP0087 Waalre, provincie N.Brabant

Lg nr	Horizont code	Diepte begin	eind	M	Org.st. %	vs	Textuur <2	50	M50	K	R	Geo frm	K vrz	C	D	Opmerkingen
1	1A/B	0	35		2.0		11	160	411					B2		10YR 3.5/5
2	1Ce1	35	50				11	160	411					O2		10YR 5.5/6
3	1Ce2	50	100				11	160	411					O2		2.5Y 6/4
4	1Ce3	100	150				6	180	411					O1		2.5Y 6.5/2
5	1Cr1	150	175				11	160	411					O2		2.5Y 6.5/2
6	1Cr2	175	180				20	130	412					O3		2.5Y 5.5/2

Top-krtnr	Veld-krtnr	Bor. nr	Datum	Opst.	X	Y	Vlaknr	Hoogte	Kroonboring	
52C	1	48	10-98	KNO	181475	383543		24.30m+ NAP		

STANDAARDPUNTENCODE tv	subgr	cijf	k	toev.eind	v	Gt	GHG	GLG	Bew. diepte	Bod. gebr	A	B	
	c4k	432				VIIo	90	180	40	GR			

BIJZONDERHEDEN: 52CL0044 Deurne, provincie N.Brabant

Lg nr	Horizont code	Diepte begin	eind	M	Org.st. %	vs	Textuur <2	50	M50	K	R	Geo frm	K vrz	C	D	Opmerkingen
1	1Aa	0	10		2.0		12	160	692					B2		10YR 4/3
2	1Ahgb	10	40		3.0		12	160	411					B2		10YR 3/2
3	1Cg	40	70				8	160	411					O1		2.5Y 6.5/4
4	1Cu	70	180				12	155	411					O2		2.5Y 7/4
5	1Cr	180	200				40	90	412					O4		2.5Y 5/2 zepig

Top-krtnr	Veld-krtnr	Bor. nr	Datum	Opst.	X	Y	Vlaknr	Hoogte	Kroon boring		
52D	1	49	10-98	KNO	198410	384110		26.53m+ NAP			

STANDAARDPUNTENCODE tv	subgr	cijf	k	toev.eind	v	Gt	GHG	GLG	Bew. diepte	Bod. gebr	A	B	
	4h	423				Vbo	30	175	35	AK			

BIJZONDERHEDEN: 52DL0010 Horst, provincie Limburg

Lg nr	Horizont code	Diepte begin	Diepte eind	M	Org.st. %	Org.st. vs	Textuur <2	Textuur 50	Textuur M50	K	R	Geo frm	K vrz	C	D	Opmerkingen
1	1Apg	0	35		4.0		18	140				413		B3		10YR 3/2
2	1Cg1	35	70				18	140				413		O3		10YR 6/3
3	1Cg2	70	100				22	140				413		O3		7.5YR 6/6
4	1Cgr	100	175				15	155				413		O2		2.5Y 5.5/2
5	1Cr	175	185				15	155				413		O2		2.5Y 5.5/2

Top-krtnr	Veld-krtnr	Bor. nr	Datum	Opst.	X	Y	Vlaknr	Hoogte	Kroon boring		
57A	1	50	10-98	KNO	146396	372129		31.40m+ NAP			

STANDAARDPUNTENCODE tv	subgr	cijf	k	toev.eind	v	Gt	GHG	GLG	Bew. diepte	Bod. gebr	A	B	
	2r	423			g10	IIa	10	80	25	WD			

BIJZONDERHEDEN: 57AP7802 Hoogeloon, provincie N.Brabant

Lg nr	Horizont code	Diepte begin	Diepte eind	M	Org.st. %	Org.st. vs	Textuur <2	Textuur 50	Textuur M50	K	R	Geo frm	K vrz	C	D	Opmerkingen
1	1Ah	0	5		40	DZ						110		B16		10YR 2/2
2	1Bhe1	5	15		4.0		20	140				413		O3		7.5YR 3/2
3	1Bhe2	15	25		1.0		20	140				413		O3		7.5YR 3.5/2
4	1Ce1	25	35				20	140				413		O3		2.5Y 6.5/3
5	1Ce2	35	50				12	160				413		O2		2.5Y 6/3
6	1Ce3	50	80				12	160				413		O2		2.5Y 5/2
7	1Cr1	80	100				12	160				413		O2		2.5Y 5/2
8	1Cr2	100	120				3	300				413		O5	g	2.5Y 5.5/2

Top-krtnr	Veld-krtnr	Bor. nr	Datum	Opst.	X	Y	Vlaknr	Hoogte	Kroonboring		
57E	1	51	10-98	KNO	164880	371480		26.94m+ NAP			

STANDAARDPUNTENCODE tv	subgr	cijf	k	toev.eind	v	Gt	GHG	GLG	Bew. diepte	Bod. gebr	A	B	
	4k	423			F	VIId	100	240	100	BL			

BIJZONDERHEDEN: 57EL0006 Leende, provincie N.Brabant

Lg nr	Horizont code	Diepte begin	eind	M	Org.st. %	vs	Textuur <2	50	M50	K	R	Geo frm	K vrz	C	D	Opmerkingen
1	1A/Cg	0	100		2.0		25	130				412		O3		7.5YR 5/8
2	1Ce1	100	180				16	130				412		O2		10YR 6/6
3	1Ce2	180	240				20	110				413		O3		10YR 6/5
4	1Cr	240	280				20	110				413		O3		10YR 5.5/5